Freie Universität Berlin

Synthesis and Application of Water-Soluble Dendronized Rylene Dyes

Dissertation

Zur Erlangung des akademischen Grades des

Doktors der Naturwissenschaften (Dr. rer. nat.)

Eingereicht im Fachbereich Biologie, Chemie, Pharmazie

Der Freien Universität Berlin

vorgelegt von

Dipl.-Chem. Timm Heek

aus Berlin

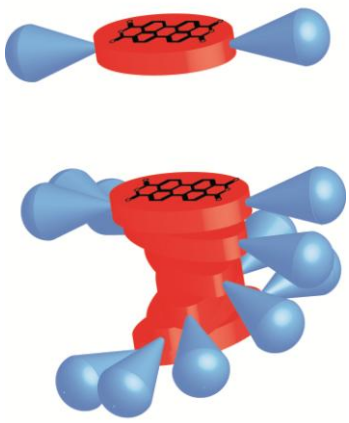

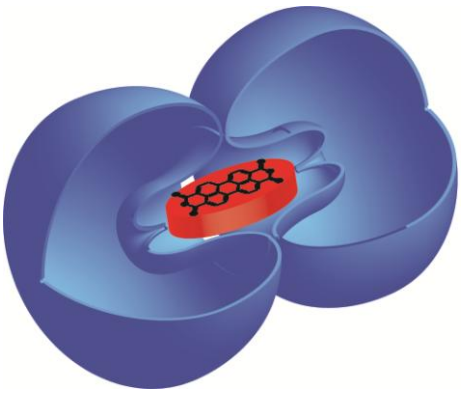

März 2013

Diese Arbeit wurde unter Anleitung von Prof. Dr. Rainer Haag im Zeitraum von Juli 2007 bis Februar 2013 am Institut für Chemie und Biochemie der Freien Universität Berlin durchgeführt.

1. Gutachter: Prof. Dr. Rainer Haag

2. Gutachter : PD Dr. habil. Kai Licha

Disputation am 24.04.2013

Acknowledgements

First of all I want to thank Prof. Dr. Rainer Haag for giving me the opportunity to do my Ph D. in his group. The interesting topics as well the freedom he granted me doing my doctoral work should be especially highlighted. Secondly I want to thank Dr. Kai Licha for interesting discussions, support in the form of cooperations, as well as for being the coreferee of this thesis. In addition I would like to thank all former and present members of the Haag group, in particular the members of the Surface Subgroup. Special thanks belong to Dipl. Chem. Aileen Justies whose enthusiastic willingness for discussion has helped me since the beginning of my chemistry studies and which always challenged me to question things. Furthermore I want to thank all members of the past and present "Kaffeerunde", Dr. Markus Meise, Dr. Ewelina Burakowska, Dr. Paul Servin, Philip Hultsch, M. Sc. Dominic Gröger, M. Sc. Harald Krüger and M. Sc. Emanuel Fleige for their advice in chemical as well as in private matters. I would also like to thank Dr. Ying Luo, M Sc. Katja Neute and Dr. Carlo Fasting I have to thank for their tolerance and forbearance as lab colleagues of mine.

Additionally, I want to thank all my cooperation partners, especially Dr. Antonio Setaro, M. Sc. Frederike Ernst, Prof. Dr. Stefanie Reich, Dr. Jörg Nikolaus, M. Sc. Roland Schwarzer, Dr. Pia Welker, Prof. Dr. Andreas Herrmann, and Prof. Dr. Frank Würthner for their fruitful collaboration.

Lastly, I would like to thank all members of the service and analytical department of the FU Berlin for their kind support and numerous measurements throughout my doctoral work.

For my family

Table of Contents

1 Introduction

1.1 Color and Dyes

When looking back on the history of mankind, one finds that the development and application of dyes and pigments has always been a focus of research. Even in the very beginning of human history, in prehistorical times, man has dyed furs, textiles, and other objects for aesthetic reasons. The oldest reported findings of applied color pigments so far maybe the cave paintings in the Cauvet-caves in France which have been estimated to originate 33000 years B.C.[1] Since then a broad variety of pigments and dyes have been developed and used. Indigo, ancient purple, and alizarin have been extensively used as colorants since antiquity because they could be obtained from natural resources. However, due to the differences in the availability of the natural resources from which the dyes had been extracted, not every color was equally valuable. For example, ancient purple was extracted from a gland of the purple snail. As every snail produces only a small amount of the dye around 12000 snails were needed to obtain about 1.4 grams of pure dye.[2] This, of course, made that color among the most valuble dyes and was mainly used for staining clothes of high ranking persons like cardinals and emperors.[3]

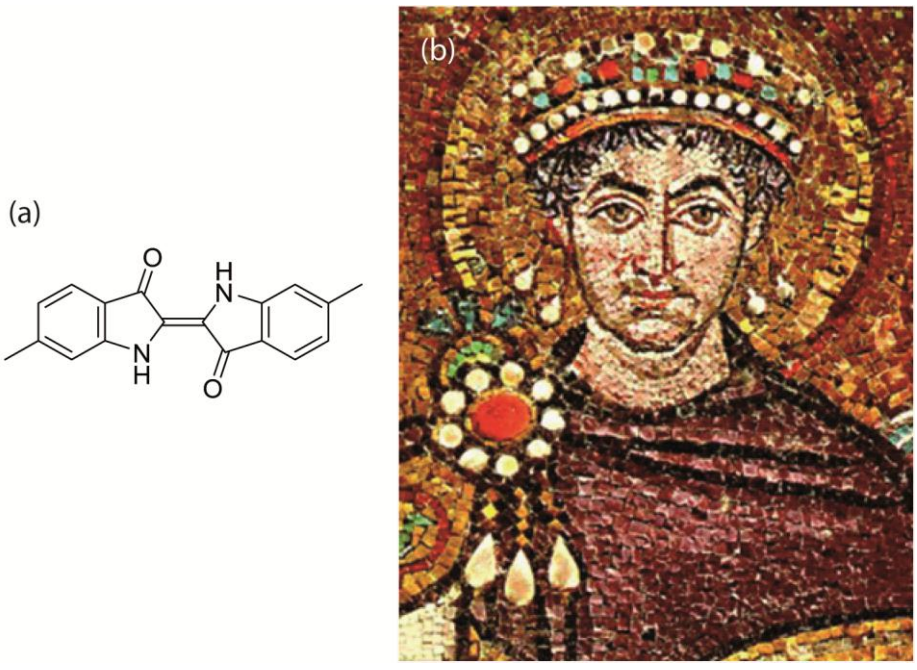

Figure 1. (a) Chemical structure of 6,6´-dibromoindigo, which is the main component in ancient purple. (b) Mosaic of Justinian I. clad in ancient purple, 6th century

These circumstances have led to an increased interest in the development of cost effective synthetic routes to dye materials. From the 18th century on, many synthetic milestones in dye chemistry were achieved, for example, in the development of Berliner Blau from Diesbach in 1706,[4] the synthesis of

mauveine from Perkin in 1856[5] or indigo by Baeyer in 1878.[6] In fact, the amount of dyes obtained from natural resources which were used in textile industry decreased to 10% until the early 1900.[7] As the textile industry was the main customer of the resulting dye products, the focus in dye research was mainly on the development of color pure dyes with a high color intensity and easy to apply staining methods. Today the interest in dye development has shifted from a simplistic use to more technical advanced and specialized topics in the fields of electronics, laser technology and medicine, to name just a few.[8] As the requirements for these dyes go beyond their simple color properties, the term "functional dyes" was developed.

1.2 Functional Dyes

The term functional dyes developed from the necessity to differentiate between dyes which are not used due to their aesthetic appearance but because of their physical or chemical properties.[9] As the color of these materials is of lower interest, the wavelength covered by functional dyes is broadened to 200 - 1500 nm. Therefore dye structures that absorb in the UV (<400 nm) or the near infrared (NIR) (>750 nm) region, which cannot be sensed with the human eye, belong to the group of functional dyes, as well. One of the best examples is β-carotene which is used as food coloring.

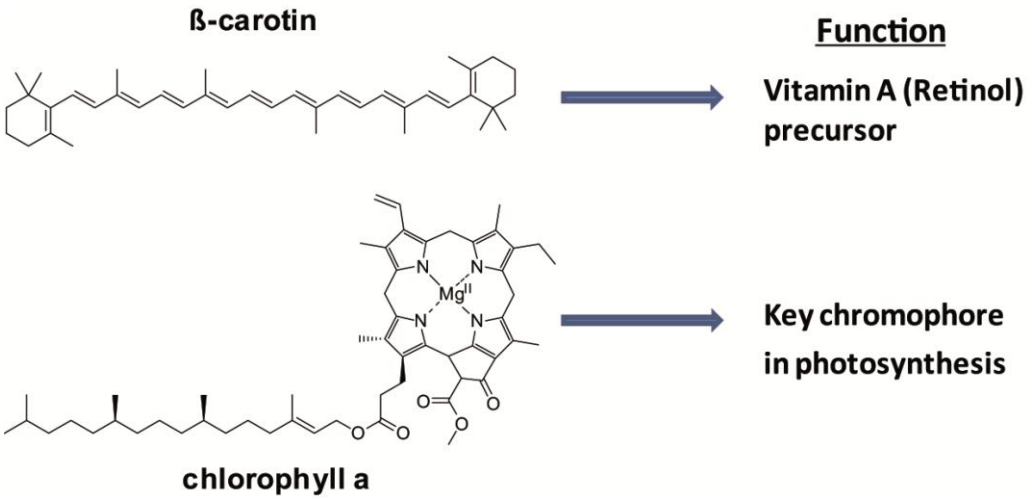

Figure 2. Everyday life examples of functional dyes.

β-carotene not only serves the function of staining treated food but also acts as a precursor for Vitamin A in the human body.[10] Another famous example from nature is chlorophyll. Without it life in the present form would not be possible. It is the key element in photosynthesis which transforms solar energy into chemical energy which then serves as fuel for biological processes.[11] Besides these simple examples from everyday life, there is a magnitude of other examples available. Many of these

functional dyes are based on polyaromatic scaffolds, i.e. rylene dyes which have become increasingly important in recent years.

1.3 Rylene dyes

The term rylene dyes describes a family of dye scaffolds which consist of naphthalene units connected via the peri positions to each other (Figure 3). Therefore if one looks at them in a polymeric way they belong to the class of the poly-peri-naphtalenes (PPNs). For the nomenclature the following names are used: perylene (n = 0), terrylene (n = 1), quaterrylene (n = 2), pentarylene (n = 3), and hexarylene (n = 4).[12] A common substitution pattern of these dyes is at the outer peri positions with imide functions leading to the respective monoimides or bisimides. Due to their electron withdrawing nature this increases the photostability of the chromophor drastically.[13] Other important substitution positions are the so-called bay position, providing a cis-butadien like structure and the ortho position next to the imide function.[14]

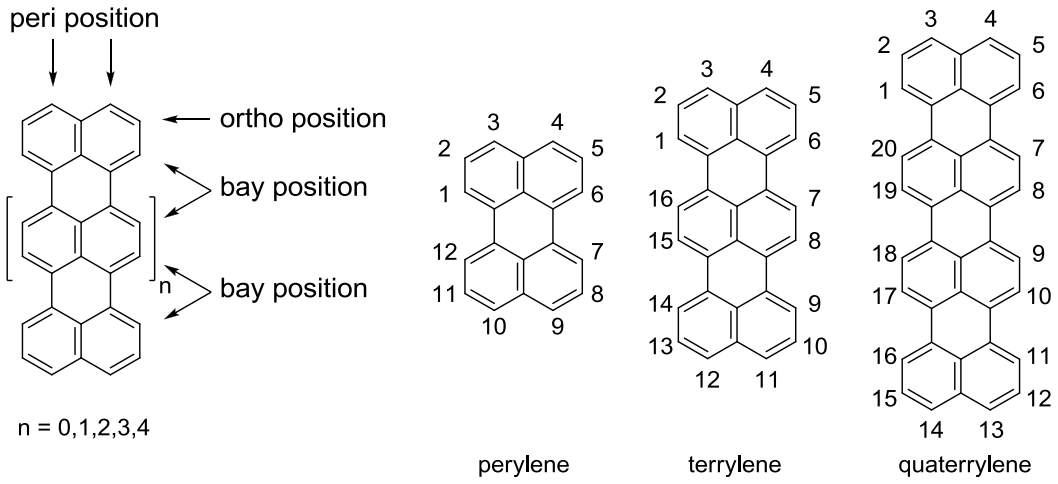

Figure 3. General structure and nomenclature of rylene dyes.

1.3.1 Perylene dyes and -pigments

Perylene bases dyes and pigments are among the most used rylene dyes in different scientific fields ranging from supramolecular chemistry[15] over organic electronics[16] to solar cell research.[17] Especially derivatives of 3,4,9,10-perylenetetracarboxibisanhydride (PBA) **5** have been the starting point of many synthesized dyes and pigments. The industrial access towards this substance class was developed by Kardos in 1912-13 [18] (Scheme 1) using acenaphtene **1** as starting material. In a first step an oxidation with vanadiumpentoxide as catalyst gave 1,8-naphtalene-dicarboxanhydride **2**. The imidization with ammonia produced 1.8-naphtalene-dicarboximide **3**. A final oxidative coupling in an alkaline melt gave the dimerized perylene-3,4,9,10-tetracarboxibisimide (PBI) **4** which was

hydrolyzed with sulfuric acid at high temperatures (220 °C) to give perylene-3,4,9,10-tetracarboxidibisanhydride (PBA) **5**.

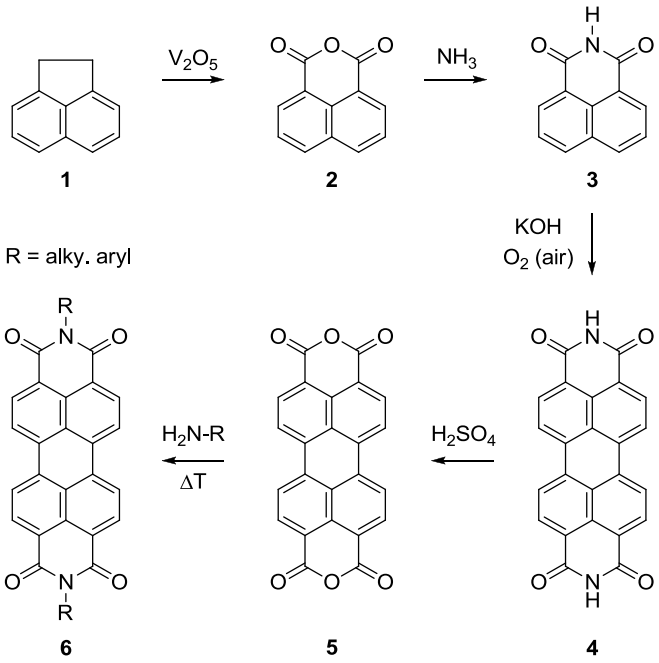

Scheme 1. Synthetic route towards 3,4,9,10-perylenetetracarboxibisimides (PBIs).

The resulting bisanhydride **5** could be easily converted into different PBIs **6** via simple coupling with aromatic or aliphatic amines at high temperatures.[19] As the solubility of these first PBIs was poor due to pronounced π-π interactions they were mainly applied as insoluble organic pigments in car paints and lacquers.[20] The fact that PBIs are subject to a strong crystallochromic effect gave access to different colored pigments based on the same chromophore ranging from bright red to black[21] (Figure 4).

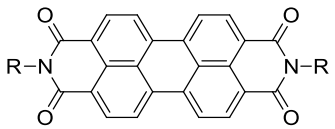

R =	**Color**
CH_3	red
	red - maroon
	red – violet
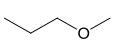	Black

Figure 4. Structures of different colored PBI pigments.

This strong crystallochromicity results from differences in the packing in the solid state which leads to a different degree of orbital overlap and therefore to a different color. In general the better the overlap between adjacent PBI molecules the more bathochromically the absorption is shifted.

A dramatic improvement in solubility of PBIs was achieved by introducing sterically demanding residues at the imide positions (Figure 5) that hampered the strong aggregation tendency. Especially, ortho substituted anilines[22] or secondary branched amines[23], so-called swallow tail substituents, have been shown to be excellent aggregation blockers that produce PBIs with a solubility in organic solvents > 100 g/l.

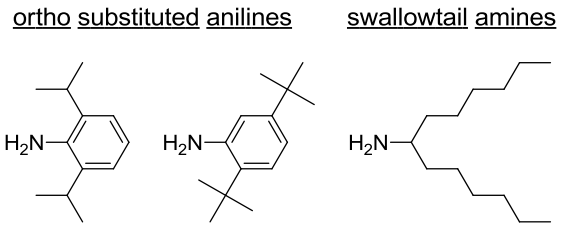

Figure 5. Typical sterically demanding substitutens used for highly soluble PBI derivatives.

In contrast to the situation in the solid state, in solution nearly all core unsubstituted PBIs possess the same absorption properties and color (Figure 6). The main absorption, resulting from the electronic S_0-S_1 transition which has a dipole moment along the long molecular axis, shows a characteristic strong vibronic fine structure.[24] In addition, most PBIs possess fluorescent properties with a fluorescence signal of nearly perfect mirror image symmetry with small stokes shifts indicating only minor changes in geometry upon excitation. The substituent at the imide position has only limited influence on the form and shape of the absorption as well as the fluorescence signal because

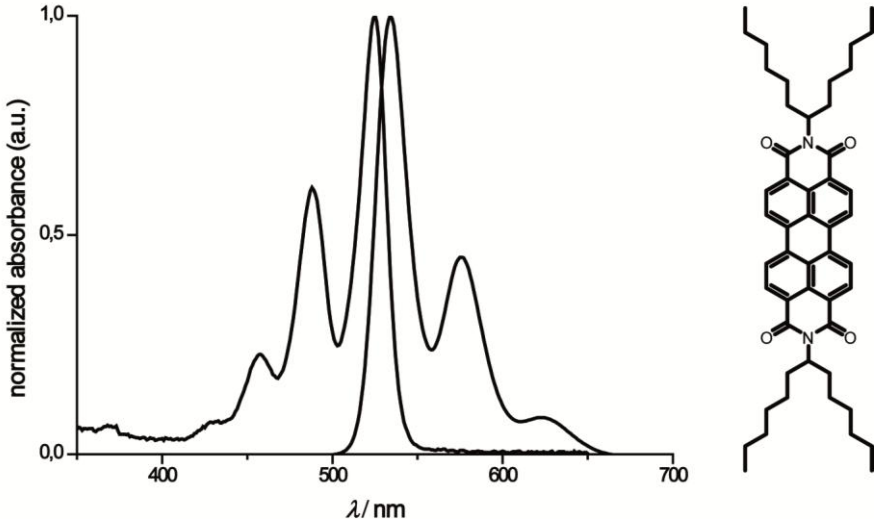

Figure 6. UV-Vis and fluorescence spectrum of hexylheptyl substituted PBI in CH_2Cl_2.

there are nodes at the imide nitrogen atoms in the HOMO and LUMO.[25]

One of the most intriguing features of PBIs are the photophysical properties of the fluorescence with exceptionally high fluorescence quantum yields (FQY) of up to ϕ_{fl}= 100 % and only a negligible triplett population rate.[24b, 26] As already mentioned, the form and shape of the absorption and fluorescence signal differ only slightly with varying imide substitutens. In contrast, the FQY can be dramatically decreased upon substitution with electron rich aromatic groups at the imide positions via a concurrent photoinduced electron transfer process.[27]

The solubility increase extended the applicability of PBIs beyond their use as organic pigments into many other fields like laser dyes[28] or fluorescence collectors.[29] In a fluorescence collector the dye is solubilized into a transparent high refractive polymer matrix (mainly polymethylmethacrylat-matrixes). When light is shined on it, the isotropically emitted light from the fluorophore is totally internally reflected (TIR) at the horizontal edges of the polymer block and therefore concentrated at the outer edges. The concentrated light can then be used in a connected solar cell to increase the efficiency. In addition, fluorescence collectors allow efficient harvesting of diffuse light which makes it unnecessary to permanently adjust the solar panels perpendicular to the incident sun light.

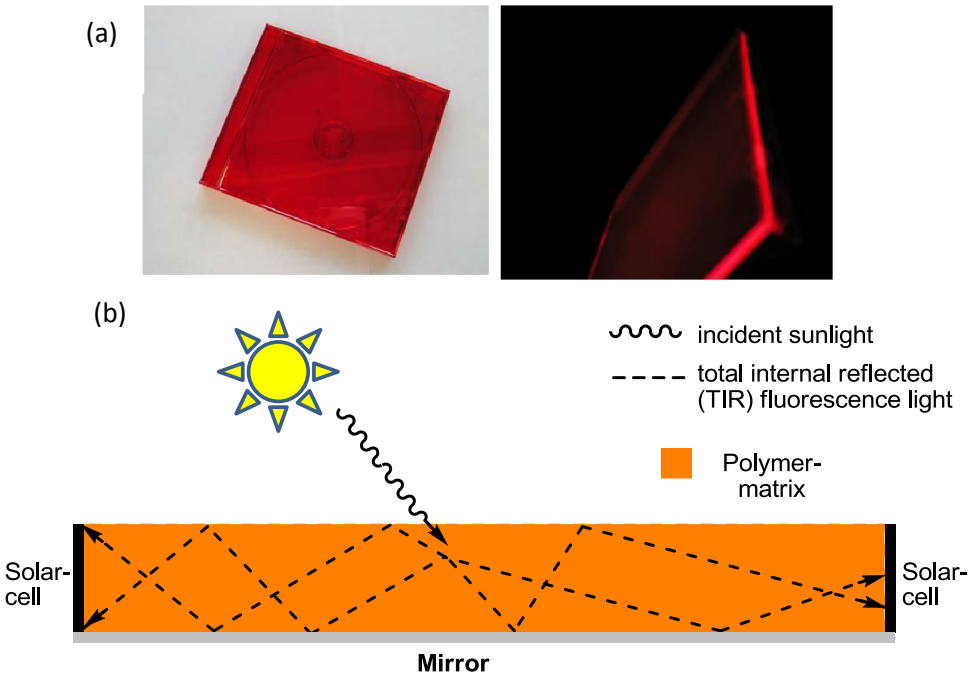

Figure 7. (a) Polystyrene imbedded fluorescent dye showing the principle of a fluorescence collector. Under illumination the edges are far more bright than the main surface area. (b) Schematic working principle of a fluorescence collector. The incident light is reemitted and totally reflected within the polymer matrix and therefore accumulated at the edges where a solar cell is placed. [30]

1.3.2 Synthesis and optical tuning of perylene based dyes

One of the main reasons why perylene based dyes are used in so many different fields is due to their optical and photophysical properties which can be controlled by a magnitude of different substitution patterns. The most important examples including their synthesis are shown in the following.

1.3.2.1 Diamidine PBIs

A treatment of PBA **5** with aromatics bearing adjacent amines leads to the formation of a mixture of *syn*- and *anti*-isomeric perylene diamidine dyes **7** and **8** (Scheme 2).[31] Via the extension of the

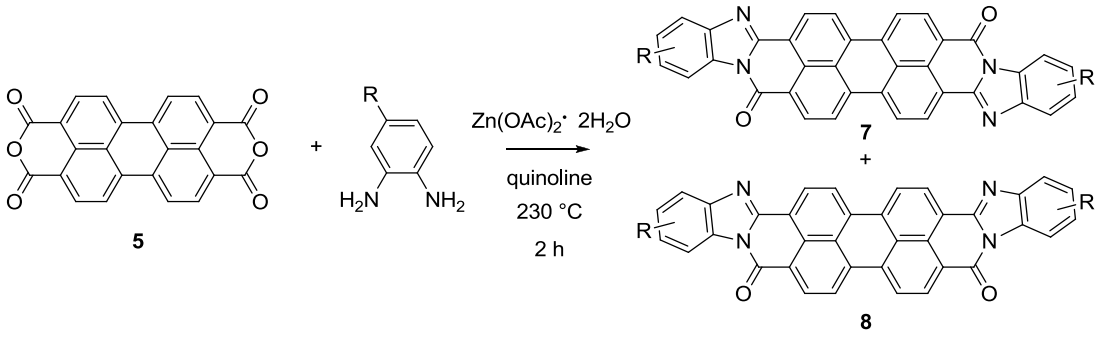

Scheme 2. Synthesis of bathochromically shifted perylene diamidine dyes.

aromatic π-system, the absorbance of these dyes is bathochromically shifted in comparison to PBIs by ~70nm to 605 nm. In consequence the fluorescence is also shifted to 623 nm together with a decrease in quantum yield to ϕ_{fl} = 37 %. These spectral properties have made these dyes attractive candidates in xerographic applications.[32] Besides the substitution with 1,2-phenyldiamine derivatives, the substitution with more extended aromatic diamines like 1,8-diaminonaphtalene or 1,8-diaminophenantrene leads to an even longer extension of the π system (Scheme 3).[33] Therefore the absorbance of the bisnaphtalene and the bisphenantranen substituted diamidines **9** and **10** is further red shifted to 643 nm and 659 nm, respectively. However, this additional shift is not solely related to the extension of the π-system along the molecular axis but also to the tetraphenoxylation in the bay region (see Chapter 1.3.2.3). This additional core substitution was necessary as the solubility of the core unsubstituted material was too low for a proper preparation. The fluorescence properties of the two dyes differ significantly from each other. While for the bisphenantranene PBI **9** a fluorescence at 680 nm is observed, the bisnaphtalene PBI **10** shows nearly no fluorescence. This arises from differences in geometry of the amidine substituents. While the amidines incorporated into five-membered rings, as in the case of **7**, **8,** and **10,** possess a completely planar structure, the

amidines incorporated into six-membered rings as in **9** are twisted out of the aromatic plane.[34] This leads to a broadening of the absorption profile and therefore to a strong reabsorption effect which quenches most of the fluorescence.

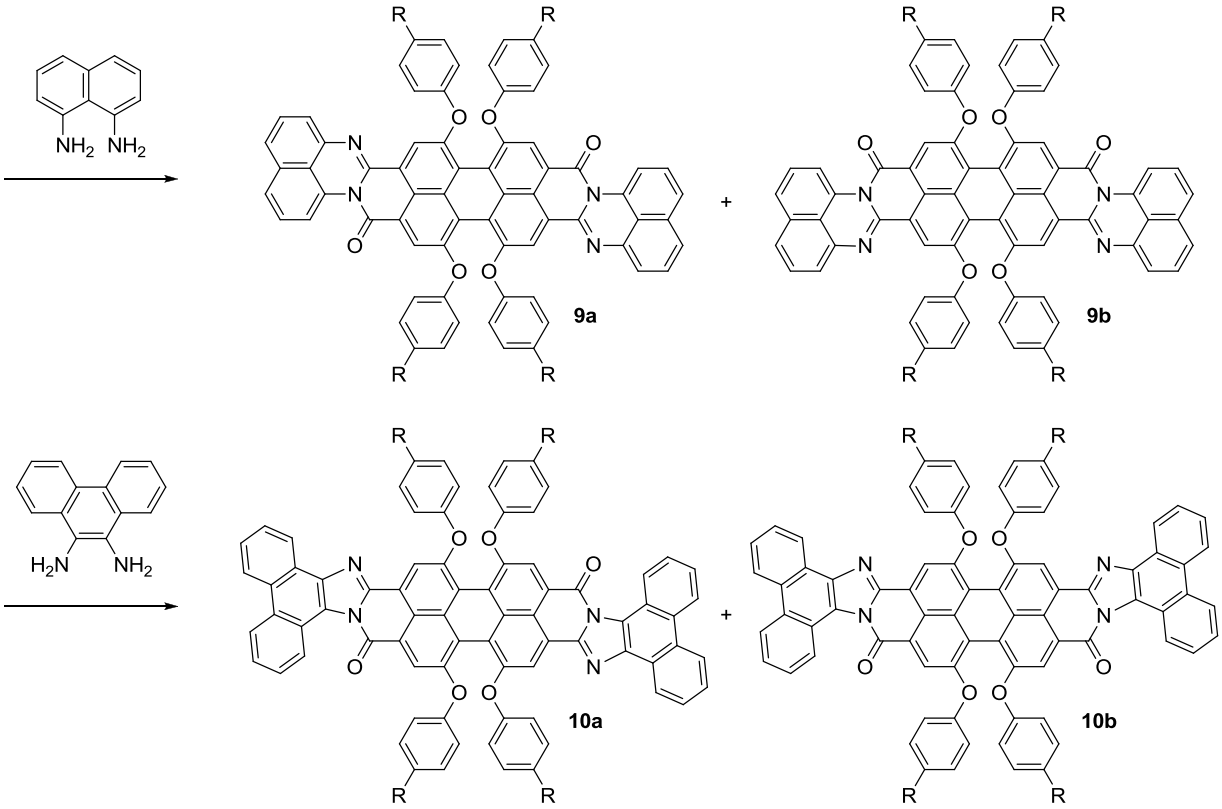

Scheme 3. Structure of red shifted perylenediamidine dyes 9 and 10.

1.3.2.2 Halogenated PBIs

Key intermediates in the synthesis of bay substituted PBIs are the 1,6,7,12-tetrachlorinated and tetrabrominated PBAs **11** and **12**. They are produced via the direct chlorination of PBA in sulfuric acid with elemental chlorine[35] or in the case of bromination by adding oleum and elemental bromine to the reaction mixture (Scheme 4).[36] In contrast to the chlorination, the bromination can also be used to obtain mainly dibrominated PBA **13** by adjusting the reaction times and the temperature.[37] One has to note that in all cases a purification of the resulting halogenated bisanhydrides is not possible due to their low solubility. The corresponding halogenated PBIs **14** and **15** can only be separated by common purification methods, e. g. column chromatography, after a subsequent imidization with sterically demanding primary amines. Since their discovery it was assumed that dibromination only led to the 1,7 regioisomer. However, besides the 1,7 isomer the 1,6 isomer can also be formed. This issue did not catch any further attention as the resulting brominated bisimides were only distinguishable upon using high field (>400 MHz NMR) ^{1}H-NMR and were in principle not separable by common purification techniques like column chromatography. The existence of this problem was

first discussed by Würthner et al. in 2004 who also was the first one to obtain regioisomerically pure 1,7 dibrominated PBIs via repetitive crystallization, which still is the only way to produce large amounts of regioisomerically pure 1,7-substituted PBIs.[38]

Both the di- and tetrahalogenated PBIs serve as starting materials for a magnitude of **D**onor or **A**cceptor core functionalized PBIs as will be shown in the next chapter.

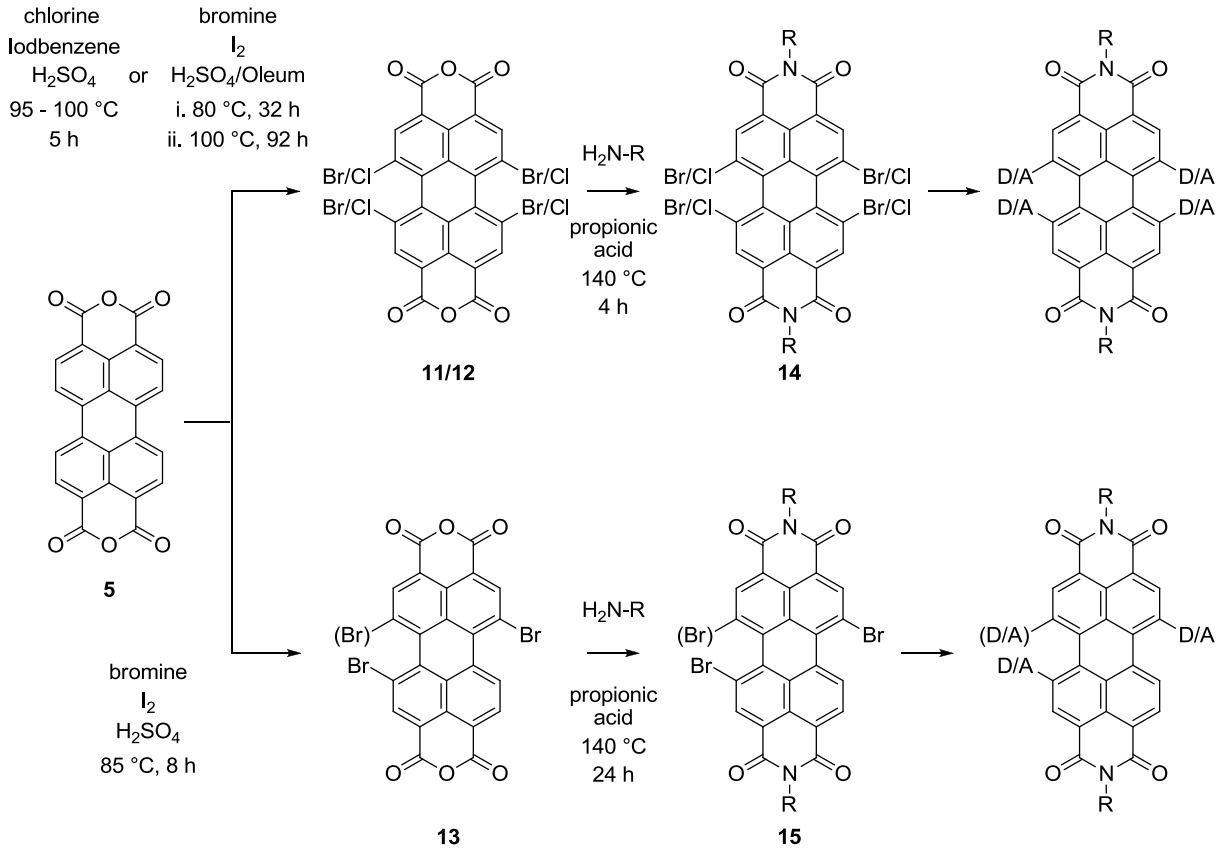

Scheme 4. Classical synthetic routes towards bay halogenated and bay substituted PBIs.

As this synthetic route may be of disadvantage in regard to the used amount of amine for the formation of the PBI, the synthetic access towards brominated PBIs has been more recently expanded by the selective bromination of PBIs under mild conditions (Scheme 5).[39] Thereby the PBIs are first prepared by the condensation of PBA with the corresponding primary amines, which are then dissolved in dichloromethane and treated with bromine at refluxing temperatures (50 °C). This route leads exclusively (>90%) to dibrominated PBIs in high yields. Upon lowering the temperature monobrominated PBIs (>50%) are also accessible via this route.

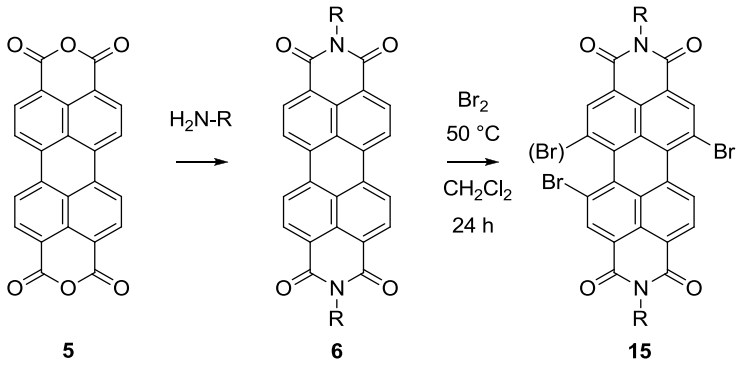

Scheme 5. Alternative reaction pathway towards dibrominated PBIs using mild conditions.

1.3.2.3 Core substituted PBIs

As shown for the diamidine perylene dyes (see Chapter 1.3.2.1) bay phenoxylation of halogenated PBIs is one of the most common ways to increase the solubility of perylenedyes. This increase mainly results from a twisting of the perylene core which reduces the tendency towards π-π self-aggregation. [40] Synthetically they are accessible via a simple one-step reaction starting from the halogenated precursor which is treated with the corresponding phenol derivate under basic conditions (Scheme 6).[28,41] Besides the solubility increase, the optical properties of phenoxylated PBIs are strongly altered. For example, the di- and tetraphenoxylated PBIs **17**[42] and **18**[43] substituted with simple phenol groups possess red-shifted absorptions in comparison to core unsubstituted PBI with maximas at 540 nm and 573 nm, respectively.

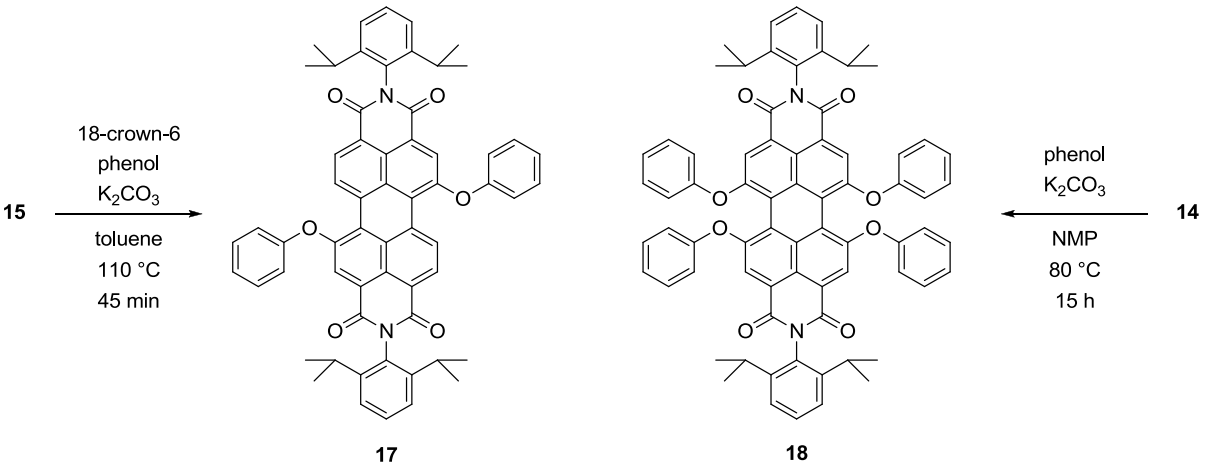

Scheme 6. Red shifted diphenoxylated and tetraphenoxylated PBIs.

Accordingly, the fluorescence from these dyes is shifted to higher wavelength, for PBI **17** and PBI **18** to 571 nm and 608 nm. Also the extremely high quantum yield of its core unsubstituted precursor is retained with FQYs of ϕ_{fl}=100 % and ϕ_{fl}=96 %, respectively.

However, it has been pointed out in literature that the bathochromic shift is mostly attributed to the electron donating ability from the ether oxygens rather than the extension of the π-system.[44] Therefore the orientation of the phenoxy groups relative to the perylene core has a major influence on the optical properties, as it leads to a different degree of conjugation from the oxygen molecular orbitals to the perylene core. This has been perfectly shown by the work from Osswald et al.[45] They synthesized different bridged macrocyclic tetraaryloxy-substituted PBIs (APBI) where the conformation of the phenoxy groups was restricted by using different lengths of oligoethyleneglycol chains (Figure 8). While the lateral bridged APBIs **20** showed mainly the same optical behavior as the non bridged reference **19,** severe differences of the optical behavior were observed in the diagonally bridged APBIs **21** in terms of a strong hypsochromic shift of the optical transitions.

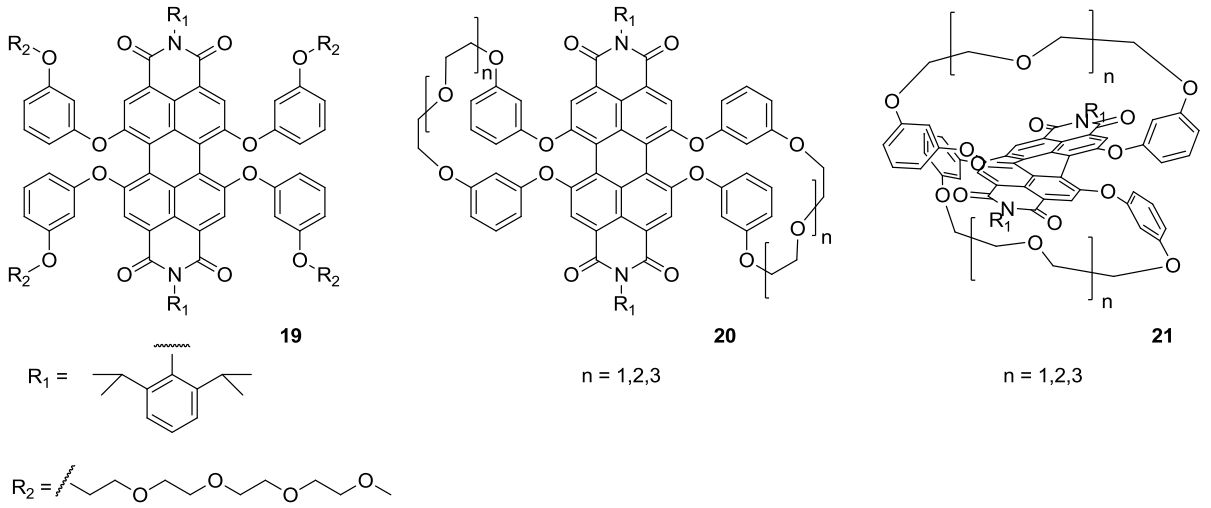

FIgure 8. Macrocyclic bridged tetraaryloxylated PBIs as conformation restricted probe molecules.

In addition, the same systems demonstrated that the actual fluorescence quantum yield of APBIs is mainly influenced by the electron donating ability (oxidation potential) from the phenoxy substituents due to a competitive charge transfer processes from the electron rich phenoxy groups to the electron poor perylene core rather than the conformation. [46]

Besides phenoxylation many other electron donating or withdrawing substituents can also be introduced to the PBI-core at the bay positions (Scheme 7). For example, cyclic amines like pyrrolidine can be easily introduced by stirring of dibrominated PBIs at moderate temperatures resulting in diaminated PBI **27**.[47] Through the strong electron donating ability of the amine groups the main absorbance as well as the fluorescence are drastically red shifted by ~150 nm to extremely high wavelength of 709 nm and 748 nm respectively.[48] In contrast to the core unsubstituted PBIs the optical transition of these bay amine substituted dyes gets a strong quadrupolar charge transfer character resulting in a moderate solvatochromic effect.[47,48] Substitution with electron acceptors

like fluorine and cyanine, on the other hand, leads to the corresponding PBIs **25**[49] and **26.**[50] In contrast to phenoxylated or pyrrolinated PBIs, the perylene core remains flat and untwisted and only small shifts in absorption and fluorescence are observed.

Transition metal catalyzed carbon-carbon couplings like Sonogashira or Suzuki couplings can also be easily performed with halogenated PBIs yielding alkynelated and arylated PBIs **28**[51] and **24**.[52] These dyes mainly serve as intermediates for the synthesis of a new class of core extended PBIs – the homologues series of coronene tetracarboxibisimides (CDIs).[53] Although the aromatic core of these new dyes is enlarged, the smallest CDI **29** shows a hyspochromically shifted main absorption at 428 nm and fluorescence at 517 nm. Semi-empirical calculations showed that this shift results from a decrease in the HOMO energy level and an increase in the LUMO energy level in contrast to core unsubstituted PBIs leading to a larger HOMO-LUMO band gap. However, upon increasing the core extension, the absorption becomes red shifted again to 494 nm for dibenzo-CDI **22** and 573 nm for dinaphto-CDI **23**. The latter one does not show the typical vibronic progression for PBIs anymore. Instead it resembles a more anthracence like structure. In all cases, a moderate to strong fluorescence is observed with QYs ranging from ϕ_{fl} = 42-80 %.

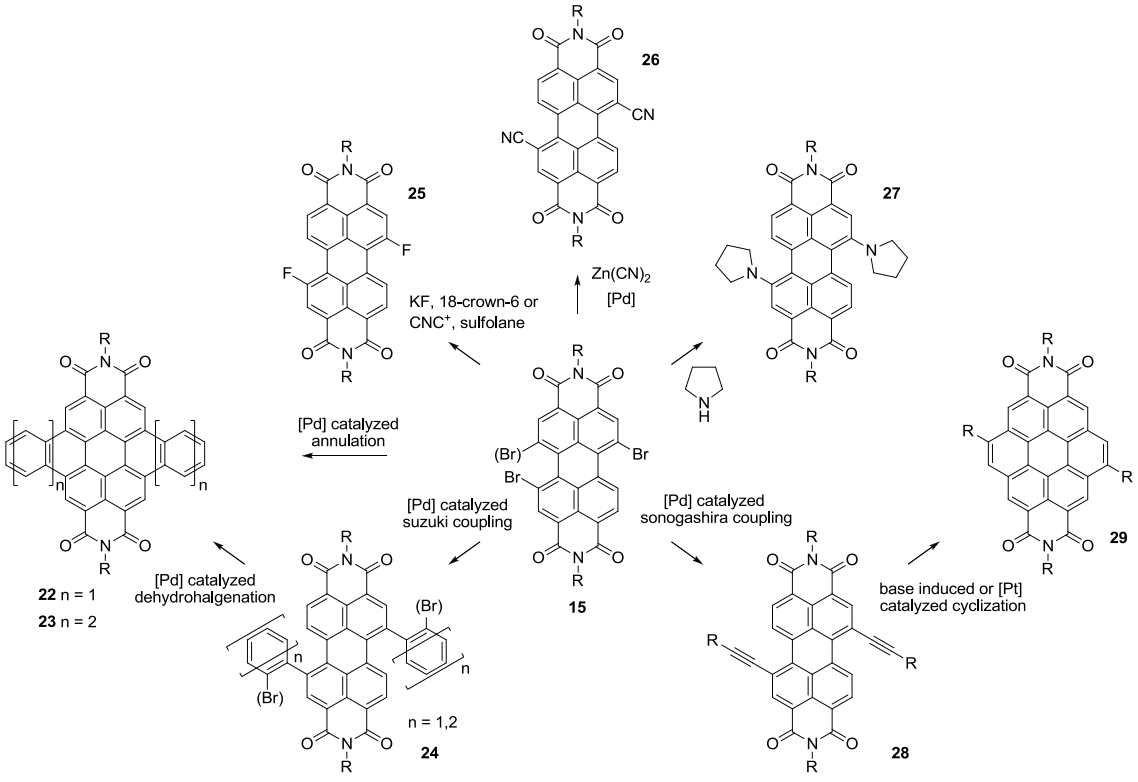

Scheme 7. Synthetic routes towards various bay substituted PBIs.

Another way to core enlarged PBIs proceeds via Diels-Alder reaction from a core unsubstituted PBI with maleic anhydride under drastic conditions (Scheme 8) yielding PBI **30**[54] possessing an anhydride

functionality at the bay region which can be further transformed with primary amines or *peri*-diaminonaphtalenes yielding trisimides **31** or **32**. Likewise as for CDIs, the absorption is shifted hypsochromically to 465 nm and 464 nm, respectively. While the fluorescence is still present in **31** with a QY of ϕ_{fl} = 45 %, it is completely quenched for **32**. All these examples clearly demontrate that a core enlargement along the short molecular axis of PBIs leads to hypsochromically shifted rylene dyes.

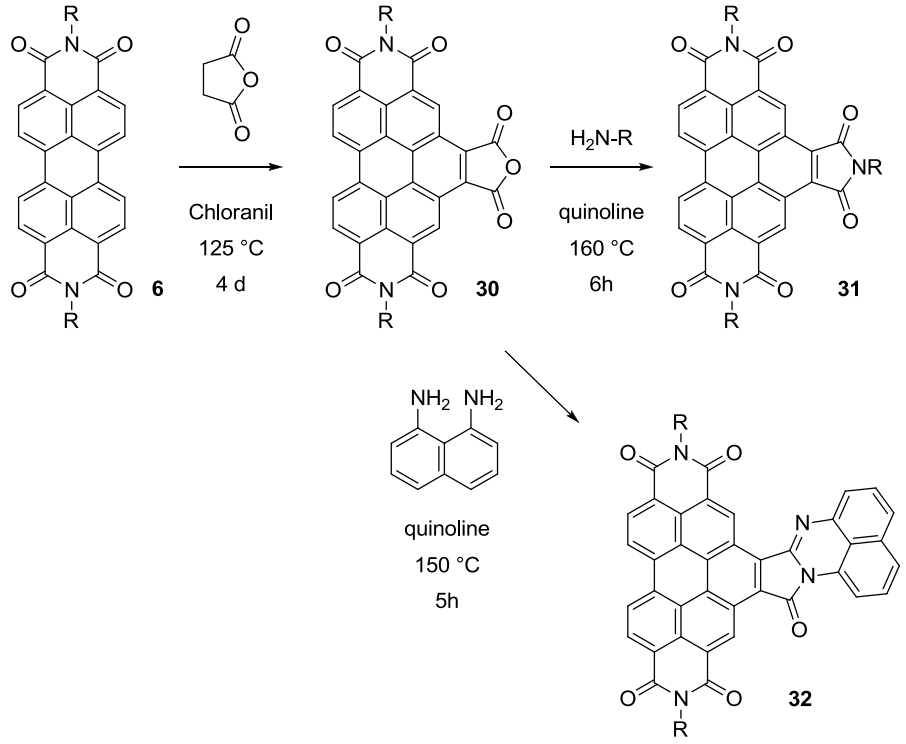

Scheme 8. Synthesis of core enlarged PBIs via Diels-Alder reaction.

This hypsochromic shift is also observed in heterocyclic enlarged PBIs containing sulfur bridges at the bay region like PBI **33**[54] and **34** (Scheme 9).[55] Both dyes still possess their fine vibronic absorption pattern with maxima at 501 nm and 480 nm respectively and mirror image shaped fluorescence at 511 nm and 488 nm with QYs of ϕ_{fl} = 71 % and ϕ_{fl} = 15 %.

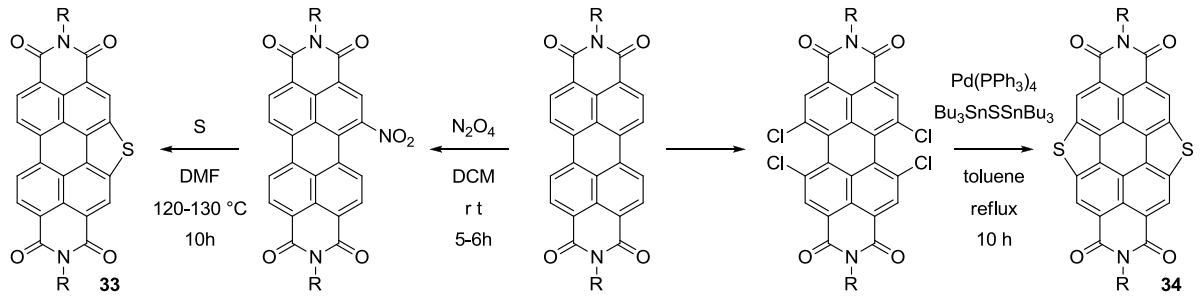

Scheme 9. Synthesis routes towards heterocyclic core enlarged PBIs.

An exception of the hypsochromic shift of lateral core extended PBIs is observed when increasing the core by two bridged donor substituents in a six-membered ring as in PBI **35**[54] and **36**[56] (Scheme 10). This leads to a strong bathochromic shift of the optical transitions due to the alpha-donor effect of this arrangement. Therefore the one side bay-substituted PBI **35** has its absorbance shifted by approx. 130 nm to 650 nm and for the double substituted PBI **36** an extreme shift of about approx. 260 nm to 778 nm is observed. Both dyes possess fluorescent properties with the maxima of fluorescence at 775 nm and 837 nm, but with no quantum yields reported. It is interesting that although these properties make these dyes interesting fluorophores in various application fields, no other reports about alpha donor substituted PBIs can be found.

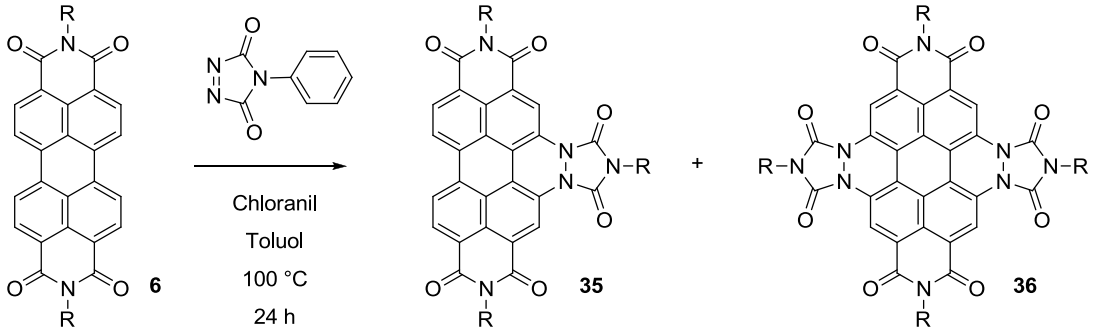

Scheme 10. Core enlarged PBIs with alpha-effect donor groups.

1.3.2.4 Perylenemonoimides

Similar to core halogenated PBIs the related halogenated 3,4-perylenemonoimides (PMI) constitute key intermediates in rylene dye synthesis. They are readily available in large scale via a two-step process (Scheme 11). In a first step the imidization of PBA with under stoichiometric amounts of sterically demanding amines under high temperatures and pressure yields core unsubstituted PMIs **37**.[57] Afterwards a selective bromination either yielding monobrominated PMI **38** or trisbrominated PMI **39** is possible by adjusting the solvent and reaction temperature.[58] Due to the loss of one electron withdrawing imide functionality the absorbance of core unsubstituted PMIs is slightly shifted towards shorter wavelength; in the case of core unsubstiuted PMI **37** to approx. 510 nm. Likewise as PBIs they are highly fluorescent showing extremely high FQY of ϕ_{fl} = 90 %.[59]

In principle, similar reactions as for halogenated PBIs e.g. phenoxylation,[60] substitution with various amines,[61] and metal catalyzed carbon-carbon couplings[62] are possible and lead to a diversity of PMIs. In contrast to PBI chemistry, trisbrominated PMIs offer the easy possibility to functionalize the same core with different substituents, as the bromine at the peri position possesses different reactivity than the bay bromines. By using this principle, push-pull PMIs **40**-**44** covering most of the visible wavelength region up to the NIR could be synthesized.[63] Due to this versatility this dye class

has found nearly as many applications as PBIs. In addition they constitute the key building blocks in the synthesis of higher rylene homologs as will be shown in the next chapter.

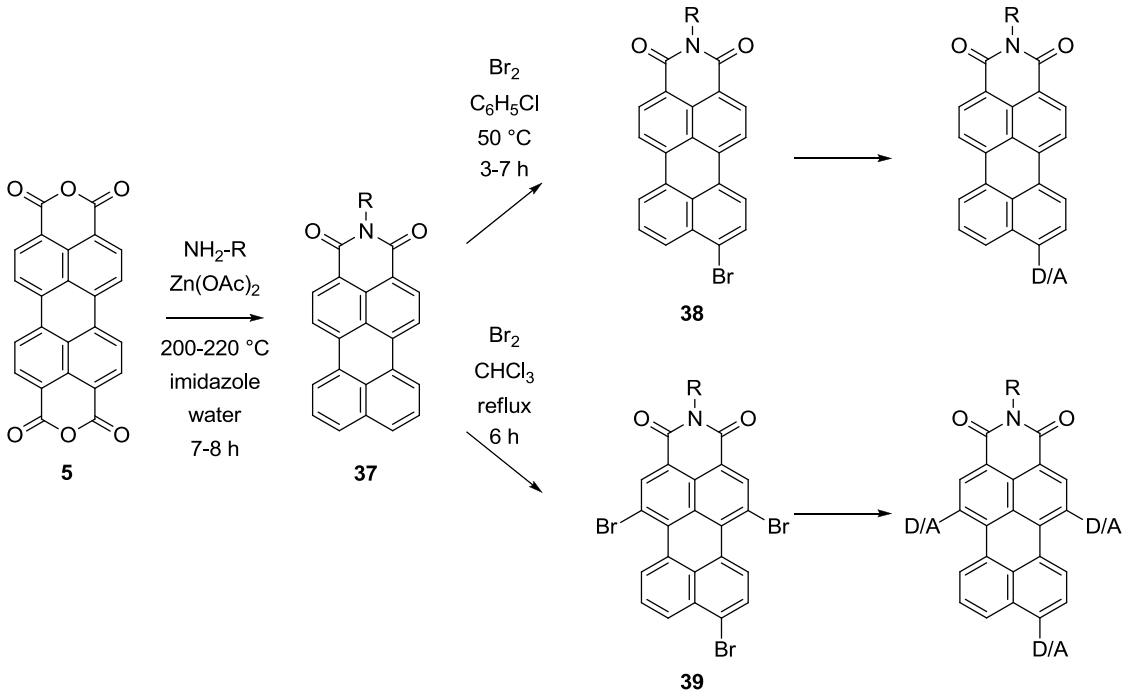

Scheme 11. Synthetic pathways to halogenated PMIs.

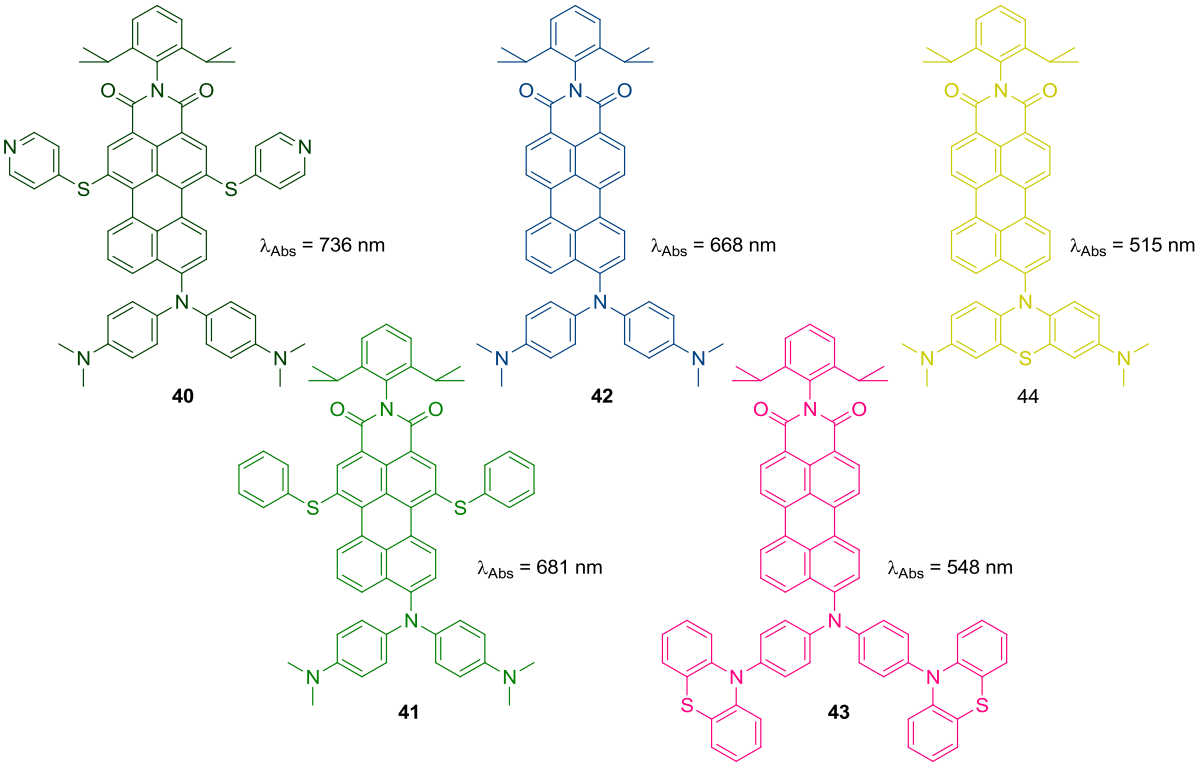

Figure 9. Push-pull PMIs covering the visible to NIR wavelength region.

1.3.2.5 Higher rylene bisimide homologs

Besides core extension along the short molecular axis, the extension of the π-system by adding additional naphthalene units along the long molecular axis leads to the higher rylene homologs terrylene-(TBI), quaterrylene-(QBI), pentarylene- (PtBI), and hexarylene bisimides (HBI). The synthetic access towards these core elongated rylene dyes was mainly encouraged by improvements in the synthesis of QBI **48**. Therefore different routes (Scheme 12) have been developed. First attempts using an analogous route as for PBIs, by merging two perylenemonoimides under high temperatures and strong basic conditions in a nickel vessel, showed only poor yields of 4% and were not applicable for large scale synthesis (Route I).[64] Although this route was improved later on, by using a one pot protocol with copper bronze and high concentrations of perylenemonoimideanhydride **46** as starting material (Route II),[65] another route which was developed at the same time in the group of Prof. Müllen (Route III) using transition metal mediated aryl-aryl coupling, proved to be much more reliable.[66] Starting with monobrominated perylenemonoimid a homocoupling under Yamamoto conditions[67] using Bis(1,5-cyclooctadien)nickel [Ni(cod)$_2$] as coupling reagent yielded bisperylene **47**. The resulting bisperylene was further cyclized under strong basic conditions using molten KOH and glucose as oxidation agent at high temperatures.

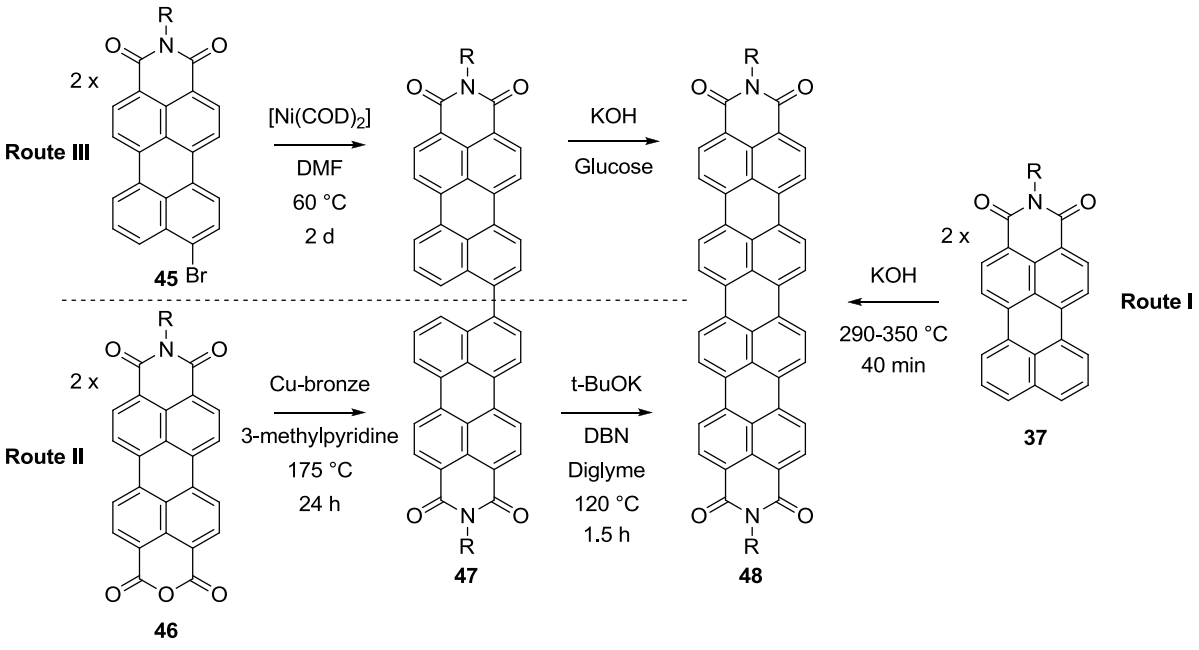

Scheme 12. Synthetic routes towards QBIs**.**

The main drawback of this route was the use of the highly toxic Nickel-COD complexes and the distinct side reactions like debromination which decreased the yield significantly. Therefore alternative routes were developed using stannylated or borylated PMIs **49** and **50** as key building

blocks in the aryl-aryl coupling.[68,69] Besides the reduction in toxicity (at least for the borylated PMIs) these pathways also opened the easy access towards unsymmetrical substituted QBIs in high yields. In addition these building blocks were also successfully applied in the synthesis of the smaller homologes TBI **52** (Scheme 13), which were not accessible via the nickel promoted route as this only led to the corresponding homocoupled bisperylenes. Therefore, PMI **49** or **50** were simply coupled with brominated napthalenemonoimides (NMIs) to yield NMI-PMIs **51**. A subsequent cyclodehydrogenation under strong basic conditions gave the final TBIs **52** in high yields.[70,71]

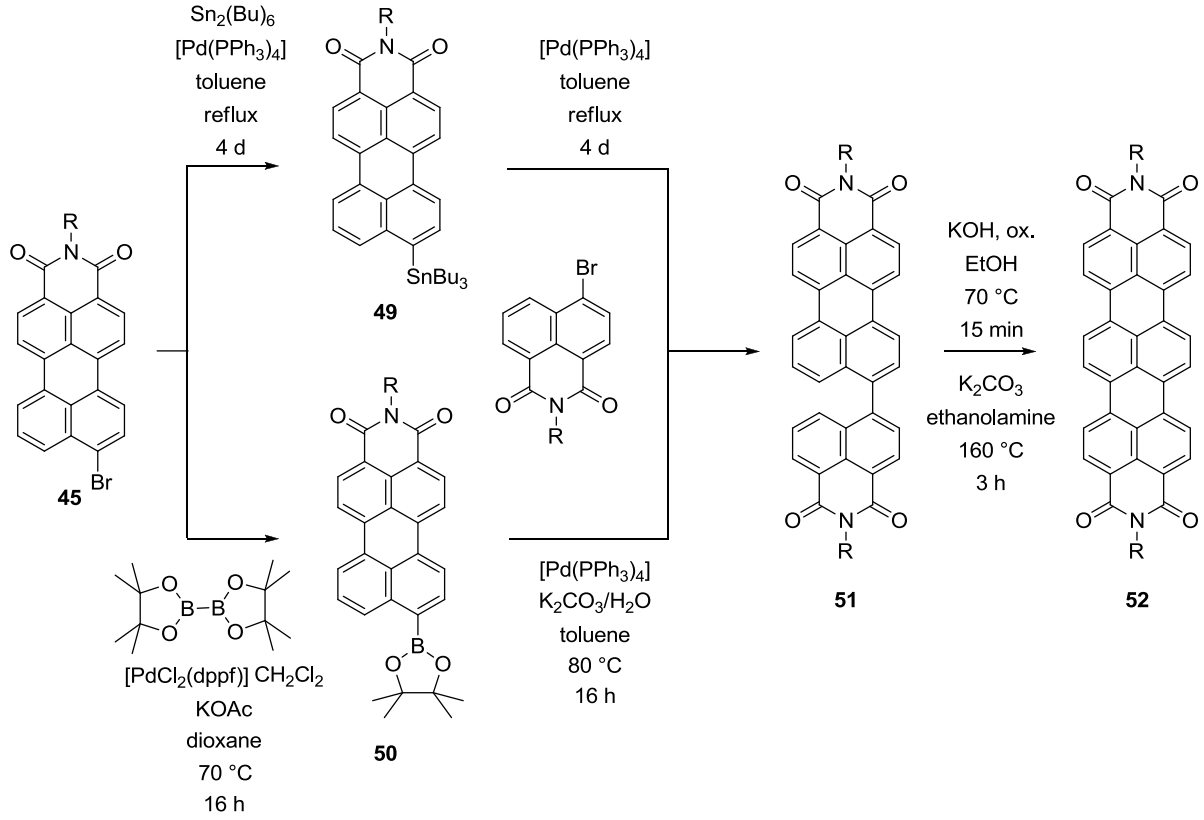

Scheme 13. Synthetic routes towards TBIs.

The Suzuki-type reaction protocol has also been applied to synthesize the next higher homologs PtBI **59** and HBI **60** using bisbrominated naphthalene **53** or perylene **54** building blocks as core elements (Scheme 14). After the carbon-carbon bond formation between the core and the outer PMIs a stepwise oxidation using first ironchloride and nitromethane and subsequently potassium carbonate in ethanolamine yielded the fully conjugated systems.[72] Due to the decreasing solubility with increasing the π-system, the use of bay phenoxylated PMIs as starting materials provided better yields than with core unsubstituted PMIs.

In contrast to the lateral core-enlarged rylene bisimides, the extension along the long molecular axis leads to a stepwise decrease in the HOMO-LUMO gap and therefore to a bathochromic shift about

~100 nm per naphthalene unit added (650 nm for TBI[70], 764 nm for QBI[68] and 831 nm for PtBI[72]). Thus the resulting dyes appear blue (TBI), turquoise (QBI), and colorless (PtBI). Likewise, as their smallest homolog PBI, all core enlarged rylenebisimides retain their unique combination of high photo-, chemical, and thermal stability.[66-72] In contrast, the fluorescence properties of higher rylene bisimides are drastically altered upon increasing the aromatic core size. While core unsubstituted TBIs still show an extremely high FQY of ϕ_{fl} = 90 %,[70] the yield drops down to ϕ_{fl} = ~5% for core unsubstituted QBIs[68] and no fluorescence has been reported so far for PtBIs and HBIs.

Similar to their smallest homolog PBI, substitution at the bay region of these scaffolds is possible. For example, tetraphenoxylation at the bay region increases the solubility and shifts the main absorbance bathochromically to 675 nm for TBI,[70,71] 781 nm for QBI,[66] 877nm for PtBI,[72] and 953 nm for HBI.[72] The introduction of these groups can either be achieved by using already phenoxylated PMIs as starting materials (as in the case for PtBI and HBI) or by a stepwise halogenation and subsequent substitution as in the case for TBI and QBI (Scheme 15).

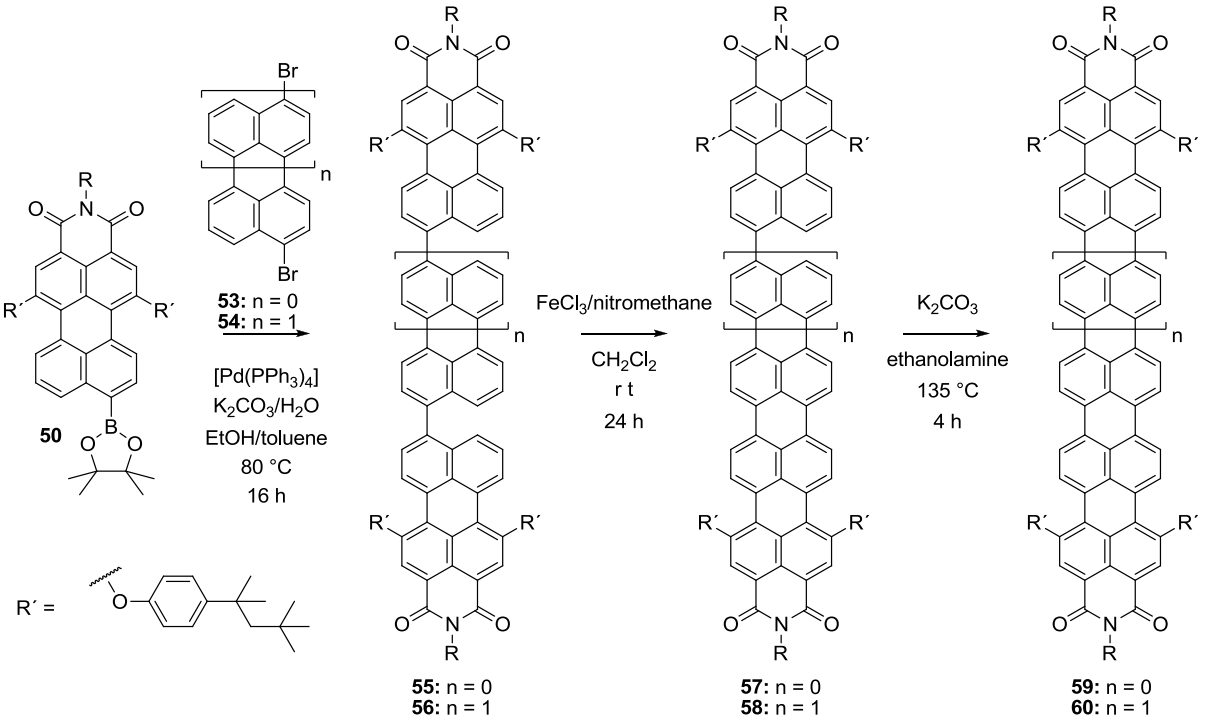

Scheme 14. Synthetic route towards highest rylene homologs pentarylene- and hexarylene bisimide.

Therefore in a first step the corresponding bisimide is halogenated with elemental bromine yielding either tetrabrominated TBI **61**[73] or hexabrominated QBI **64**.[74] A subsequent introduction of the phenoxy groups under basic conditions yields the tetraphenoxylated TBI **62**[70] and QBI **65**.[74] In the case of QBIs the inner bromines are not accessible to phenoxylation even under prolonged reaction time.[74] Besides phenoxylation the tetrabrominated TBI also undergoes nucleophilic substitution

with cyclic amines producing strongly bathochromically shifted TBI **63** with the absorption maximum shifted by approx. 170 nm to 819 nm. [70]

Besides bay functionalization a first example of using a ruthenium catalyzed ortho substitution has been recently reported (see Chapter 1.3.2.6). The resulting ortho-TBI show an increase in solubility without altering the photophysical properties.[75]

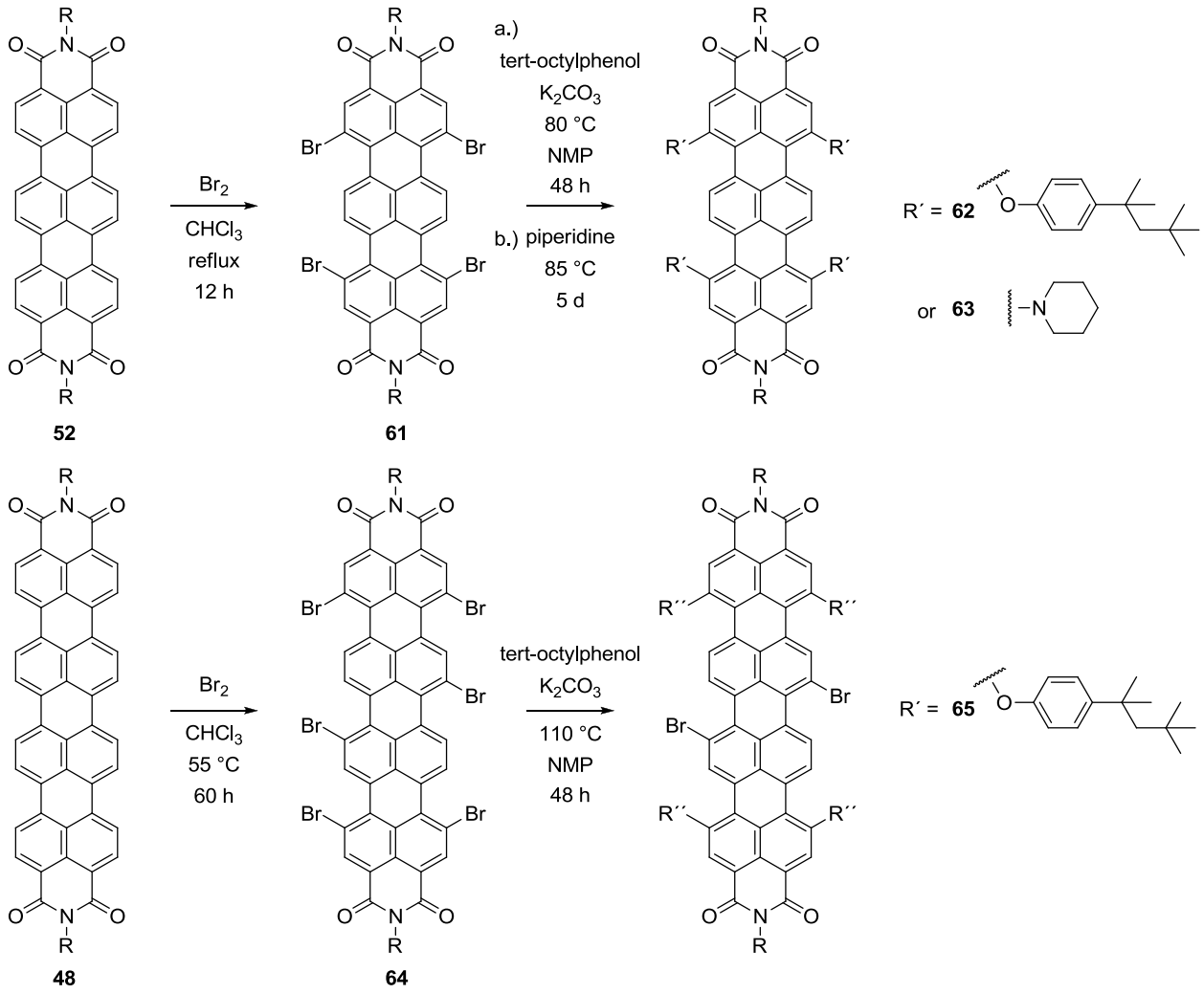

Scheme 15. Synthetic route towards core substituted TBIs and QBIs.

1.3.2.6 Ortho substituted PBIs

In addition to the classical functionalization at the bay or the peri positions of peryleneimides, which has been known since the early 1980s, more recently the synthetic access towards the ortho positions has been achieved. Therefore core unsubstituted PBIs were treated with a ruthenium catalyst under Murai–Chatani–Kakiuchi conditions[76] yielding ortho alkylated[77] and arylated[78] PBIs **66** and **67** via C-H activation and addition. The same reaction conditions were also applied onto core unsubstituted TBIs yielding the first ortho-TBIs.[75]

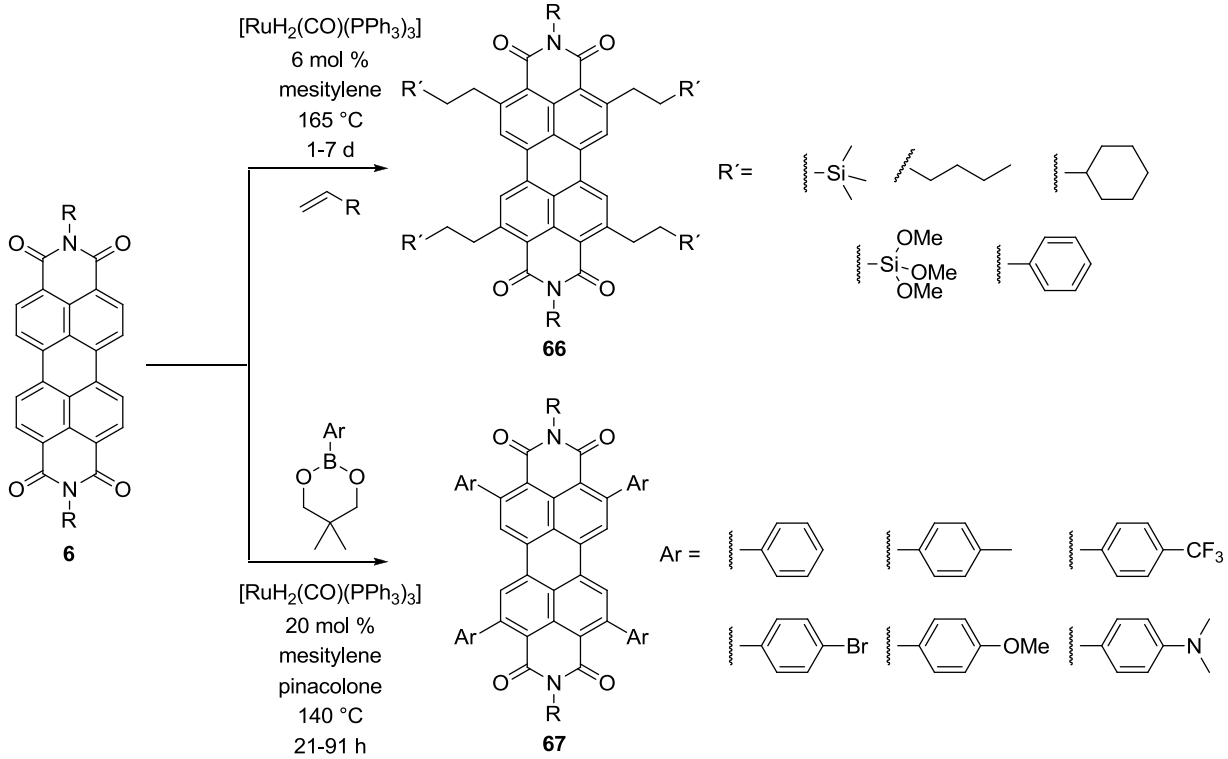

Scheme 16. First reported synthetic routes towards ortho-functionalized PBIs.

The optical characteristics in solution of aliphatic substituted ortho-PBIs are not influenced by the residues attached and resemble their unsubstituted counterparts with high FQY of up to ϕ_{fl} = 94 %. However in the solid state the optical properties change drastically. While the fluorescence of core unsubstituted PBIs is nearly completely quenched due to strong interchromophoric interactions and H-aggregate formation[79] (see Chapter 1.3.2), ortho-PBIs retain a high quantum yield of up to 59 % due to differences in the packing.[77] A slightly different behavior is observed for arylated ortho-PBIs. Due to the orthogonal arrangement of the aromatic substituents to the perylene core the absorption profile shows an unaltered fine vibronic structure from the perylenecore together with an absorption at lower wavelength from the added aromatic unit. Unlike aliphatic ortho-PBIs and similar to bay phenoxylated PBIs the fluorescence intensity is strongly correlated to the electron donating ability

from the aromatic unit. Consequently, the quantum yield varies from non fluorescent up to ϕ_{fl} = 15% for the electron rich aromatics while an electron poor CF_3-aryl substituted compound still possesses a high FQY of ϕ_{fl} = 75 %.

To bypass restrictions concerning the available substituents in the ruthenium catalyzed routes, e.g., strongly deactivated aromatics, the tetraborylated ortho-PBI **68** was synthesized shortly afterwards via the treatment of core unsubstituted PBIs with diboronpinacolester using either a new iridum catalyzed route[80] or the above mentioned ruthenium catalyzed route.[81]

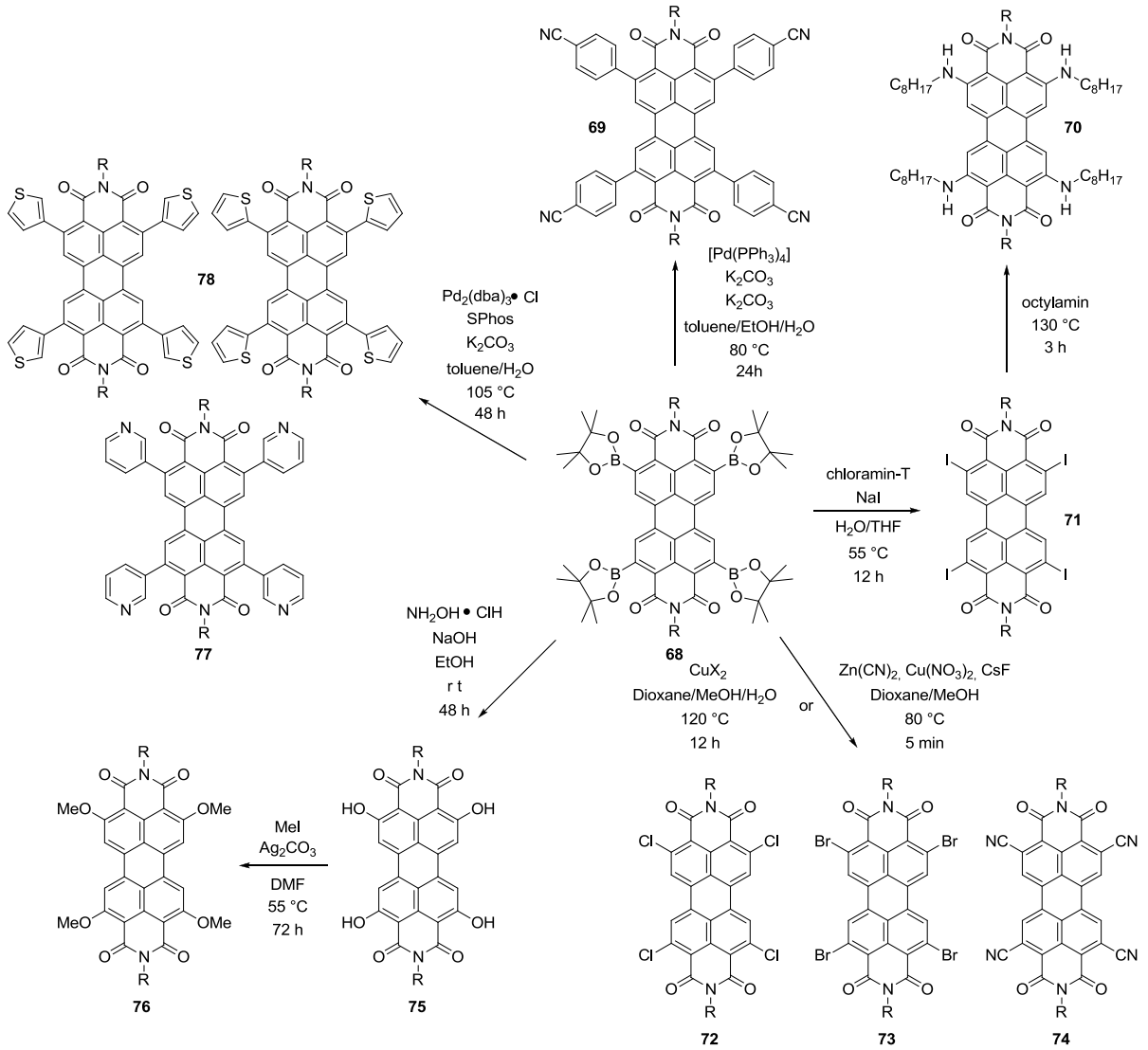

Scheme 17. Tetraborylated ortho-PBI as new building block in PBI synthesis.

Starting from this newly synthesized compound, a variety of ortho-PBIs (**69**-**78)** were prepared that were not accessible via the direct ruthenium catalyzed route. Hence, in analogy to the halogenated intermediates for bay substituted PBIs, the tetraborylated ortho-PBI represents the key building block in follow up functionalization at that position. However, in contrast to classical bay substituted

PBIs the wavelength region accessible by these ortho-PBIs remains rather low between 505 and 538 nm.

1.3.2.7 Perylenetetraesters and -diesters

Besides the imide functionalization another common substitution pattern of 3,4,9,10—perylenebisanhydrides are the corresponding perylenetetraesters (PTEs) **79**. Although the first preparation of these dye materials was reported in the 1980s[82] (Scheme 18), they did not attract as much attention in research during the last decades as their related PBIs. This might be due to the fact that they do not offer the easy possibility of introducing different functional groups onto the dye scaffold.

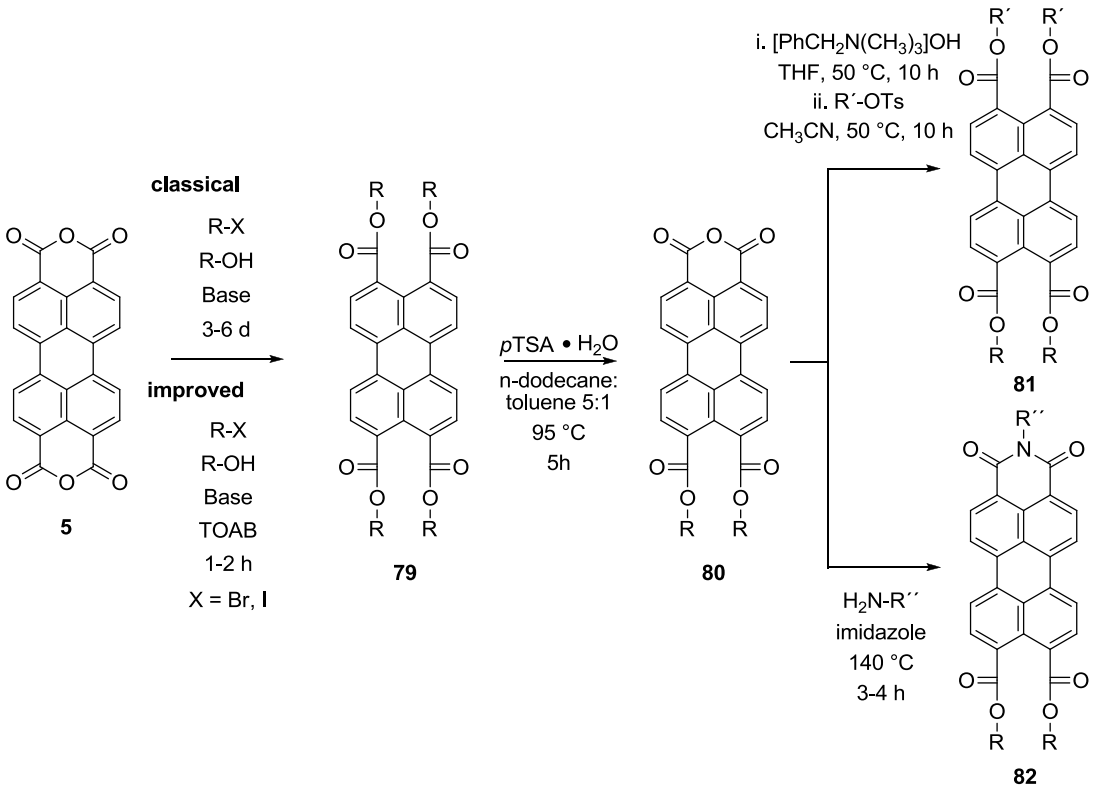

Scheme 18. Synthetic routes towards PTEs and PIDEs.

The classical synthesis of PTEs involves long reaction times (3-6 d), high temperatures, and strong basic conditions.[83] A major improvement of this method has been made by applying phase transfer agents to the reaction mixture which significantly decreases the reaction times to 1-2 h.[84] However, this simple one-pot reaction approach only gave access to symmetrically substituted PTEs. The access towards unsymmetrical substituted PTEs has been reported quite recently.[85] It involves a two-step reaction protocol, where a symmetrical PTE is prepared in the first step and in the second step two ester groups on the same side of the perylene core are cleaved under acidic conditions. These

reaction conditions should in consequence lead to the formation of the corresponding starting material PBA. But, by properly adjusting the reaction time and solvent mixture, the intermediate formed perylenemonoanhydridediester (PMAD) **80** precipitates and can be obtained in relatively high yields. A subsequent treatment of the PMAD under PTC conditions yielded the first asymmetric PTE **81**. In addition the reaction of PMAD **80** with aliphatic amines opened the synthetic pathway to a new subclass of the rylene dye family – the perylenimidodiesters **82** (PIDEs).

The spectral properties of PTEs and PIDEs are very similar to PBIs. Both dye classes show characteristically fine vibronic absorption patterns with the maxima hypsochromically shifted to ~472 nm for PTEs[86] and to ~505 nm for PIDEs[87] due to the less strong electron withdrawing capacity of the ester groups. Both dye classes are also highly fluorescent with fluorescence maxima at 492 nm for PTEs and 525 nm for PIDEs and reported FQY of up ϕ_{fl} = 99 %[88] and ϕ_{fl} = 96 %[89] respectively. Although these properties make these dyes interesting fluorophores, their main application has been in the solid state due the fact that they easily form liquid crystalline phases.[90]

1.3.2 Water-soluble rylenedyes

The importance of fluorescent dyes in science today is steadily increasing. Especially in the fields of medical, pharmaceutical and biochemical research they have become virtually indispensable. Hereby their main function lies in the specific staining of certain biomolecules, regions, and areals within a biological system to allow a deeper insight into its working principles.[91] For example proteins can be easily tagged with conjugatable fluorescent markers and therefore allowed to track their ways and functions within biological processes on a cellular level.[92] The requirements to fluorescent dyes are quite versatile. Although the importance of the following points can vary upon their concrete application, there are properties which are favorable for most applications:

- High brightness (product of extinction coefficient and fluorescence quantum yield)
- High photochemical & chemical stability
- No or only low cytotoxicity
- Fluorescence emission above ~500 nm to decrease auto fluorescence from cells.
- Water solubility

The detection method of choice for a magnitude of the current fluorescent based investigations is the usage of a fluorescence microscope. In the last few years more advanced methods than simple wide field microscopy, so-called super-resolution methods,[93] like, e.g., stimulated emission depletion (STED),[94] stochastical optical reconstruction microscopy (STORM),[95] and photoactivated localization microscopy (PALM)[96] and others,[97] have been developed, that allow a spatial resolution

far below the diffraction limit of light. As the requirements of those methods to the used fluorophore are very harsh, especially in terms of photostability for ensemble based methods like STED, and the number of emitted photons for single molecule based methods like STORM or PALM, the amount of small organic dyes that can be used is rather limited. In this context the high photostability of rylene dyes makes them superior to many other already existing fluorophores like fluorescein or rhodamin based dyes.[98,128]

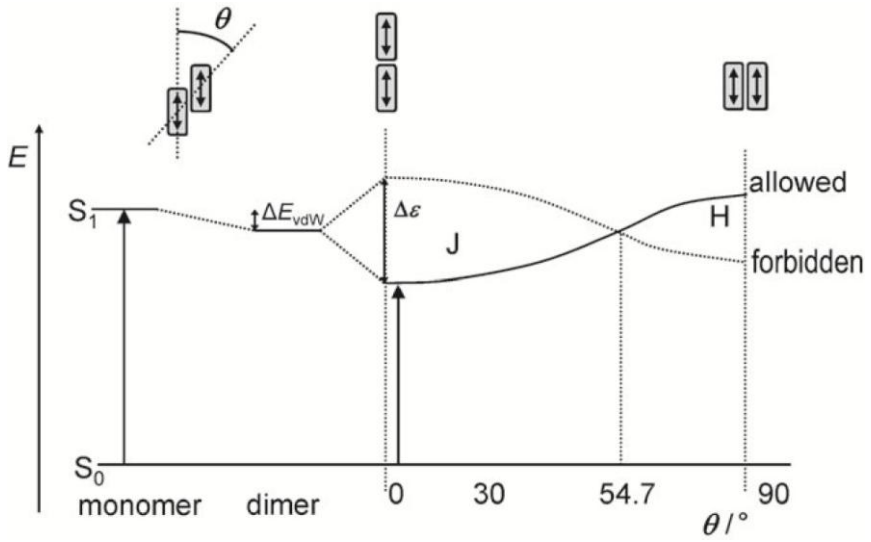

Figure 10. Schematic energy diagram for aggregated dimers taken from ref. [105].

One major drawback of highly extended π-systems is their tendency to form aggregates which in most cases leads to a drastic change of the optical properties.[98] The molecular exciton theory therefore differentiates between two main types of dye aggregates: H-aggregates and J-aggregates. The name, J-aggregate, derives from the name of one of its discoverers, E. E. **J**elley in 1936.[100] Alternatively these aggregates are also called Scheibe-aggregates due to G. Scheibe who independently discovered the same phenomenon one year later in 1937.[101] J-aggregates are characterized by a bathochromic shift of the absorption in comparision to its monomeric unit. Most of them are fluorescent and the QY of the aggregate-fluorescence can be as high as the monomeric one.[102] In contrast to that, H-aggregates are characterized by a **h**ypsochomic shift of the absorbance and are mostly low or non-fluorescent.[103] This is rationalized by different special arrangements of the dye molecules, and therefore to different interactions of their transition dipole moments. In both cases, the interaction between at least two dye molecules leads to two different states (Davydov-splitting): one of higher and one of lower energy.[104] Depending on the angle θ between the transition dipole moments not every transition into these aggregate states is allowed. In J-aggregates the individual chromophores are oriented in a collinear (θ < 54.7°) fashion. Therefore only the transition into the lower lying state is possible, which leads to the bathochromic shift. In H-

aggregates the transition dipole moments are parallel (θ > 54,7°) and consequently only the transition into the higher lying state is allowed.

The majority of rylene dyes aggregate in an H-type manner leading to a strong decrease in FQY. For example, the fluorescence QY of organic soluble PBI **83** decreases from 96% to 6% upon aggregation in ethanol by increasing the concentration from 10^{-5} M to 10^{-3} M.[106] This aggregation tendency is solvent dependent and is most pronounced in an aqueous environment due to the addition of hydrophobic effects.[107] These circumstances were may have hampered the application of rylene dyes as fluorescent dye material in an aqueous environment for such a long time. Nevertheless, there has been a strong interest in producing water-soluble rylene dyes, as will be shown in the following chapters.

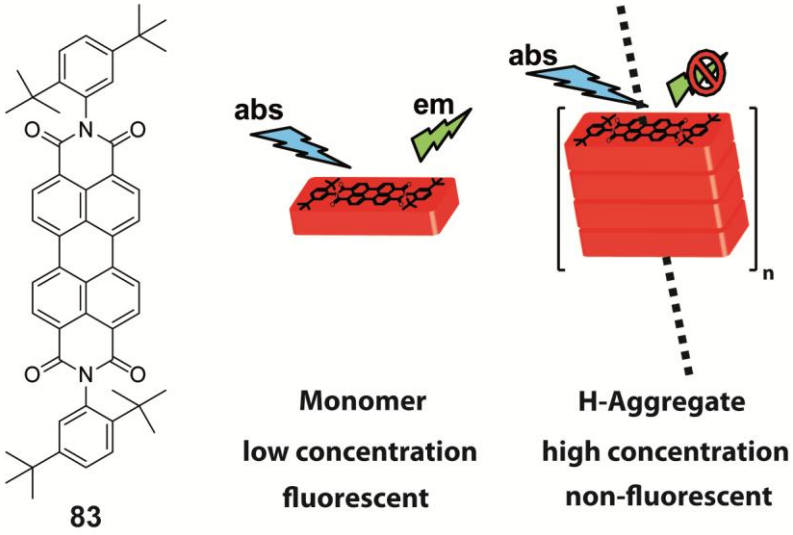

Figure 11. Schematic illustration of PBI aggregation into non-fluorescent H-aggregates.

1.3.2.1 Perylene based Dyes

Already in the 1980s and early 1990s the substitution with ionic groups at the imide position led to water-soluble PBIs **84,**[108] **85,**[109] and **86**.[110] Later on neutral substituents like crown ether in PBI **87,**[111] and polyethylenegylcol chains like in PBI **88,**[112] and **89**[113] have also been used to induce water solubility (Figure 12). However in all of the reported cases the resulting compounds showed pronounced aggregate formation in the forms of micelles, rods and microcrystals and therefore strongly altered optical properties with reduced fluorescence FQY.

Besides introducing the water-solubilizing groups at the imide positions, other synthetic approaches involving the modification of the bay region were more successful. For example, in 2001, in the group of Prof. Müllen, the tetraphenoxylation of a PBI core with polypeptides gave the first water soluble core substituted PBIs **90** and **91** with a reported fluorescence in water.[114] Although no aggregation

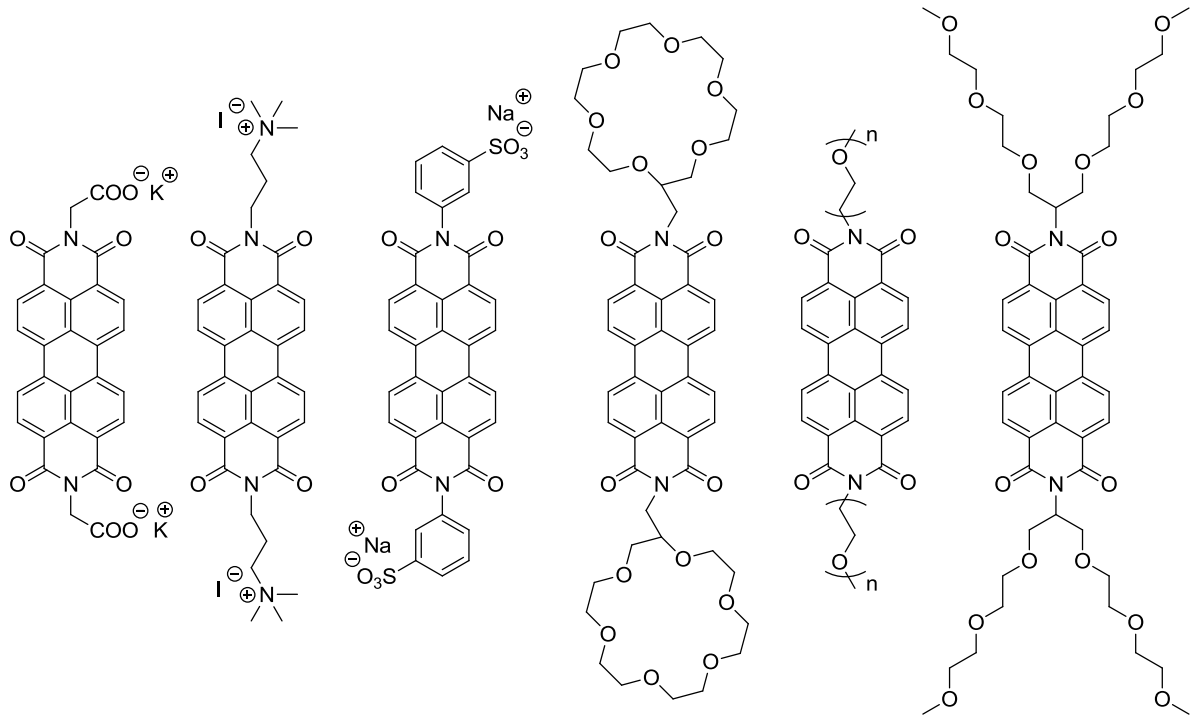

Figure 12. Chemical Structures of water soluble core unsubstituted PBIs.

behavior was observed for these compounds, the reported FQY of the resulting material was rather low with a FQY of ϕ_{fl} = 3 % for PBI **91**.[115] Other tetraphenoxylated perylene derivatives bearing polymeric solubilizing groups like PBI **92**, which consist of an inner shell of sterically demanding polyphenylene dendrons of different generations to prevent aggregation and an outer shell of a polymeric amine as water-solubilizing groups, also showed strongly reduced QYs between ϕ_{fl} = 11 % to ϕ_{fl} = 17 %, depending on the dendron generation and the size of the outer amine polymer shell.[116] In both cases, no explanation for this strong reduced FQY has been stated. But when looking at the structures it seems plausible to assume that it mainly arises from an increase in flexibility and therefore non radiative deactivation pathways.[117]

Although these examples showed that tetraphenoxylation can be an efficient method to introduce water-solubilizing groups to PBI cores, the resulting polymers possessed high molecular weights of up to 200 kg/mol. This made them unfavorable for specific applications such as fluorescent label for bioimaging, where small organic dyes are better due to reduced interference with the function and/or shape of the biomolecules.[118] In 2004 a great improvement in the synthesis of water-soluble PBIs was developed by using low molecular weight phenoxy derivatives which were transformed into ionic groups via subsequent sulfonation or quarternization (Figure 14).[119] The resulting PBIs **94**-**96** were highly water-soluble and moderate to high quantum yields in an aqueous environment with FQY of ϕ_{fl} = 58 % for **94**, ϕ_{fl} = 66 % for **95** and ϕ_{fl} = 98 % for **96** were reported for the first time. These

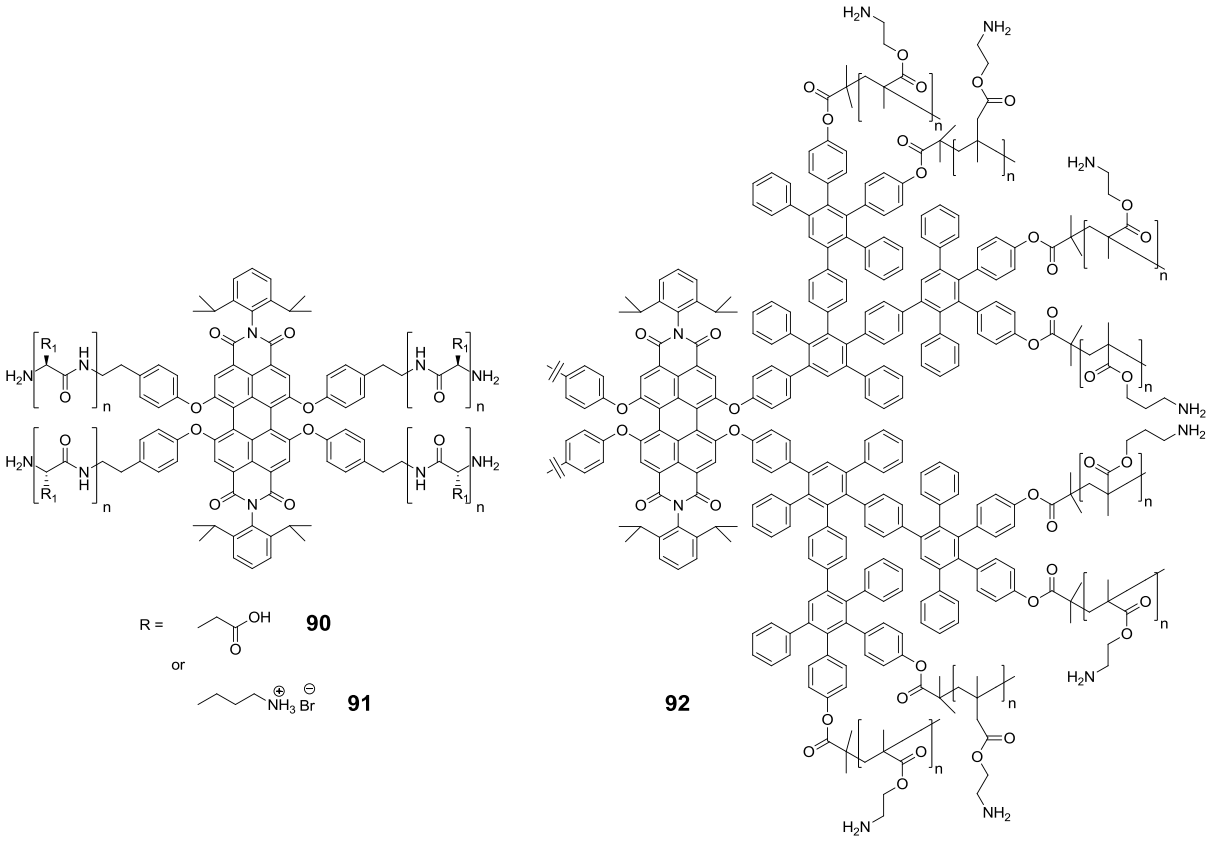

Figure 13. Water-soluble PBIs based on polymeric tetraphenoxylated perylene cores.

.

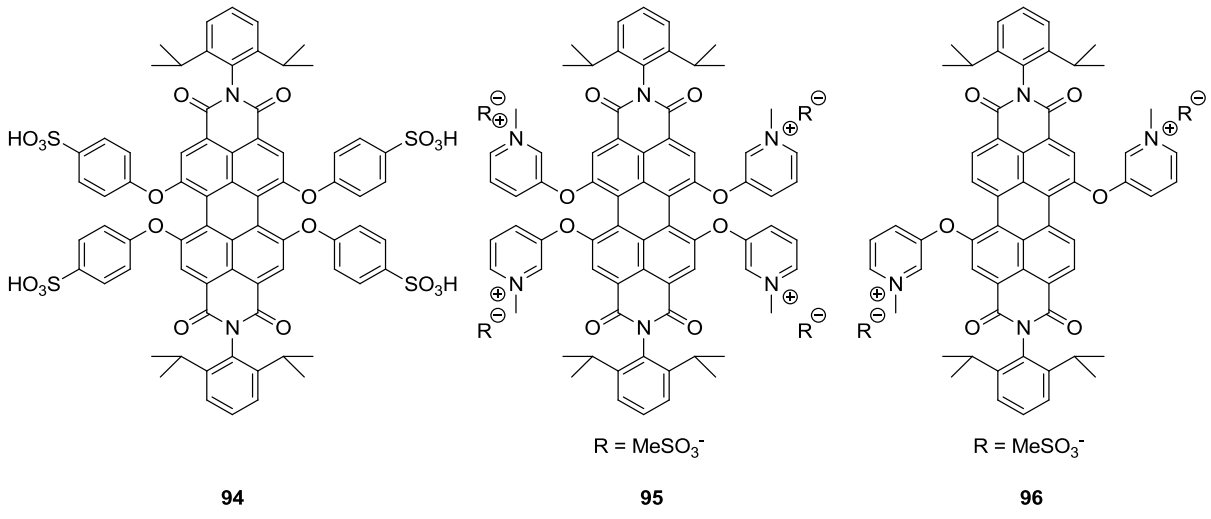

Figure 14. Water-soluble PBIs based on the introduction of small ionic groups to the bay region.

high FQYs were mainly attributed to the decreased π-stacking tendency due to the distortion of the PBI cores (see Chapter 1.3.2.3) in combination with the electrostatic repulsion forces caused by the ionic groups.

Follow up studies on PBI **94** and **95** by treating them with oppositely charged surfactants gave deeper insight into the photophysics of the materials and the authors stateed that the water-soluble PBIs are not molecularly dissolved but rather exist in an aggregated form (mostly dimers) with a geometry that induces only limited fluorescence quenching.[120] It is surprising to denote that although PBI **96** showed the highest reported QY of PBIs it has not been further used as fluorescent dye material in any of the following research. Sulfonated tetraphenoxylated PBI **94** has become instead the main scaffold for the development of functional water-soluble PBIs. For example unsymmetrical PBIs **97** and **98** (Figure 15) that possess a maleimide or a NHS-ester functionality for the active labeling of amine or thiol groups of biomolecules have been synthesized and used to label phospholipase (PLA1).[121] Due to their high photochemical stability this allowed real time single particle tracking of single enzymes on a phospholipid layer.

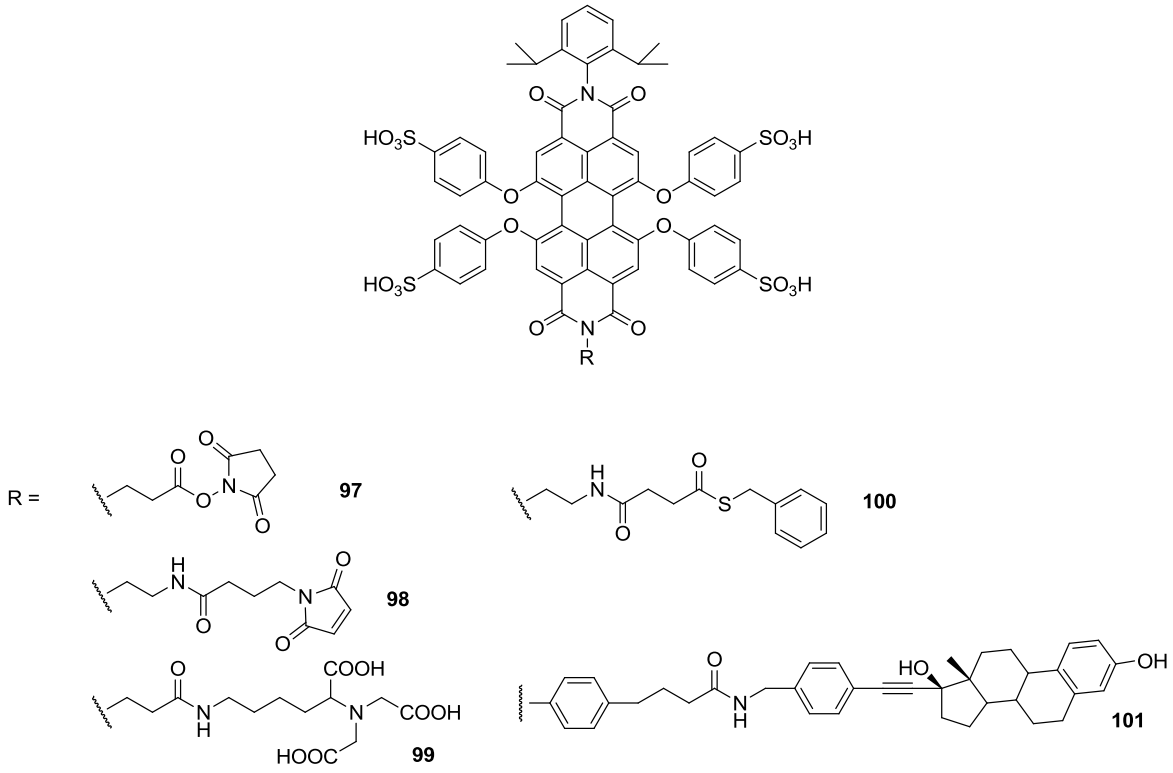

Figure 15. Functional water-soluble PBIs used for biolabeling and enzyme tracking.

Other functional PBIs which have been successfully applied contain a nitrilotriacetic acid (NTA) moiety[122] (PBI **99**, ϕ_{fl} = 15%), a thioester functionality[123] (PBI **100**, ϕ_{fl} = 54%) and a 17β-estradiol[124] (PBI **101**, ϕ_{fl} = 36%). These examples demonstrate that bay substitution with water-solubilizing groups is a very successful approach in perylene dye chemistry.

However, this structure design possesses one main disadvantage which is the blocking of the bay positions. As shown in Chapter 1.3.2 these are the positions where the optical properties of rylene

dyes are fine tuned. Therefore one reduces the spectrum of accessible wavelengths through this substitution pattern, which is one of the main advantages of perylene dyes. It would be of great benefit to find a substituent which introduces water solubility at the imide position but at the same time suppresses the aggregation tendency. Due to their unique properties, e.g., the easy control in size and shape, dendrimers, and dendrons (see Chapter 1.4) constitute an ideal substance class for this purpose.

In addition to the reports shown in chapter 3, other water-soluble PBIs using water-soluble dendrimers at the imide position as water-solubilizing groups e.g. Newkome- or PEG-Dendrons have been published in recent years. The reader is referred to the corresponding references [125] and [126] which are also discussed in the individual papers.

1.3.3.2 Higher rylene dyes

As the synthetic access to higher rylene dyes is not as old as for the corresponding perylene derivatives, the number of available water-soluble derivatives is limited. For many biological applications, however, especially in vivo studies, the red-shifted absorption and emission profiles are beneficial because tissue material is most transparen at longer wavelengths in the so-called optical window between 650 nm – 1450 nm that allows a detection of the fluorescent marker deeper in the tissue.[127] In principle, the methods for introducing water solubility to higher rylene dyes have been the same as for perylene based materials. Therefore it is not surprising that the first reported water-soluble terrylene- and quaterrylene bismides are based on polypeptides, which are introduced on the bay positions as can be seen in TBI **102** and QBI **103** (Figure 16).[128] In contrast to the corresponding water-soluble PBIs, however, no fluorescent properties were reported for these compounds. As no further studies have been conducted on these dye scaffolds, it remains unclear what is the main driving force for that fluorescence quenching.

As the tetraphenoxylation and subsequent transformation into ionic groups was rather successful in the case of PBIs, the same approach was also applied to TBIs yielding TBI **104**[129] and **105**.[130] Contrary to the water-soluble PBIs, only TBI **105** bearing four positively charged pyridoxy substitutents showed no aggregation in the aqueous phase while the typical optical properties of a H-aggregated species were observed for TBI **104**. This difference is also reflected by the fact that a fluorescence signal in water was only observed for TBI **105**. The quantum yield was rather poor though with a FQY of ϕ_{fl} = 1.6% in contrast to ϕ_{fl} = 90% for organic soluble TBIs.[70] Although no reason for this dra-

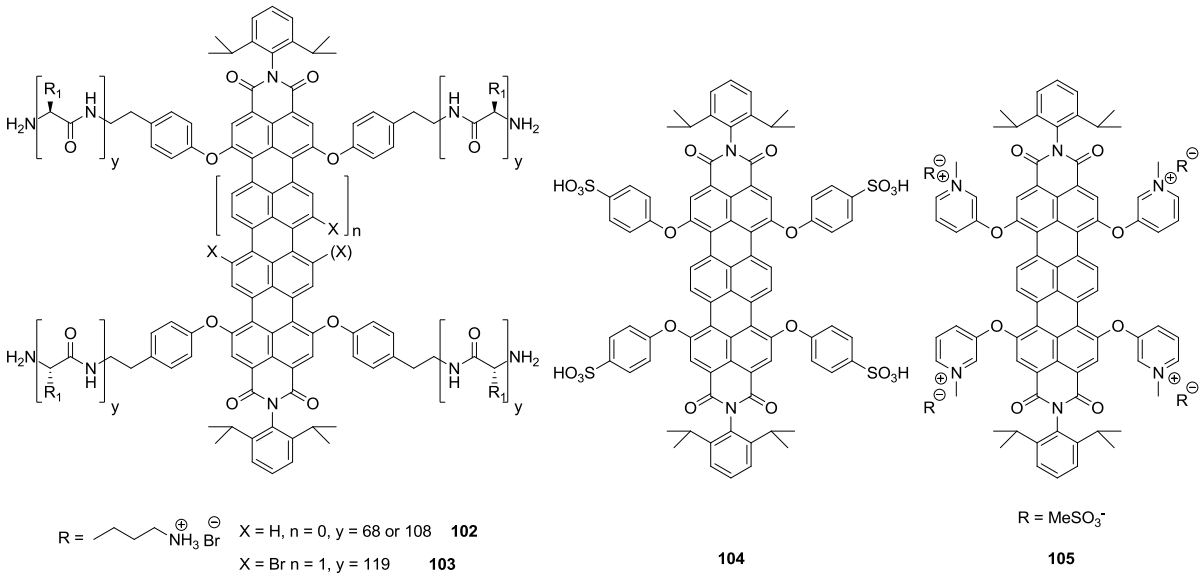

Figure 16. Structures of water-soluble higher rylene homologs TBI and QBI via bay substitution.

matic loss is given, it seems reasonable to assume that a photoinduced electron transfer process from the pyridoxy groups to the TBI core is responsible for this quenching, because an encapsulation of the dye into a micellar environment (Pluronic) increases the FQY to ϕ_{fl} = 3.9% and photoinduced processes are strongly dependent onto the polarity of the surrounding environment.[131]

Although it shows a strong tendency towards aggregation, based on the tetraphenoxylated sulfonated TBI **104**, monofunctional water-soluble TBIs like TBI **106**-**108** have been synthesized bearing NHS or maleimide functionalities for the labeling of amine or thiol groups of biomolecules or an aliphatic chain for lipid membrane affinity (Figure 17).[121,130] TBI **106** was successfully used in coupling experiments with short DNA strands and the photophysical properties of the resulting complexes were compared to a DNA strand labeled with ATTO647N, which is a common commercial

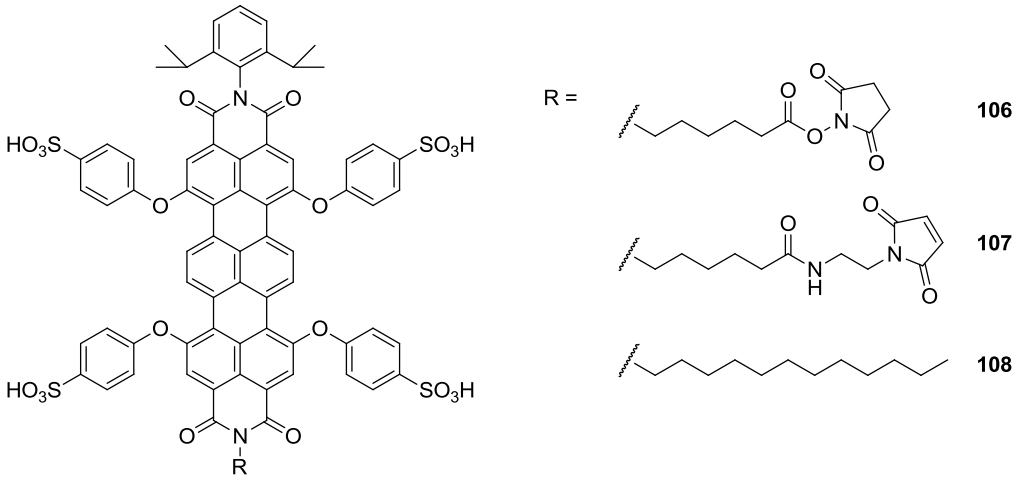

Figure 17. Functional water-soluble TBIs**.**

labeling dye with similar spectral characteristics. The TBI conjugate showed in this direct comparison a higher photon emitting rate with less blinking behavior, although the lifetime before photodegradation was nearly the same. This makes this dye superior in single molecule experiments.

In all of the above-mentioned TBIs, the water-solubilizing groups have been introduced via bay substitution. Thus the same disadvantages as mentioned for the water-soluble PBIs (Chapter 1.3.2.1) holds true for this compound class which facilitates alternative approaches that introduce the water-solubility via the imide positions. The first report about a water-soluble TBI **109**[132] bearing swallow tailed PEG chains at the imide positions was only quite recently published (Figure 18). However, it shows a strong H-aggregation behavior and is therefore non fluorescent in the aqueous phase.

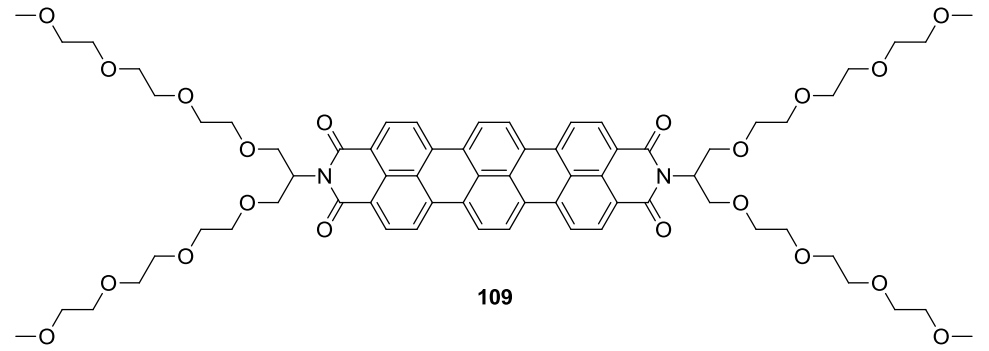

109

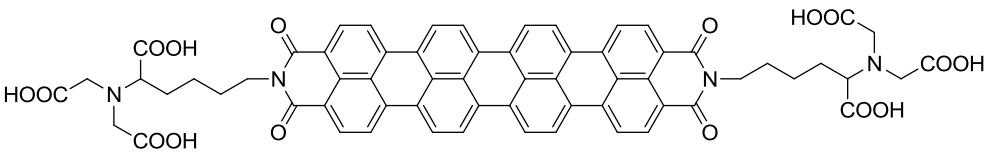

110

Figure 18. Examples of water-soluble higher rylene dyes with solubilizing groups at the imide postions.

Besides the polylysine substituted example QBI **103,** there are even fewer examples of other water-soluble QBIs, although the spectral characteristics of absorbing and emitting at wavelength > 750 nm make it an ideal fluorophore for bioimaging applications. In fact, to the best of the authors knowledge, only QBI **110** has a reported solubility in water. [133] It has been used as surfactant molecule in the selective solubilization of single-walled carbon nanotubes (SCWNT) according to their helicity. However, no details about the spectral characteristics or the aggregation state have been reported.

1.4 Dendrimers and dendrons

The first dendritic molecules were synthesized in 1978[134] by Vögtle et al., although at that time they were named cascade molecules, as he compared them to a big waterfall which divides up into different smaller waterfalls.[135] The synthetic approach towards these first molecules relied on a sequential Michael- addition and a subsequent reduction process. In the concrete example a twofold Michael-addition of a primary mono-amine with acrylnitrile led to the bisnitrile **111**. A following hydrogenation of the nitrile groups with sodiumborohydride resulted in the diamine **112**. Through repetition of these simple reaction steps a structural well defined and highly branched molecule was obtained for the first time.

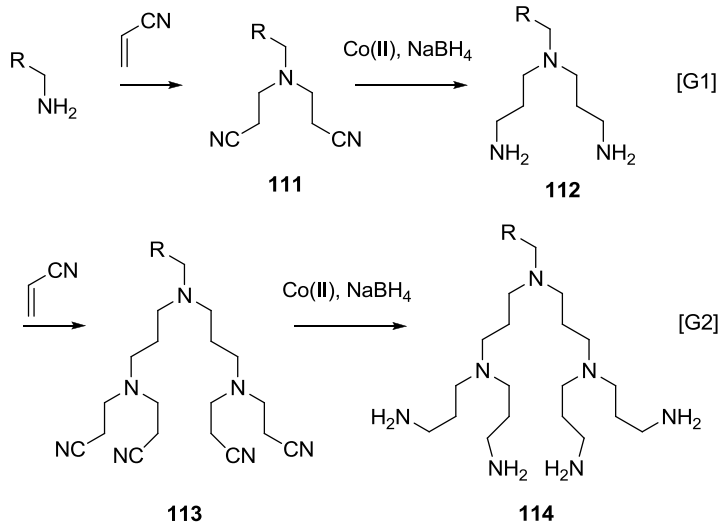

Scheme 19. First reported dendrimer synthesis by Vögtle.

Despite the novelty and simplicity of that synthetic approach only few "cascade"-like molecules were reported within the following years. This was mainly due to major difficulties in the synthesis and especially the purification and analysis of the materials. Nevertheless the exploration of this new substance class continued in theoretical regards mainly by the work from Maciejewski[136] (densely packed cascade like polymers), De Gennes and Hervet[137] (generation limit in starburst-dendrimers) as well as in synthetic optimizations mainly by Denkewalter[138] (Polylysine) und Tomalia[139] (polyamidoamine). Tomalia also was the first one using the name „dendrimer", which is derived from the greek words dendron (tree) and meros (part). Since then this nomenclature has become accepted and is nowadays commonly used.

1.4.1 Synthetic approaches towards dendrimers and dendritic molecules

Dendrimers can be synthesized via different methods.[140] The most convenient methods are the divergent and convergent syntheses (Figure 19). Each approach has its own advantages and disadvantages, however. The divergent approach, which was the first one to be applied and is perhaps the most common, starts from a polyfunctional core onto which the building blocks are

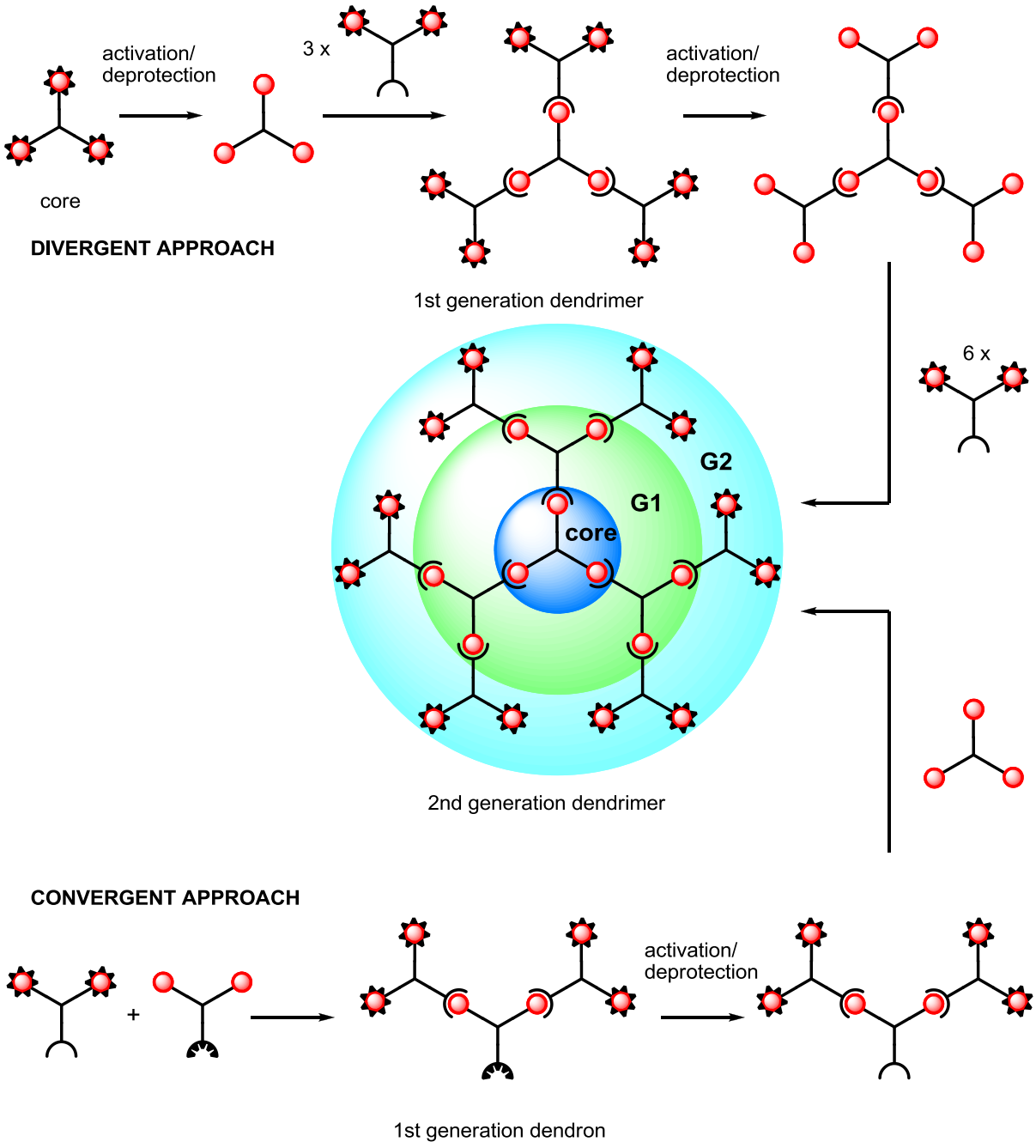

Figure 19. Synthetic approaches for dendrimer preparation.

added in a stepwise so that the dendrimers grow from the inside to the periphery. The main drawback of this approach is the difficulty in purification upon reaching high dendron generations due to the high amount of surface active groups which need to be coupled. For example, theoretical calculations on the synthesis of a generation five ([G5]) poly (propylene imine) dendrimer (64 amine end groups, 248 reactions) showed that even if the individual coupling reaction has a yield of 99.5% the yield of defect free dendrimer will only be 29 %.[141] This seems to be a rather drastic value, but one has to keep in mind that the polydispersity of the resulting material (PDI = 1.002) is still narrower than for any other conventional polymer.

The convergent approach was first established by Fréchet in 1990.[142] The first step here is the synthesis of different generations of "dendrons" which are the individual wedges of a perfect dendrimer that bear a protected coupling unit at the focal point. The core function is then deprotected and coupled again to another protected branching unit. This reaction sequence can be repeated until the desired generation is reached. A final coupling to a symmetric core leads to the formation of the perfect dendrimer. Obviously the advantage of this synthetic method is that only a small number of synthetic steps (mostly one or two) on the given dendron is necessary for every increase in generation, therefore also allowing lower yielding reaction types for the dendron synthesis. In addition the purification becomes easier than in the divergent approach. The difference in mass and polarity in imperfect dendrons in comparison to perfect dendrons is higher and a separation is easily performed via common chromatographic methods like HPLC. The major drawback of this route is the fact that the final coupling proceeds at the focal point of the dendrons. This leads to a decrease in yield upon going to higher generations due to the increasing steric hindrance. Consequently, the convergent approach gives only satisfactory yields up to generation five.

Via these two approaches many different dendrimer scaffolds like Poly(propyleneimine) (PPI),[143] Poly(amidoamine) (PAMAM),[139] Poly(ether),[144] Poly(ester),[145] Poly(lysine),[138] and also heteroatom containing (e.g. silicon or phosphor) dendrimers[146] have been synthesized and the number of new scaffolds is still increasing.

1.4.2 Application of dendrimers for site isolation of fluorophores

Due to their unique molecular features and properties ,like precise control of functional groups on the surface and the high functional group density, dendrimers have found application in various scientific fields ranging from catalysis over surface modification up to their use as drug delivery agents.[147] An intrinsic feature is their capability of shielding functional cores from the outer environment by providing a local microenvironment which is predominantly dictated by the

dendrimeric architecture.[148] This intriguing feature has been applied to tune and optimize the properties of a magnitude of different functional cores. For example, redox active cores like porphyrines have been focused on in dendrimer research since they can be regarded as simplified model for natural heme-containing proteins such as cytochrom c.[149] Not only could the aggregation of the dye core be suppressed in these systems, the actual redoxproperties strongly varied with dendron generation as well. In the zinc porphyrine **115** (Figure 20), for example, the reduction potential becomes more negative in comparison to the undendronized core (E_{red}=-1.6 V) upon increasing the dendron generation from [G1] to [G3] by 90 mV (E_{red}=-1.69 V) and 300 mV

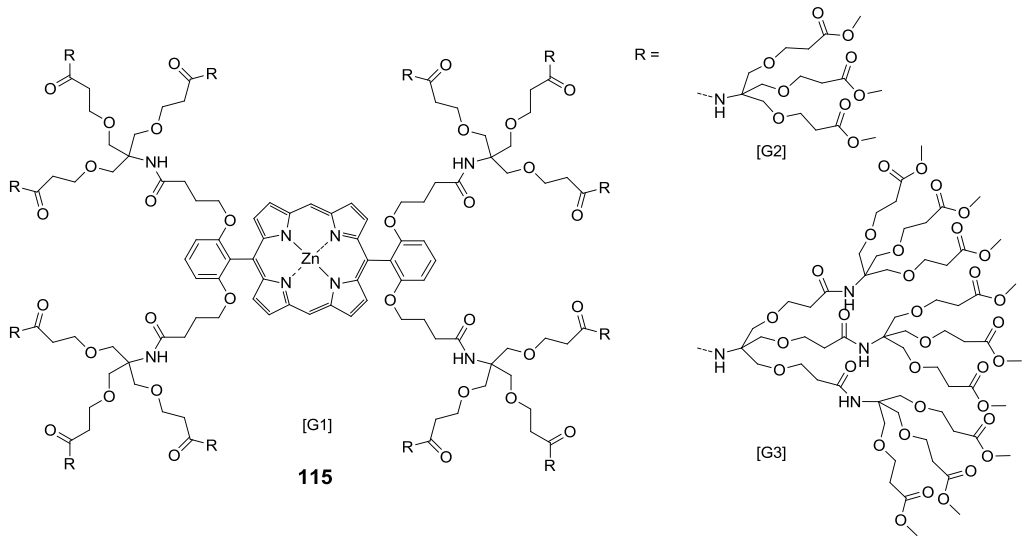

Figure 20. Dendronized Porphyrine as artificial cytochrom c model.

(E_{red}=-1.9 V), respectively.[150] This was explained by the increasing influence of the microenvironment introduced by the Newkome-dendrons which became more and more electron rich and therefore hampered the addition of an electron to the core. Due to the increasing importance of highly fluorescent dyes in the field of bioimaging (see Chapter 1.3.2), dendrimers are also increasingly applied as a solubilizing agent and aggregation suppressor of hydrophobic fluorophores. Consequently, the focus lies here on the utilization of water-soluble dendrimers. However, most dendrimers consist of a completely hydrophobic backbone. Only after a functionalization of the endgroups with water-soluble substituents e.g. sugars,[151] oligo-[152] or polyethyleneglycols,[153] hydroxyl[154] or ionic groups,[155] does a magnitude of water-soluble dendrimers become available. The improvement of the optical properties of fluorophores due to conjugation with dendrimers has been demonstrated, for example, onto monomeric[156] or polymeric[157] fluorine derivatives, cyanines,[158] and metalloporphyrines[159] or squaranines[160] (Figure 21). In all these cases a high water solubility and reduced aggregation behavior of the dendritic material was achieved, which ulti-

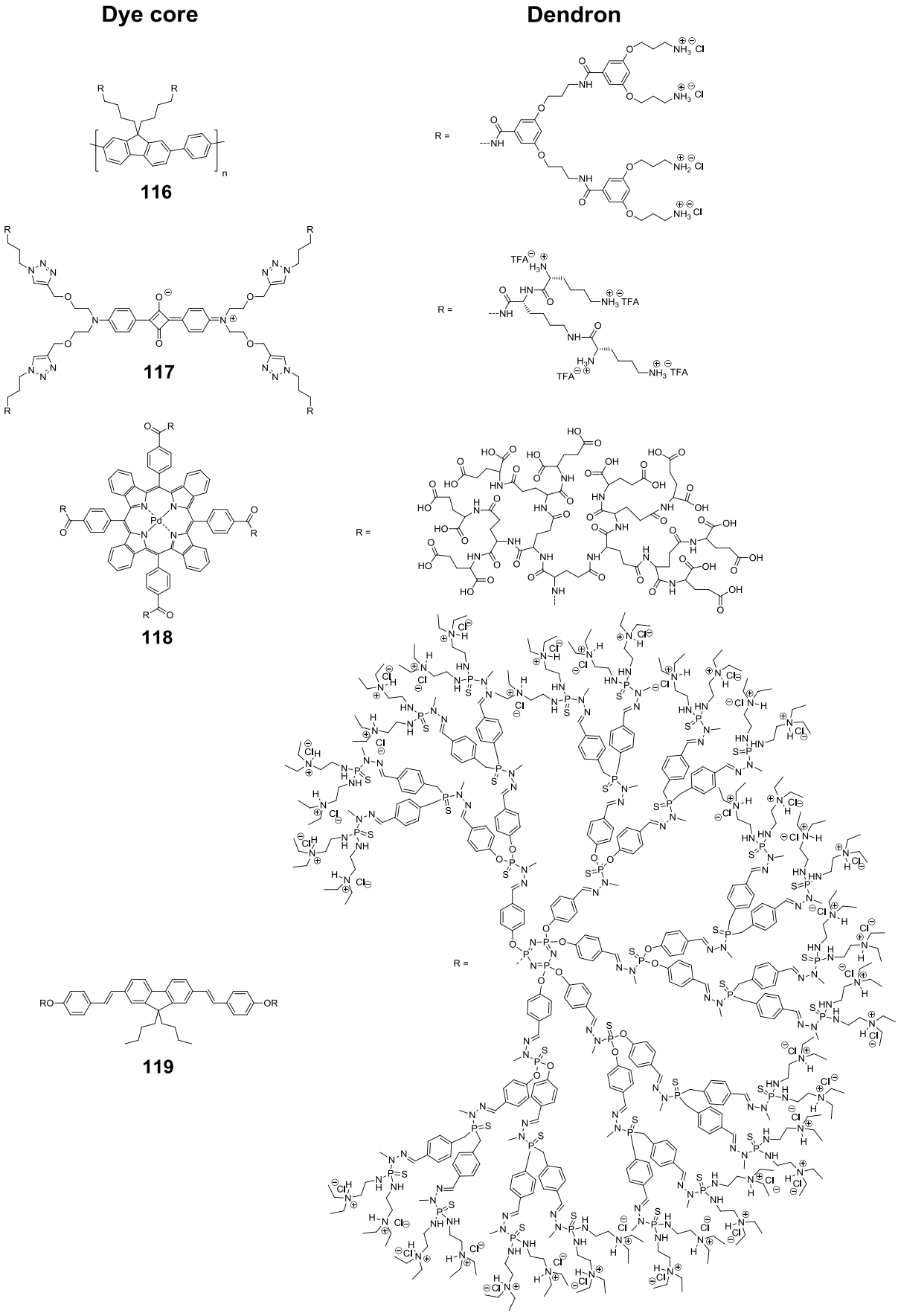

Figure 21. Examples of dendronized fluorophores.

mately led to a retained or even improved fluorescence quantum yield. Water-soluble dendrimers with excellent properties for application in biological systems are polyglycerol dendrimers.

1.4.3 Polyglycerol Dendrimers and Dendrons

Polyglycerol dendrimers and dendrons belong to the subclass of poly(alkyl ether) dendrimers.[161] Due to their highly branched structure, the high amount of hydroxyl endgroups, their biocompatibility and their extremely high water-solubility, they have been successfully applied as solubilizing substituents or agents for hydrophobic functional core molecules.[162-164] The first synthesis of glycerol monomers in a dendritic architecture was reported by Nemoto et al. in 1992.[165] Herein via a convergent approach starting from benzyl alcohol and epichlorhydrine PG-dendrons up to the 2nd generation were successfully prepared. After a final conjugation of the central hydroxyl group with a propargyl unit, carbaboranes could easily be attached. This way, the completely water-insoluble carbaboranes became highly soluble and therefore could be used in boron neutron capture therapy.

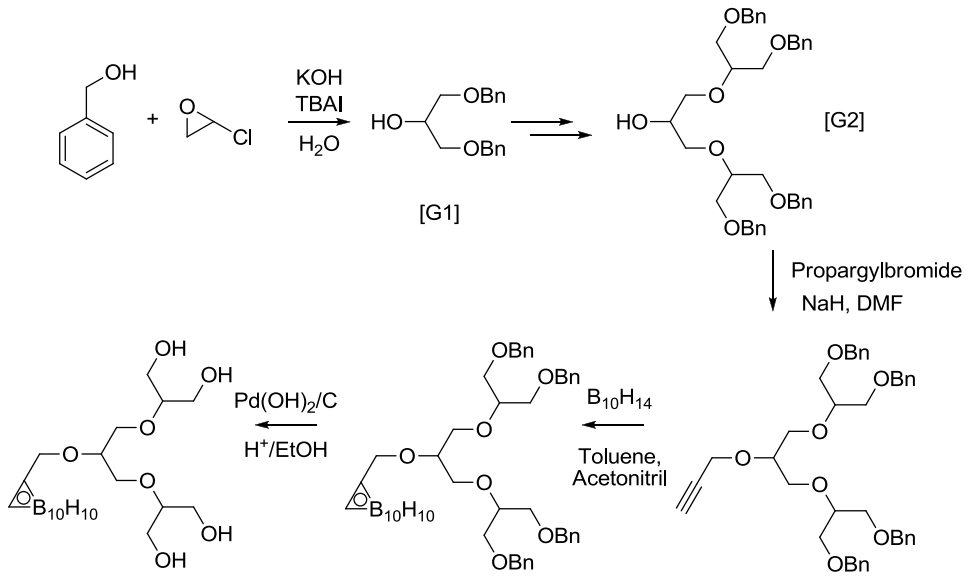

Scheme 20. First synthesis of polyglycerol dendrons.

Based on the [G1] derivative Jayaraman et al. modified and improved the synthesis leading up to [G5] dendrimers using a C_4-building block.[166] In this process he introduced methallyl chloride as the core building block. This had two advantages. Firstly, the allylic functionality enhanced the nucleophilic substitution at both electrophilic sites and secondly the double bond itself served as a protected coupling group which could be easily converted into a primary alcohol via hydroboration. However, due to the additional CH_2-unit within the dendrimeric backbone, the perfect glycerol structure was abandoned.

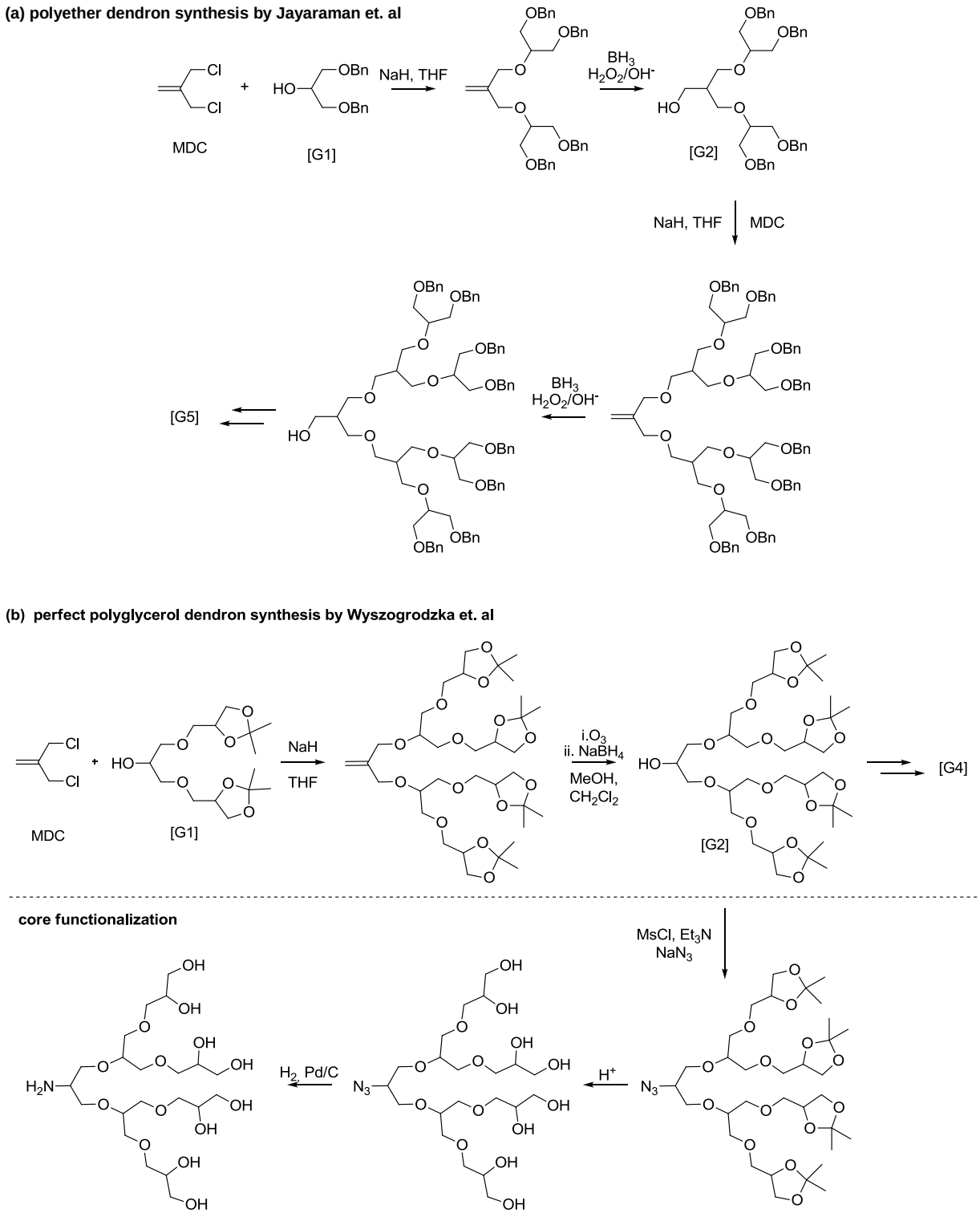

Scheme 21. Modified convergent approaches towards core functional PG-Dendrons: (a) route by Jayaraman et al. generating poly(ether)-dendrons with glycerol units at the surface, (b) route by Wyszogrodzka et al. generating perfect PG dendrons with modifiable core.

Perfect polyglycerol dendrons were finally available by a further adjustment of the synthetic protocol by Wyszogrodzka et al.[167] By changing the hydroboration step into an ozonolysis, the glycerol

structure could also be retained in the dendritic backbone. As starting material, cyclic acetal protected triglycerols were used, since they are readily accessible from commercial triglycerol rendering this synthesis efficient on large scale. Furthermore, the core functionality could be changed into azide or amine groups via a simple mesylation, azidation, and reduction protocol which made the dendrons very versatile in amide or copper catalyzed click couplings. Beside this very efficient convergent approach a divergent method was also invented by Haag et al. Starting from trimethylolpropane (TMP), a subsequent repeated allylation of the hydroxyl groups under phase transfer conditions and osmium tetroxide catalyzed dihydroxylation of the allylic double bond led to PG dendrimers in high yields (75% for [G3] overall).[168] Although useful in drug delivery applications, e.g., the efficient encapsulation of the hydrophobic drug PTX,[169] these systems did not possess a

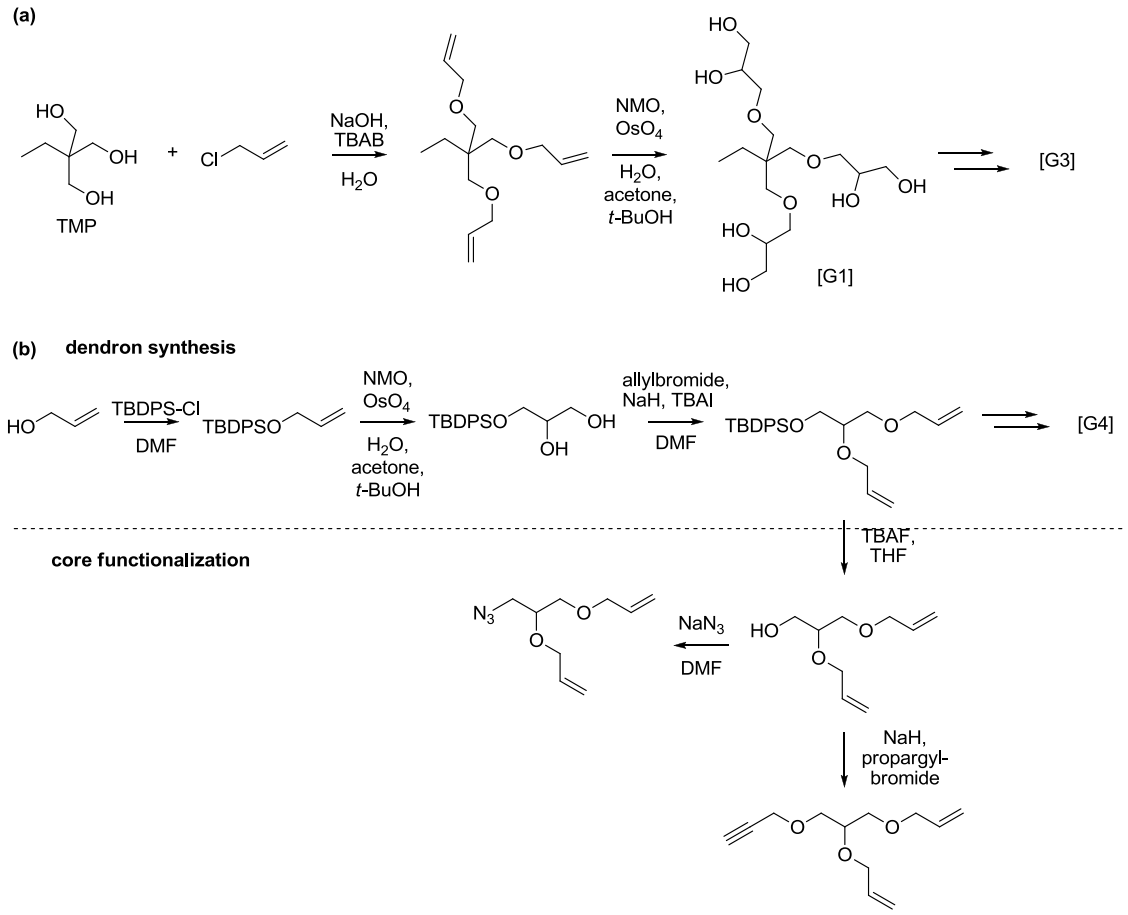

Scheme 22. Divergent approaches towards PG-Dendrons: route by (a) Haag et al. introducing the allylation, dihydroxylation sequence, (b) by Zimmermann using monoprotected glycerol as core.

functional core. This problem was solved in the group of Prof. Zimmermann by using mono tert-butyldiphenylsilyl (TBDPS) protected glycerol as starting mojety instead of TMP which introduces a protected hydroxyl into the core at the cost of one branching unit. A further functionalization with

e.g. propargyl or azide groups renders these dendrons as versatile as the convergent ones.[170] Due to their high biocompatibility,[171] which is as high or even higher than for PEG, its high water-solubility and highly branched structure PG-dendrons are perfect substituents for the site isolation of fluorophores.

2 Motivation and objectives

As shown in the introduction, rylene dyes represent an exceptional versatile class of dyes. Their good fluorescent properties, the high chemical and photochemical stability, as well as the easy synthetic possibility to fine tune the optical properties over a broad range of wavelengths have led to the development of a multitude of functional rylene dyes. Although water-solubility could be induced by many different approaches, the efficient solubilization and effective site isolation of these dyes in the high polarity medium water, is still a challenging task. Monofunctional polyglycerol dendrons, on the other hand, can be produced on large scale and constitute a very effective tool for solubilizing aliphatic materials in an aqueous environment. In addition they possess a highly branched structure which makes them ideal for site isolation purposes.

Therefore the following points were the central objectives in this work:

1) Synthesis and optical characterization of polglycerol dendronized perylene bisimides, whereby the correlation between dendron generation and their impact on the optical properties in an aqueous environment should be clarified.

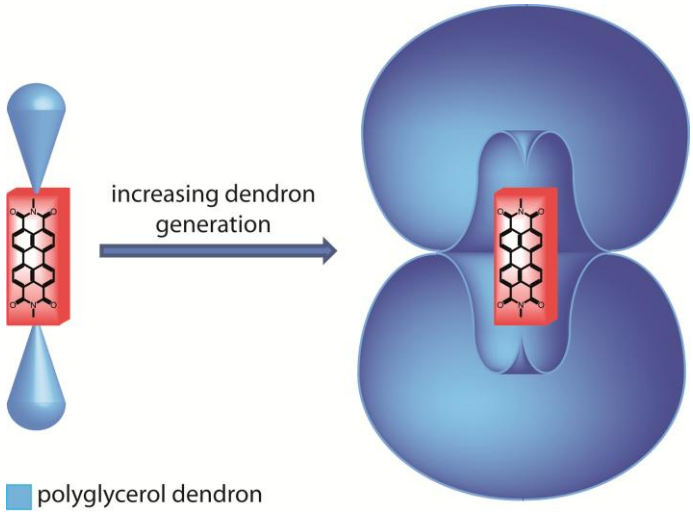

Figure 23. Schematic illustration of target structures bearing polyglycerol dendrons of increasing generation.

2) Extension and evaluation of the polyglycerol dendronization principle onto bathochromically shifted rylene dyes. Therefore, core-substituted perylene bisimides as well as higher rylene homologs should be synthesized and characterized.

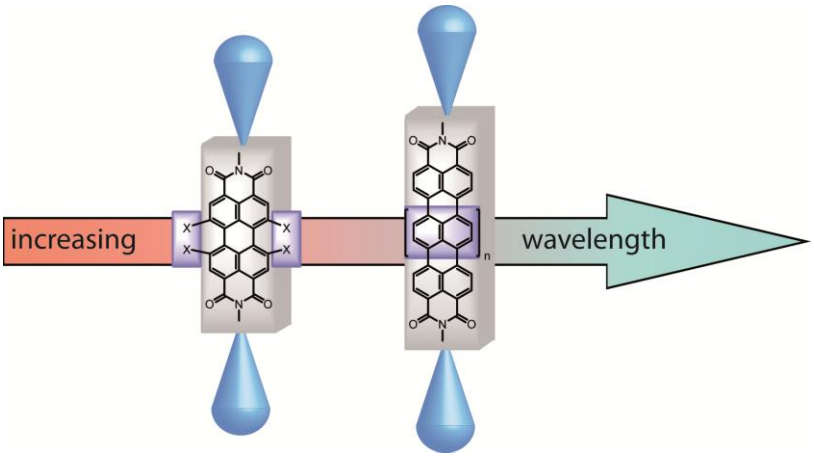

Figure 24. Schematic illustration of target structures possessing bathochromically shifted optical properties.

3) Synthesis and optical characterization of amphiphilic polyglycerol dendronized perylene dyes and evaluation of their possible application as functional dyes in the fields of bioimaging and energy transfer systems.

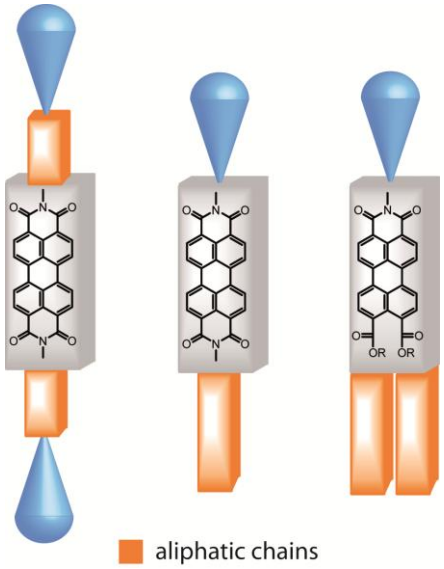

Figure 25. Schematic illustration of target structures possessing amphiphilic character .

3 Publications and manuscripts

In the following chapters, the published articles are listed with a specification of the authors´ contribution.

3.1 Highly fluorescent water-soluble polyglycerol-dendronized perylene bisimide dyes

Timm Heek, Carlo Fasting, Christina Rest, Xin Zhang, Frank Würthner*, and Rainer Haag*

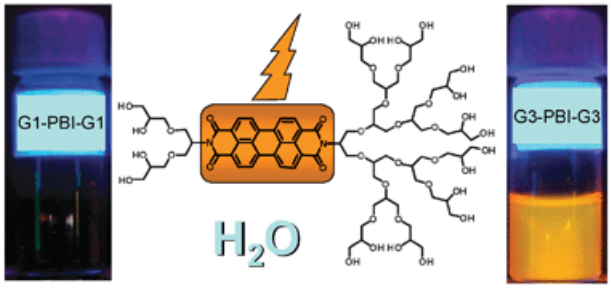

In this publication the author contributed the idea, synthesis and characterization of the reported perylene – polyglycerol dyes. The photophysical studies, especially the quantum yield measurements, were performed by cooperation partners from the group of Prof. Würthner.

This article was published in the following journal:

Timm Heek, Carlo Fasting, Christina Rest, Xin Zhang, Frank Würthner, and Rainer Haag, *Highly fluorescent water-soluble polyglycerol-dendronized perylene bisimide dyes,* Chemical Communications, **2010**, *46*, 1884-1886. (DOI: 10.1039/B923806A)

Highly fluorescent water-soluble polyglycerol-dendronized perylene bisimide dyes†

Timm Heek,[a] Carlo Fasting,[a] Christina Rest,[b] Xin Zhang,[b] Frank Würthner*[b] and Rainer Haag*[a]

Received (in Cambridge, UK) 12th November 2009, Accepted 11th December 2009
First published as an Advance Article on the web 16th January 2010
DOI: 10.1039/b923806a

Water-soluble perylene tetracarboxylic acid bisimides (PBIs) with terminally linked polyglycerol dendrons of four different generations have been synthesized. These PBI dyes reveal a strong dendritic effect, enabling outstanding fluorescence quantum yields in water up to almost 100% for the highest dendron generation.

Perylene-3,4:9,10-tetracarboxylic acid bisimides (PBIs) have been used as pigment colorants for many years, as they possess outstanding thermal and photophysical stability and are available over a broad color range.[1] While their extremely low solubility is a desired property for application as pigments, this particular feature has prevented the utilization of these fluorophores in other research fields, despite their excellent optical and redox properties. To increase the solubility of PBIs, additional side groups have been introduced directly on the perylene core or in the imide positions.[2,3] In particular, the latter strategy using swallow-tail alkyl chains provided highly soluble PBIs with fluorescence quantum yields of up to 100% in almost any common organic solvent.[4] Inspired by this development, PBI dyes were intensively investigated as fluorophores in dye lasers,[5] as fluorescent labels in life sciences[6] and fluorescence sensors,[7] as novel materials for molecular wires and switches,[8] and as photofunctional supramolecular building blocks.[9] However, there are only a few reports on the physical and optical characterization of PBIs in aqueous systems, which is relevant for fluorescence labeling applications in biological systems. Owing to the strong aggregation of these chromophores in water,[10] and hence the loss of fluorescence intensity,[11] the most powerful strategy to circumvent these has been the derivatization with bulky substituents at the perylene core introduced by Müllen and coworkers.[12] By this approach, perylene aggregation could be suppressed and high fluorescence quantum yields. The fluorescence color of the fluorophore, however, is shifted into the red spectral region.

[a] *Freie Universität Berlin, Institut für Chemie und Biochemie, Takustrasse 3, 14195, Berlin, Germany. E-mail: haag@chemie.fu-berlin.de; Fax: +49 30 838 53357; Tel: +49 30 838 52633*
[b] *Universität Würzburg, Institut für Organische Chemie, Am Hubland, 97074, Würzburg, Germany. E-mail: wuerthner@chemie.uni-wuerzburg.de; Fax: +49 931 888 4756; Tel: +49 931 318 5340*

† Electronic supplementary information (ESI) available: General methods and materials, synthesis and characterization of compounds **1a–1d** and supporting figures S1–S5. See DOI: 10.1039/b923806a

Therefore, other strategies to prevent aggregate formation of PBIs in water, in particular for the parent core-unsubstituted derivative with green-yellow emission, are still in demand. To achieve this, permanently or reversibly charged substituents have been introduced in the imide positions, such as dendritic Newkome-type carboxylates[13] and phosphate surfactants.[14] Additionally, several polar but uncharged moieties, such as PEG chains,[15] cyclodextrins,[7] or crown ethers,[16] have been employed. Although water-solubility was achieved for these compounds, high fluorescence quantum yields in aqueous media have not been reported so far, which might be attributed to fluorescence quenching by aggregation or an excited-state proton transfer between hydrogen-bond donor solvents and the imide oxygens.

The goal of this work was to explore whether the parent core-unsubstituted PBI fluorophores exhibit high fluorescence intensity in water if their aggregation is completely suppressed. Towards this goal, bifunctional polyglycerol (PG) dendrons appear quite promising because they are well known to introduce water-solubility, if covalently attached to hydrophobic compounds, and have previously been used for the creation of nanotransporters with hydrophobic cores and hydrophilic shells.[17] We have utilized here terminally aminated PG dendrons of generation 1 (G1, 4 hydroxy groups) to 4 (G4, 32 hydroxy groups), which were prepared according to literature procedures.[18]

The condensation of perylene tetracarboxylic acid bisanhydride (PBA) with the respective aminated PG dendron was performed in molten imidazole at 140 °C to furnish the desired symmetric perylene bisimides **1a–1d** in high yields (Scheme 1). It is noteworthy that all putative products are water-soluble and do not require further deprotection. Thus, purification was achieved by simple filtration of its aqueous solution, followed by dialysis to remove imidazole and remaining starting materials.

In order to obtain analytically pure samples, reversed phase column chromatography was further applied to compounds **1a–1d**. The spectroscopic properties of these dendronized PBIs **1a–1d** and their aggregation behavior were investigated in aqueous solution by concentration-dependent UV/Vis and fluorescence spectroscopy. From the UV/Vis measurements (Fig. 1) a drastic difference in their aggregation behavior can be observed. The [G1] dendronized PBI **1a** (Fig. 1, top) exists in an aggregated state over the whole accessible concentration range, as evidenced by the characteristic shape of the absorption band with its maximum at 501 nm. Similar spectra have been observed for PBI chromophores in organic solvents

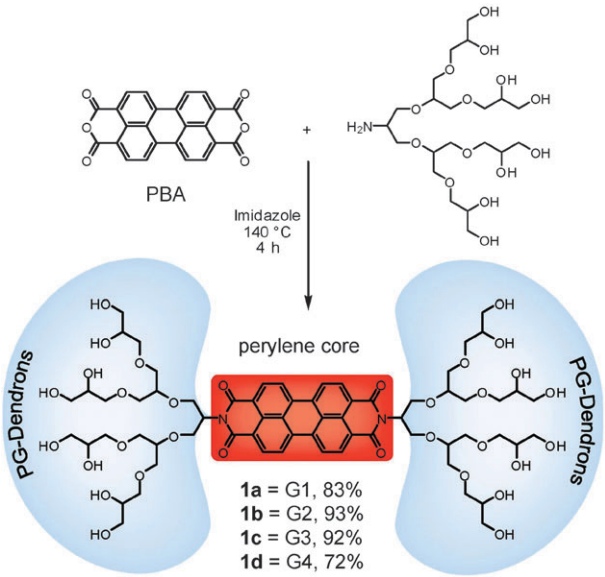

Scheme 1 Synthesis of the PBIs shown for [G2]-PBI **1b** as an example.

and were interpreted in terms of H-type aggregates based on exciton coupling theory (for cryo-TEM pictures see ESI, Fig. S5†).[19] This indicates that the [G1] dendron substituents are too small to interfere with the strong interchromophoric π–π interactions of the PBI cores. In contrast, for [G2] dendronized PBI **1b**, an almost complete transition from aggregated dyes (absorption maximum at 501 nm) to monomeric dyes (absorption maximum at 534 nm) is observed upon dilution in the concentration range between 10^{-4} and 10^{-6} M (Fig. 1, middle). Finally, both dendronized PBIs of higher generations, [G3] **1c** (Fig. 1, bottom) and [G4] **1d** (ESI, Fig. S2†) show well-resolved absorption spectra with a maximum absorption at 531 nm and a vibronic fine structure which are characteristic for monomeric PBIs, over the whole investigated concentration range. This reflects the increasing steric demand of the higher generation dendron substituents and their ability to inhibit the aggregation of the perylene cores by shielding the π-faces. This is further supported by AM1 modeling (ESI, Fig. S1†). Hence, the perylene derivatives **1c** and **1d** exist in monomeric state at all the concentrations used here.

We further investigated the concentration-dependent fluorescence behavior of all four conjugates (Fig. 2 and ESI, Fig. S3†). For the most dilute solutions (10^{-7} M), a well-resolved vibronic pattern is observed for all derivatives which is characteristic for monomeric PBIs. For **1b–1d** this fluorescence band is a mirror image of the respective absorption band, while a significant deviation is observed for **1a**. Accordingly, for **1a** which contains the smallest generation number dendron, the absorption spectra are dominated by aggregated species, while the emission spectra are attributed to monomers. These results provide strong evidence for an efficient fluorescence quenching in the aggregated state. Only at quite high concentrations (10^{-4} M), where monomers are almost absent, a weak and broad aggregate emission can be observed with a maximum at 688 nm (Fig. 2, top). Such a characteristic PBI emission band has previously been observed in organic

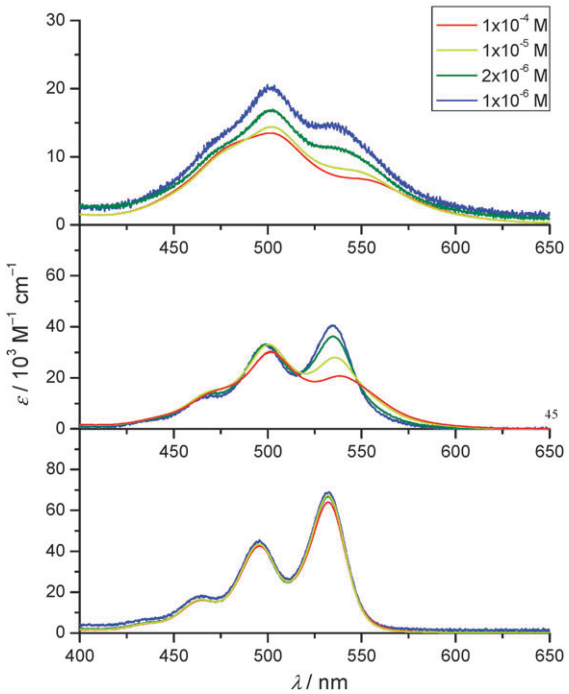

Fig. 1 (a) UV/Vis absorption spectra of aqueous solutions of PBIs **1a** (top), **1b** (middle), and **1c** (bottom) at 25 °C for concentrations from $c = 10^{-4}$ M to 10^{-6} M.

solvents, and the pronounced bathochromic shift was attributed to an excimer-type excited state.[20] Interestingly, for **1b** (Fig. 2, middle) a less pronounced band displacement is observed which might be an indication for the prevalence of smaller aggregates, *i.e.*, dimers, or, more likely, the prevention of the structural reorganization of the excited aggregate into a relaxed excimer state owing to the larger sterical congestion imposed by the second generation dendron.‡ Finally, for **1c** (and likewise for **1d**, see ESI†) no characteristic aggregate emission band could be observed, even at higher concentrations (Fig. 2, bottom).§

To get a quantitative insight into the operating fluorescence quenching mechanisms for PBI fluorophores in water, we have determined the fluorescence quantum yields (FQY) for the most dilute solution (10^{-7} M) of all four dendronized PBIs (Fig. 3). One can recognize a strong positive dendritic effect, revealing a continuous increase of the FQY with increasing dendron generation ranging from 33.1% for [G1] substituted PBI **1a** up to 98.9% for [G4] substituted PBI **1d**. From this study, we can conclude that PBI fluorophors are equally efficient emitters in water as well as in organic solvents if their aggregation is completely suppressed. Owing to the strong π–π interactions between these dyes and a pronounced hydrophobic effect in water,[10] however, the largest [G4] dendron number was necessary to achieve this effect.

In summary, we have synthesized a set of highly water-soluble polyglycerol-dendronized PBIs. The sterically most demanding dendron substituent afforded a dye with an outstanding fluorescence quantum yield of almost 100% in water. This result provides clarification that no specific fluorescence quenching mechanism like excited state proton transfer is operative for this important class of fluorophores in

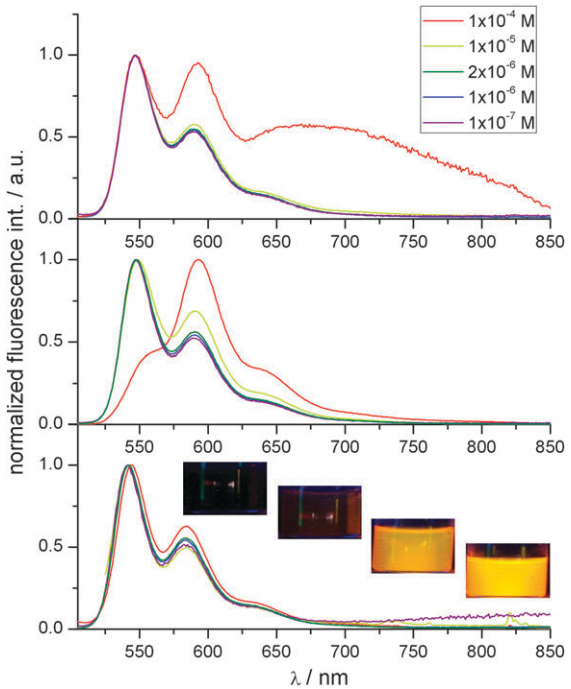

Fig. 2 Normalized fluorescence spectra of aqueous solutions of PBIs **1a** (top), **1b** (middle), and **1c** (bottom) at 25 °C for concentrations from $c = 10^{-4}$ M to 10^{-7} M, $\lambda_{ex} = 490$ nm. The inset shows a photograph of the solutions of PBIs **1a–1d** ([G1]–G[4] from left to right) under UV-light illumination ($c = 1.43 \times 10^{-4}$ M).

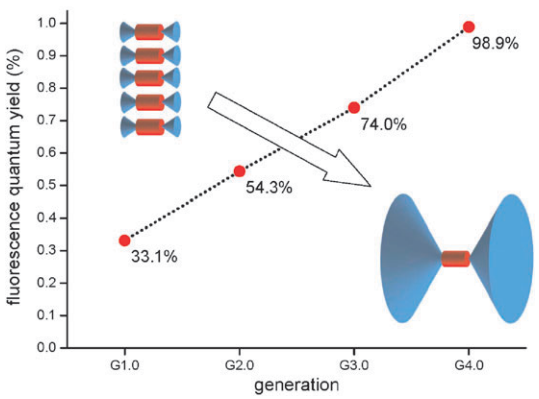

Fig. 3 Fluorescence quantum yields of **1a–1d** determined at a concentration of $c = 10^{-7}$ M and schematic illustration of the effect of dendronization of PBI chromophores.

water. Thus, strong fluorescence can be observed for simple core-unsubstituted PBIs if aggregation is efficiently suppressed. This observation should open many interesting applications, such as fluorescent labels and sensors in aqueous media.

The authors thank Dr Parveen Mohr and Andrea Schulz for AM1 modelling and Cryo-TEM measurements, respectively.

Notes and references

‡ According to ref. 20 the excimer state is characterized by an almost perfect face-to-face stacking geometry even though rotationally displaced dyes are present for PBI aggregates in the ground state.

§ The slight increase of the second vibronic band at 580 nm might arise from aggregated species, but could also be a reabsorption effect.

1 W. Herbst and K. Hunger, *Industrial Organic Pigments: Production, Properties, Applications*, Wiley-VCH, Weinheim, 3rd edn, 2004.
2 H. Langhals, *Heterocycles*, 1995, **40**, 477.
3 F. Würthner, *Chem. Commun.*, 2004, 1564.
4 S. Demmig and H. Langhals, *Chem. Ber.*, 1988, **121**, 225.
5 R. Gvishi, R. Reisfeld and Z. Burshtein, *Chem. Phys. Lett.*, 1993, **213**, 338; M. Sadrai, L. Hadel, R. R. Sauers, S. Husain, K. Krogh-Jespersen, J. D. Westbrook and G. R. Bird, *J. Phys. Chem.*, 1992, **96**, 7988.
6 W. Tuntiwechapikul, T. Taka, M. Béthencourt, L. Makonkawkeyoon and R. Lee, *Bioorg. Med. Chem. Lett.*, 2006, **16**, 4120; D. Baumstark and H.-A. Wagenknecht, *Angew. Chem., Int. Ed.*, 2008, **47**, 2612; Y. Zhao, X. Zhang, D. Li, D. Liu, W. Jiang, C. Han and Z. Shi, *Luminescence*, 2009, **24**, 140.
7 Y. Liu, K.-R. Wang, D.-S. Guo and B.-P. Jiang, *Adv. Funct. Mater.*, 2009, **19**, 2230; L. Zang, R. Liu, M. W. Holman, K. T. Nguyen and D. M. Adams, *J. Am. Chem. Soc.*, 2002, **124**, 10640.
8 M. P. O'Neil, M. P. Niemczyk, W. A. Svec, D. Gosztola, G. L. Gaines III and M. R. Wasielewski, *Science*, 1992, **257**, 63; T. M. Wilson, M. J. Tauber and M. R. Wasielewski, *J. Am. Chem. Soc.*, 2009, **131**, 8952.
9 B. Rybtchinski, L. E. Sinks and M. R. Wasielewski, *J. Am. Chem. Soc.*, 2004, **126**, 12268; S. Yagai, Y. Monma, N. Kawauchi, T. Karatsu and A. Kitamura, *Org. Lett.*, 2007, **9**, 1137; G. Golubkov, H. Weissman, E. Shirman, S. G. Wolf, I. Pinkas and B. Rybtchinski, *Angew. Chem., Int. Ed.*, 2009, **48**, 926.
10 Z. Chen, A. Lohr, C. R. Saha-Möller and F. Würthner, *Chem. Soc. Rev.*, 2009, **38**, 564.
11 J. B. Bodapati and H. Icil, *Dyes Pigm.*, 2008, **79**, 224; H. Langhals, *New J. Chem.*, 2008, **32**, 21.
12 C. Kohl, T. Weil, J. Qu and K. Müllen, *Chem.–Eur. J.*, 2004, **10**, 5297; A. Margineanu, J. Hofkens, M. Cotlet, S. Habuchi, A. Stefan, J. Qu, C. Kohl, K. Müllen, J. Vercammen, Y. Engelborghs, T. Gensch and F. De Schryver, *J. Phys. Chem. B*, 2004, **108**, 12242; K. Peneva, G. Mihov, F. Nolde, S. Rocha, J.-i. Hotta, K. Braeckmans, J. Hofkens, H. Uji-i, A. Herrmann and K. Müllen, *Angew. Chem., Int. Ed.*, 2008, **47**, 3372.
13 C. Schmidt, C. Böttcher and A. Hirsch, *Eur. J. Org. Chem.*, 2007, 5497; C. Backes, C. Schmidt, F. Hauke, C. Böttcher and A. Hirsch, *J. Am. Chem. Soc.*, 2009, **131**, 2172; C. Ehli, C. Oelsner, D. Guldi, A. Mateo-Alonso, M. Prato, C. Schmidt, C. Backes, F. Hauke and A. Hirsch, *Nat. Chem.*, 2009, **1**, 243.
14 Y. Huang, Y. Yan, B. M. Smarsly, Z. Wei and Charl F. J. Faul, *J. Mater. Chem.*, 2009, **19**, 2356.
15 X. Zhang, Z. Chen and F. Würthner, *J. Am. Chem. Soc.*, 2007, **129**, 4886; E. Shirman, A. Ustinov, N. Ben-Shitrit, H. Weissman, M. Iron, R. Cohen and B. Rybtchinski, *J. Phys. Chem. B*, 2008, **112**, 8855; J. Baram, E. Shirman, N. Ben-Shitrit, A. Ustinov, H. Weissman, I. Pinkas, S. Wolf and B. Rybtchinski, *J. Am. Chem. Soc.*, 2008, **130**, 14966; J. Gebers, D. Rolland and H. Frauenrath, *Angew. Chem., Int. Ed.*, 2009, **48**, 4480; E. Krieg, E. Shirman, H. Weissman, E. Shimoni, S. Wolf, I. Pinkas and B. Rybtchinski, *J. Am. Chem. Soc.*, 2009, **131**, 14365; X. Zhang, S. Rehm, M. Safont-Sempere and F. Würthner, *Nat. Chem.*, 2009, **1**, 623.
16 H. Langhals, W. Jona, F. Einsiedl and S. Wohnlich, *Adv. Mater.*, 1998, **10**, 1022; Y.-M. Jeon, T.-H. Lim, J.-G. Kim and M.-S. Gong, *Macromol. Res.*, 2007, **15**, 473.
17 M. Calderon, M. A. Quadir, S. Sharma and R. Haag, *Adv. Mat.*, 2010, **22**, 190; E. Burakowska and R. Haag, *Macromolecules*, 2009, **42**, 5545.
18 R. Haag, A. Sunder and J.-F. Stumbé, *J. Am. Chem. Soc.*, 2000, **122**, 2954; M. Wyszogrodzka, M. Weinhart and R. Haag, *Polym. Mater. Sci. Eng.*, 2007, **48**, 760; M. Wyszogrodzka and R. Haag, *Chem.–Eur. J.*, 2008, **14**, 9202.
19 M. Kasha, H. R. Rawls and M. A. El-Bayoumi, *Pure Appl. Chem.*, 1965, **11**, 371.
20 R. Fink, J. Seibt, V. Engel, M. Renz, M. Kaupp, S. Lochbrunner, H.-M. Zhao, J. Pfister, F. Würthner and B. Engels, *J. Am. Chem. Soc.*, 2008, **130**, 12858.

Electronic Supplementary Information

Highly fluorescent water-soluble polyglycerol-dendronized perylene bisimide dyes

Timm Heek,[a] Carlo Fasting,[a] Christina Rest,[b] Xin Zhang,[b] Frank Würthner*[b] and Rainer Haag*[a]

[a] *Freie Universität Berlin, Institut für Chemie und Biochemie, Takustrasse 3, 14195 Berlin, Germany; Correspondence: Prof. Dr. Rainer Haag, E-mail: haag@chemie.fu-berlin.de; Phone: +49 30 838 52633; Fax: +49 30 838 53357*

[b] *Universität Würzburg, Institut für Organische Chemie, Am Hubland, 97074 Würzburg, Germany; Correspondence: Prof. Dr. Frank Würthner, E-mail: wuerthner@chemie.uni-wuerzburg.de; Phone: +49 931 318 5340; Fax: +49 931 888 4756*

General Methods

^{1}H NMR spectra were recorded on a Bruker ECX 400 spectrometer (400 MHz and 100 MHz for ^{1}H and ^{13}C, respectively) at 25 °C and calibrated against residual solvent peaks as internal standard. The UV/Vis absorption spectra were recorded for different concentrations on a Perkin Elmer Lambda 40P spectrophotometer with cuvettes of 0.1 cm path length (for **G2.0**, **G3.0** and **G4.0** at a concentration of $1\text{x}10^{-4}$ M) and 1.0 cm path length for all other measurements. The steady-state fluorescence spectra were recorded on a PTI QM4-2003 fluorescence spectrometer and corrected against photomultiplier and lamp intensity. The fluorescence spectra were measured with cuvettes of 0.1 cm path length (for **G2.0**, **G3.0** and **G4.0** at a concentration of $1\text{x}10^{-4}$ M) and 1.0 cm path length for all other measurements. Fluorescence quantum yields were calculated from the integrated intensity under the emission band (*I*) using the following equation:

$$\Phi = \Phi_r \frac{I}{I_r} \frac{OD_r}{OD} \frac{n^2}{n_r^2}$$

where *OD* is the optical density of the solution at the excitation wavelength and *n* is the refractive index. The optical density of the solution for the calculation of quantum yields was less than 0.1 at

the excitation wavelength. *N*,*N*'-Di(2,6-diisopropylphenyl)-perylene-3,4:9,10-tetracarboxylic acid bisimide in chloroform was used as reference ($\Phi_r = 1.00$).

ESI-MS spectra were measured on an Agilent 6210 ESI-TOF, Agilent Technologies, Santa Clara, CA, USA. Solvent flow rate was adjusted to 4 μL/min, spray voltage set to 4.000 V. Drying gas flow rate was set up to 15 psi (1 bar). All other parameters were adjusted for a maximum abundance of the relative $[M+H]^+$. The samples for cryogenic transmission electron microscopy (cryo-TEM) were prepared at room temperature by placing a droplet (5 μL) of the solution on a hydrophilized perforated carbon filmed Quantifoil grid (60 s Plasma treatment at 8 W using a BALTEC MED 020 device). The excess fluid was blotted off to create an ultra thin layer of the solution spanning the holes of the carbon film. The grids were immediately vitrified in liquid ethane at its freezing point (-184 °C) using a standard plunging device. Ultra-fast cooling is necessary for an artifact-free thermal fixation (vitrification) of the aqueous solution avoiding crystallization of the solvent or rearrangement of the assemblies. The vitrified samples were transferred under liquid nitrogen into a Philips CM12 transmission electron microscope using the Gatan cryoholder and -stage (Model 626). Microscopy was carried out at -175 °C sample temperature using the microscope's low dose mode. Accelerating voltage was 100 kV and the defocus was chosen to be -1.5 μm up to -2.5 μm.

Materials

All solvents and reagents were purchased from commercial sources and used as received without further purification, unless otherwise stated. The solvents for spectroscopic studies were of spectroscopic grade and used as received. Dialysis was performed in Spectra/Por® Biotech CE dialysis tubing.

Synthesis and Characterization of Compounds 1a-1d

General method for preparation of the *N*,*N*-substituted perylene-3,4:9,10-tetracarboxylic acid bisimides

In a typical experiment, perylene 3,4:9,10-tetracarboxylic acid bisanhydride (PBA, 1.0 eq.), the [G*n*]-NH_2 dendron (2.5 eq.) and imidazole were combined. The mixture was heated to 140 °C under argon for 4 hours and cooled to room temperature. The remaining solid was dissolved in water and dialysed for three days against water to give the desired product.

1a: [G1.0]-NH_2 (74 mg, 0.330 mmol), PBA (52 mg, 0.13 mmol) and 200 mg imidazole, dialysed with MWCO 500, yield 90 mg, 0.108 mmol (83%). ^{1}H NMR (CD_3OD, 400 MHz): δ (ppm) = 7.25 (m, 8H, Ar-H), 5.30 (m, 2H, -N-C<u>H</u>-,), 4.40-3.25 (m, 28H, PG-Dendron). MS (ESI-TOF, pos. mode) m/z 857.27 $[M+Na]^+$ (calcd. for $C_{42}H_{46}N_2O_{16}$ 834.2847). UV/Vis (H_2O): λ_{max} (nm) = 501, 536; fluorescence (H_2O): λ_{max} (nm) = 590, 546, Φ_{fl} = 33.1% (c = 10^{-7} M).

1b: [G2.0]-NH_2 (100 mg, 0.186 mmol), PBA (30 mg, 0.078 mmol) and 500 mg imidazole, dialysed with MWCO 500, yield 103 mg, 0.722 mmol (93%). ^{1}H NMR (D_2O, 400 MHz): δ (ppm) = 7.86 (m, 8H, Ar-H), 5.54 (br. s., 2H, -N-C<u>H</u>-), 4.33-3.65 (m, 68H, PG-Dendron). MS (ESI-TOF, pos. mode) m/z 1449,5722 $[M+Na]^+$; 736.2811 $[M+Na]^{2+}$ (calcd. for $C_{66}H_{94}N_2O_{32}$ 1426.5790). UV/Vis (H_2O): λ_{max} (nm) = 535, 499, 468; fluorescence (H_2O): λ_{max} (nm) = 591, 548, Φ_{fl} = 54.3% (c = 10^{-7} M).

1c: [G3.0]-NH_2 (315 mg, 0.280 mmol), PBA (44 mg, 0.110 mmol) and 300 mg imidazole, dialysed with MWCO 1000, yield 264 mg, 0.101 mmol (92%). ^{1}H NMR (D_2O, 400 MHz): δ (ppm) = 8.40 (m, Ar-H), 5.63 (br. s, 2H, -N-C<u>H</u>-), 4.37 (br. s, 4H), 4.24 (br. s, 4H), 4.00-3.21 (m, 140H, PG-Dendron). MS (ESI-TOF, pos. mode) m/z 2635.1247 $[M+Na]^+$; 1329.0669 $[M+2Na]^{2+}$ (calcd. for $C_{114}H_{190}N_2O_{64}$ 2611.1674). UV/Vis (H_2O): λ_{max} (nm) = 532, 495, 464; fluorescence (H_2O): λ_{max} (nm) = 584, 543, Φ_{fl} = 74.0% (c = 10^{-7} M).

1d: [G4.0]-NH_2 (190 mg, 0.083 mmol), PBA (13 mg, 0.033 mmol) and 200 mg Imidazole, dialysed with MWCO 3500, yield 118 mg, 0.024 mmol (72%). ^{1}H NMR (D_2O, 400 MHz): δ (ppm) = 9.00 (m, 8H, Ar-H), 5.70 (br. s, 2H, -N-C<u>H</u>-), 4.37 (br. s, 4H), 4.14 (br. s, 4H), 3.95-3.06 (m, 300H, PG-Dendron). MS (ESI-TOF, pos. mode) m/z 1683.1051 $[M+3Na]^{3+}$; 1268.0764 $[M+4Na]^{4+}$ (calcd. for $C_{210}H_{382}N_2O_{128}$ 4980.3444). UV/Vis (H_2O): λ_{max} (nm) = 532, 495, 46; fluorescence (H_2O): λ_{max} (nm) = 584, 541, Φ_{fl} = 98.9% (c = 10^{-7} M).

Supporting Figures

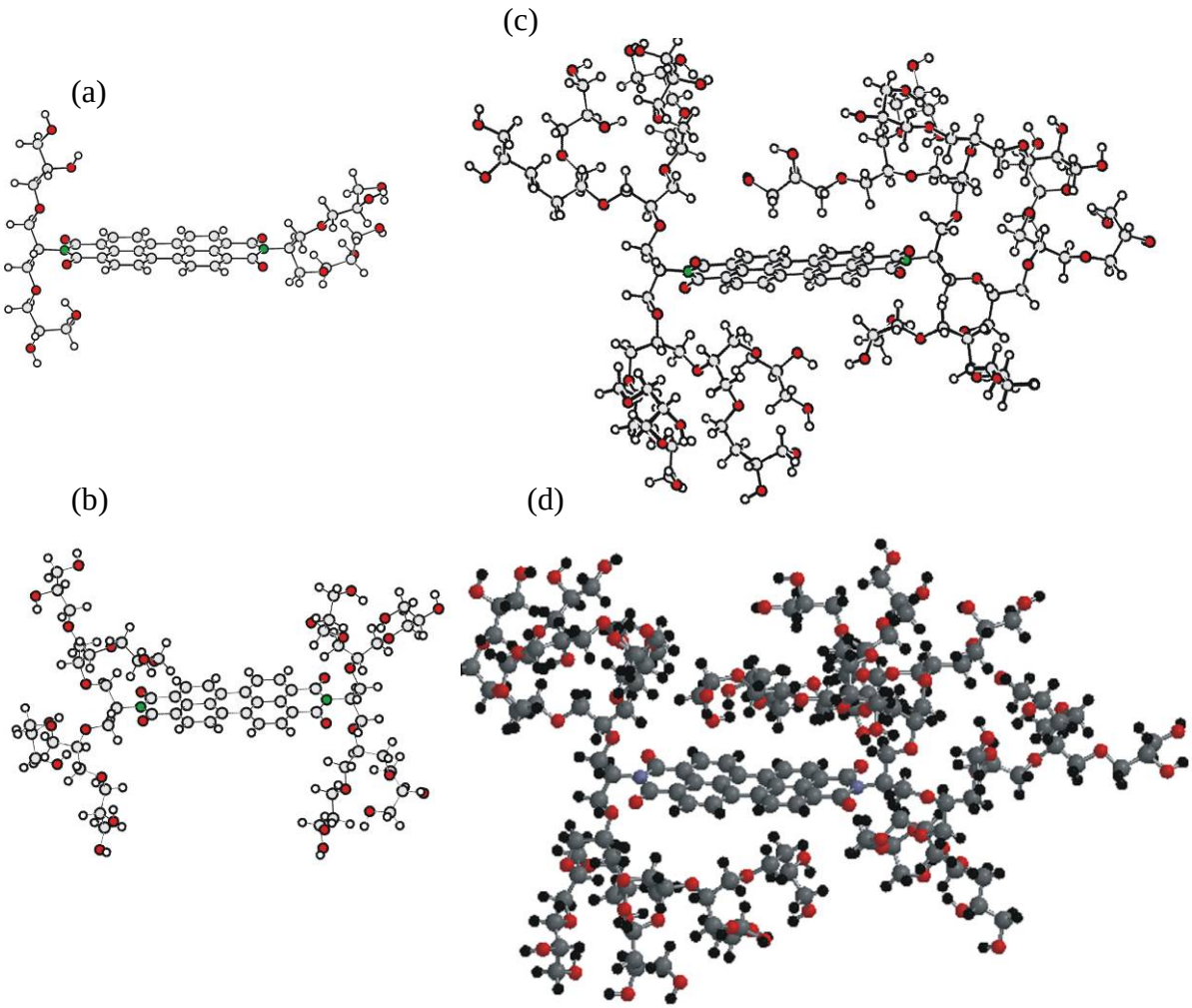

Fig. S1 AM1 modelled structures for (a) **1a,** (b) **1b,** (c) **1c** and (d) **1d**.

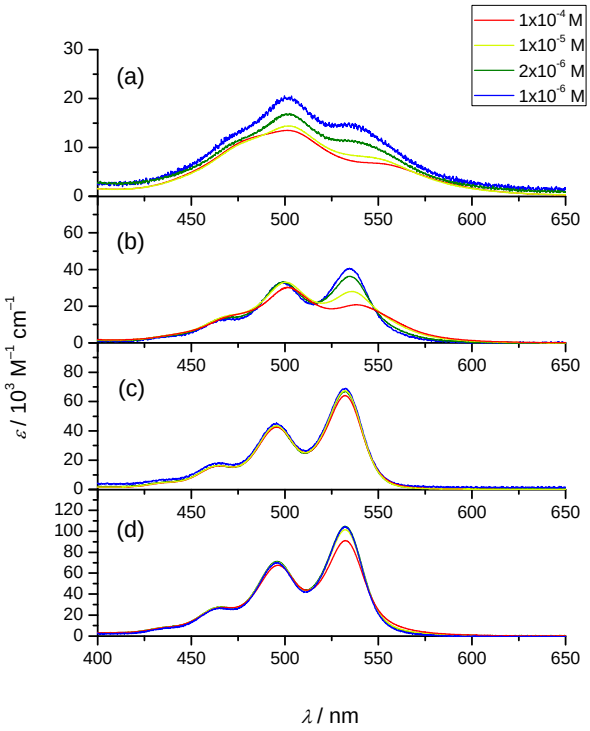

Fig. S2 UV/Vis absorption spectra of aqueous solutions of PBIs (a) **1a**, (b) **1b**, (c) **1c**, (d) **1d** at 25 °C for the concentration range from 10^{-4} to 10^{-6} M.

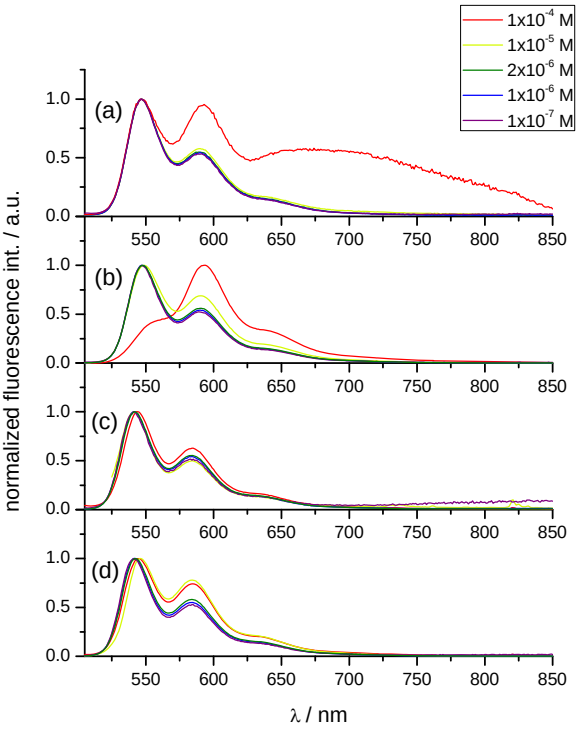

Fig. S3 Normalized fluorescence spectra of aqueous solutions of PBIs (a) **1a**, (b) **1b**, (c) **1c**, (d) **1d** at 25 °C for the concentration range from 10^{-4} to 10^{-7} M, λ_{ex} = 490 nm.

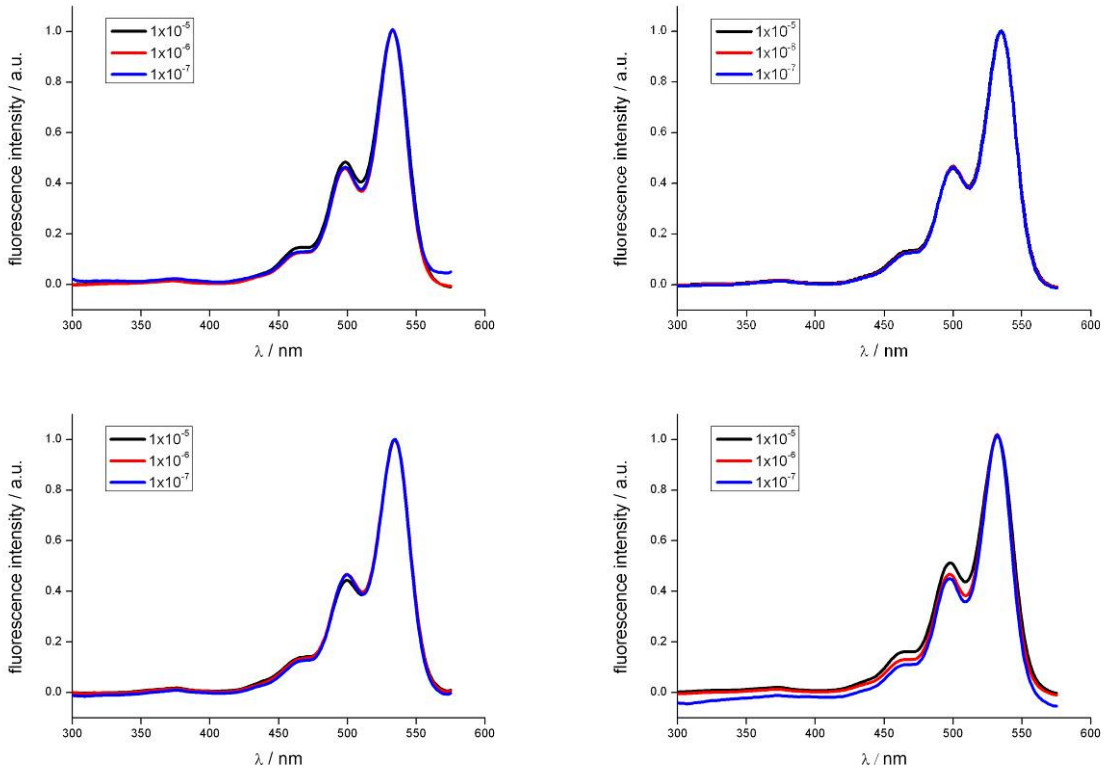

Fig. S4 Excitation spectra (λ_{ex} = 540 nm) of (a) **1a**, (b) **1b**, (c) **1c**, (d) **1d** in aqueous solution at concentrations from 10^{-5} to 10^{-7} M.

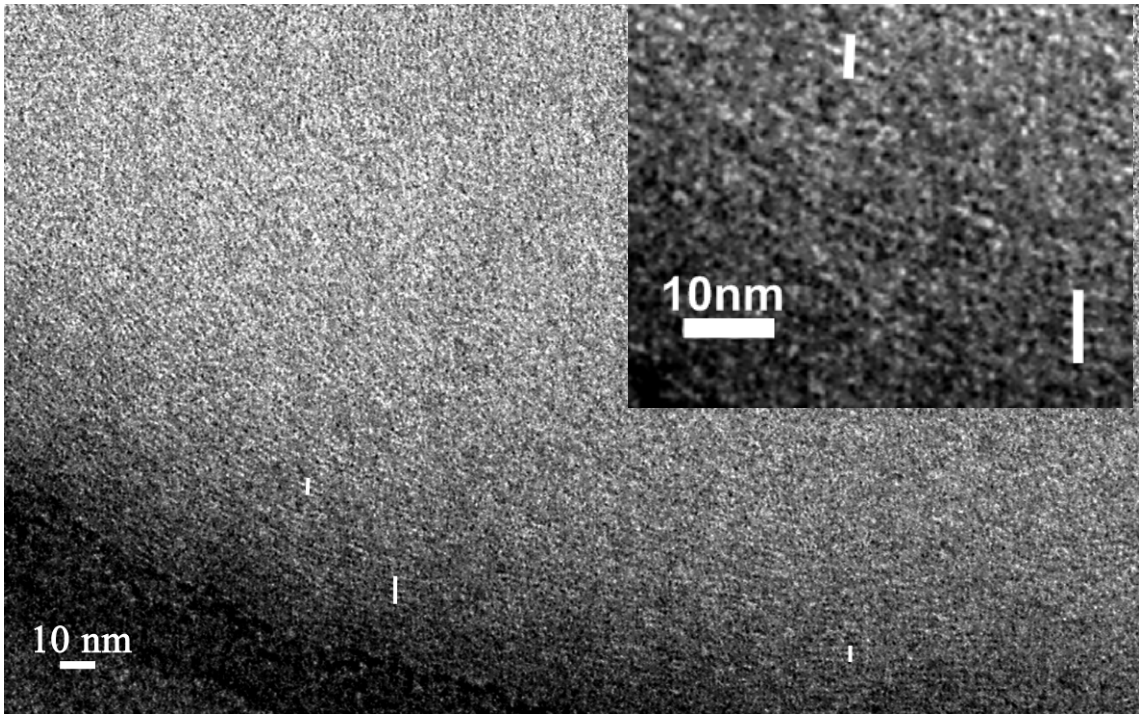

Fig. S5 Cryo-TEM image of **1a** (10 mg/ml H_2O) showing small fibres with a diameter of about 1.6 nm, as measured across the indicated white lines.

3.2 Synthesis and optical properties of water-soluble polyglycerol-dendronized rylene bisimide dyes

Timm Heek, Frank Würthner*, and Rainer Haag*

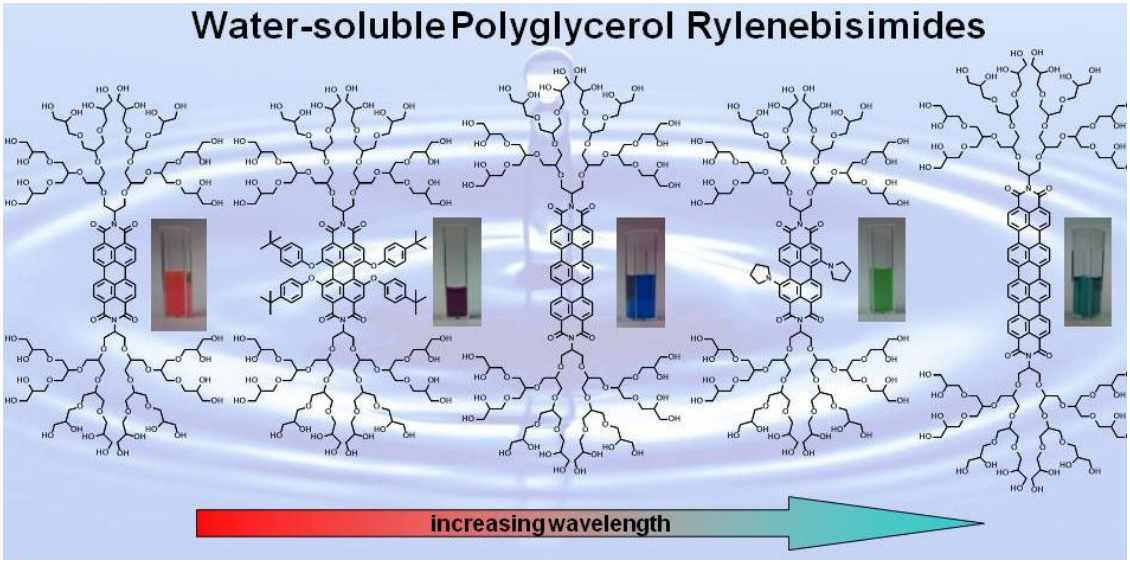

In this publication the contribution of the author was the idea, synthesis and complete photophysical characterization of the rylene - polyglycerol dyes. Frank Würthner provided one starting material and theoretical support in terms of extensive corrections and interpretation of the data.

This article was submitted for publication.

Timm Heek, Frank Würthner, and Rainer Haag, *Synthesis and optical properties of water-soluble polyglycerol-dendronized rylene bisimide dyes*, Chemistry – A European Journal, **2013**, *19*, 10911-10921. (DOI: 10.1002/chem.201300556)

3.3 Energy transfer in nanotube-perylene complexes

Frederike Ernst*, Timm Heek, Antonio Setaro, Rainer Haag, and Stephanie Reich

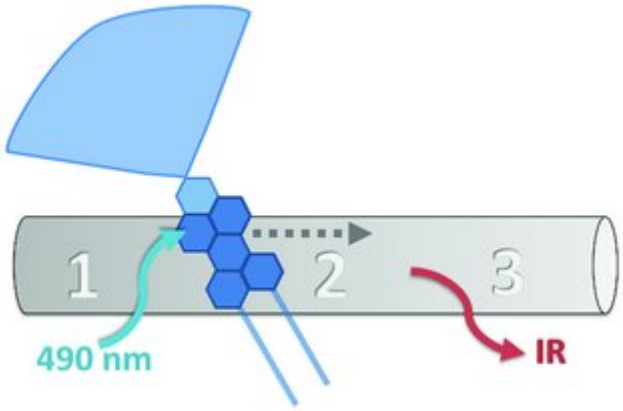

In this publication the author provided the idea and synthesis of the corresponding amphipilic perylene derivative. The photophysical characterization of the single-walled carbon nanotube (SWCNT) surfactant complex was performed by cooperation partners from AG Reich.

This article was published in the following journal:

Frederike Ernst, Timm Heek, Antonio Setaro, Rainer Haag, and Stephanie Reich, *Energy transfer in nanotube-perylene complexes,* Advanced Functional Materials, **2012**, 22, 3921-3926. (DOI: 10.1002/adfm.201200784)

3.4 Functional surfactants for carbon nanotubes: effects of design

Frederike Ernst, Timm Heek, Antonio Setaro, Rainer Haag, and Stephanie Reich*

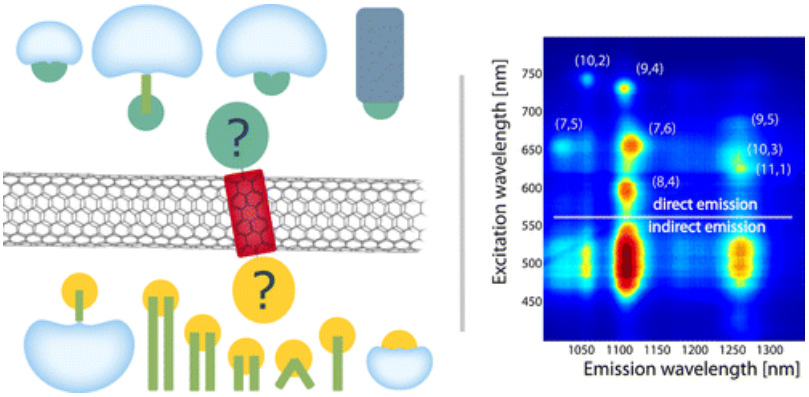

In this publication the author developed the idea for the different surfactant designs and synthesized and characterized the compounds. The photophysical characterization of the single-walled carbon nanotube (SWCNT) surfactant complexes was performed by cooperation partners from AG Reich.

This article was published in the following journal:

Frederike Ernst, Timm Heek, Antonio Setaro, Rainer Haag, and Stephanie Reich, *Functional Surfactants for Carbon Nanotubes: Effects of Design,* Journal of Physical Chemistry C, **2013**, 117 (2), 1157-1162. (DOI: 10.1021/jp3098186)

3.5 Chirally enhanced solubilization through perylene-based surfactant

Frederike Ernst*, Timm Heek, Antonio Setaro, Rainer Haag, and Stephanie Reich

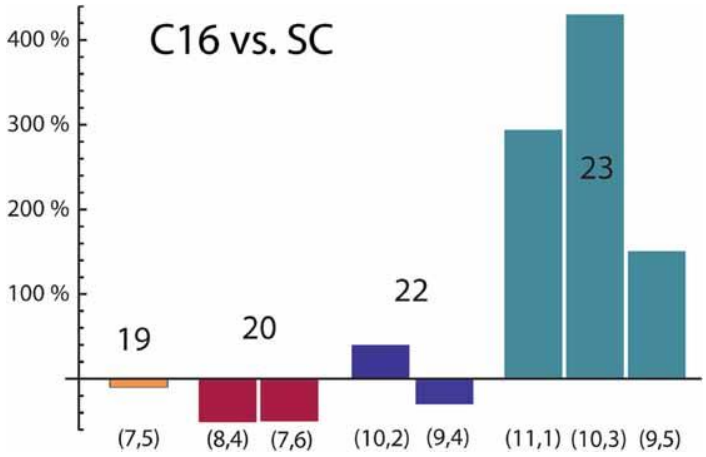

In this publication the author synthesized and characterized the used surfactant. The idea and the photophysical characterization of the single walled carbon nanotube (SWCNT) surfactant complexes were performed by cooperation partners from AG Reich.

This article was published in the following journal:

Frederike Ernst, Timm Heek, Antonio Setaro, Rainer Haag, and Stephanie Reich, *Chirally enhanced solubilization through perylene-based surfactant,* Physica Status Solidi (b), **2012**, 249, 2465-2468. (DOI: 10.1002/pssb.201200192)

3.6 An amphiphilic perylene imido diester for selective cellular imaging

Timm Heek, Jörg Nikolaus, Roland Schwarzer, Carlo Fasting, Pia Welker, Kai Licha, Andreas Herrmann* and Rainer Haag*

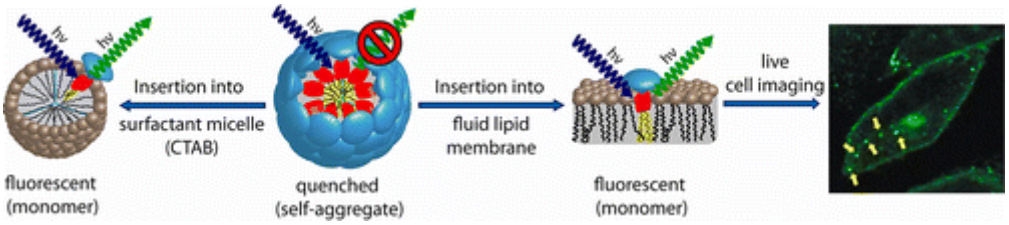

In this publication the author developed the idea, synthesis and the photophysical characterization of the perylene – polyglycerol membrane marker that was used. The biological experiments concerning cell toxicity, FACS, vesicle preparation, and confocal imaging studies were performed either in corporation with partners from the Mivenion GmbH or the AG Herrmann.

This article was published in the following journal:

Timm Heek, Jörg Nikolaus, Roland Schwarzer, Carlo Fasting, Pia Welker, Kai Licha, Andreas Herrmann and Rainer Haag, *An amphiphilic perylene imido diester for selective cellular imaging,* Bioconjugate Chemistry*,* **2013**, 24 (2), 153-158. (DOI: 10.1021/bc3005655)

4 Summary and conclusion

In this thesis the synthesis and application of polyglycerol (PG) dendronized water-soluble rylene derivatives as new functional dyes were demonstrated. In a first study it was shown that water-soluble perylene bisimides (PBIs) can be efficiently prepared by a simple condensation reaction of amine cored PG dendrons with the corresponding anhydride of perylene bisanhydride in high yields. Interestingly, the different generations of PG dendron showed only a limited influence on the coupling efficiency to the perylene core which was rather unexpected as the stericial shielding of the reactive core of a [G4]-PG dendron is quite remarkable. Although all generations revealed high water-solubility, the lower generations ([G1] and [G2]) showed a pronounced H-aggregate formation and consequently a dramatic change in optical properties, especially a dramatic decrease in the fluorescence QY. The higher generations ([G3] and [G4]) showed no signs of aggregate formation. Therefore an extremely high FQY of up to 98% in an aqueous environment was observed for the first time for core unsubstituted PBIs. These properties make these dyes promising candidates for bioimaging purposes. However, especially for in vivo imaging studies, fluorophores with more red-shifted absorption and emission profiles are of greater interest as they allow a deeper detection in the tissue material. Core substituted PBIs with red-shifted optical properties as well as higher rylene homologs TBI and QBI bearing PG dendrons were therefore synthesized in the following study, and their optical properties determined. Although a double substitution with [G3] PG dendrons showed a somewhat lower fluorescence QY in the case of core unsubstituted PBIs, due to an easier synthesis and a sufficient aggregation suppression it was chosen as benchmark generation for the new dye cores. The design of these new PG-dye conjugates followed the same approach as for the PG-PBIs, namely, by introducing the PG dendrons at the imide positions via condensation of PG amines. As the corresponding anhydrides were not readily available in high purity and yield, more elaborated synthetic pathways had to be taken. It turned out that, besides aggregation for the core substituted PBIs, concurrent electron transfer processes from the electron rich substitutents to the perylene core play a far more important role in the fluorescence quenching in the highly polar solvent water. Although successful at introducing water-solubility to the higher rylene homologs TBI and QBI, the dendron generation was too small to successfully suppress their aggregation. However, for the first time, a concentration-dependent aggregation behavior of TBIs was observed and the related thermodynamic parameters were successfully determined. This information might become essential in the future development of supramolecular architectures bases on TBIs.

In the next studies, the goal was to introduce functionality to the PG perylene based dyes. Therefore in a first study, two aliphatic chains were introduced giving the dye conjugate a classical wedge type

amphiphile character. This conjugate was successfully applied as surfactant for single-walled carbon nanotubes (SWCNT). It was shown that the prepared dispersions were stable over several months and that the surfactant could efficiently debundle SWCNTs into individual tubes. Moreover, an extremely efficient energy transfer from the dye to the SWCNT was observed upon direct excitation of the perylene moiety. Although such energy transfer processes are known for other chromophors, e.g., porphyrines, this was observed for the first time for perylene based systems. Besides this very unique property, a follow-up study revealed that the surfactant also possesses selectivity towards SWCNTs with a certain chirality which is of interest because one major challenge in SWCNT research is the preparative separation of this polydisperse material. Encouraged by these findings, a whole set of perylene based amphiphiles were synthesized in order to find a "perfect" surfactant design for SCWNT solubilization and sensitization. First it was found that PG dendrons possess a superior solubilizing power in comparison to linear polyethyleneglycol (PEG) chains. Secondly, it was shown that a wedge type amphiphile design is much better in terms of debundling capacity and long-term stability. Lastly, the length of the aliphatic chains was varied showing that there is an optimum length which should be chosen carefully, as the interaction with the SWCNTs is otherwise either too weak or, if the hydrophobicity becomes too high, the tendency of self-aggregation of the surfactant becomes dominant yielding in less surfactant bound to SWCNTs.

In a final study, one of the amphiphilic PG-perylene dyes was modified for application as fluorescent membrane marker in optical bioimaging. Therefore, the two alkyl chain concept from the surfactant design was retained and the length of the aliphatic chains chosen that the overall length of the hydrophobic part perfectly fits the length of one lipid bilayer leaflet. Due to the fact that it forms fluorescently self-quenched aggregates, it gives a good contrast to the surrounding material as free and unbound dye cannot be visualized. It was clearly shown that the quenched fluorescence of the marker can be recovered in water upon treatment with a surfactant solution by breaking up the aggregates and that it can be easily incorporated into lipid membranes by applying it in the imaging of artificial membranes of giant unilamellar vesicles. In addition, the incorporation into different lipid environments proves that the dye has a high specificity towards liquid disordered domains. Finally, it was demonstrated that the dye can be easily used in the staining of living cells and that the uptake from the dye into living cells appears via endocytic pathways after incorporation into the plasma membrane. The dye was applied successfully to different cell lines showing its potential as general membrane marker. Overall this makes it an ideal platform for the tracking and anchoring of dendron bound bioactive substances into artificial or cellular membranes.

In conclusion, it could be demonstrated that the combination of PG dendrons with rylene dye constitute an extraordinarily promising platform for the construction of functional water-soluble fluorescent dyes.

5 Outlook

Based on the findings within this thesis there are different topics of interest for further development of functional PG dendronized rylene dyes. For example, it would be interesting to find a synthetic pathway to introduce active conjugateable groups like maleimide or NHS-ester groups to the water-soluble rylene derivatives for application as fluorescent label of biomolecules. Therefore either a synthetic method to modify the PG dendron synthesis with exactly one active group seems a plausible approach or alternatively one could apply methods known in the literature for the preparation of unsymmetrical substituted rylene dyes and evaluate if higher PG generations (G4 or G5) are capable of providing sufficient water-solubility if only attached at one imide functionality.

Another simple way to introduce an additional functionality to water-soluble rylene dyes would be to introduce sulfate groups at the periphery. Pure PG-sulfates are known to be highly effective as an inflammation specific agent. Therefore one would expect a similar effect for the sulfated rylene dyes. This would be of benefit as one would be able to exactly follow individual PG rylene sulfates via optical imaging methods without the trouble of having statistically labeled polymeric bioactive material.

Although the newly reported membrane marker has been shown to be quite effective for labeling disordered lipid domains, it would be interesting to tune the dye scaffold towards a specificity of liquid ordered domains, the so-called RAFT domains, which are the site for many important cellular surface processes. This might be achieved via the introduction of a spacer unit between the water-solubilizing PG dendron and the chromophore to allow a deeper insertion into the lipid bilayer and therefore an increased probability of interaction with the RAFT domain bound cholesterol which should be detectable via time resolved fluorescence spectroscopy. Alternatively, a synthetic approach introducing a cholesterol moiety to the PG dendron rylen dye scaffold would also serve the same purpose.

Finally, due to the combination of an aliphatic interior with an enlarged aromatic scaffold, it would be interesting to investigate the aggregated membrane marker as a potential drug delivery construct, as it should be able to efficiently encapsulate hydrophobic guest molecules. As the micelles are easily broken up upon reaching the cell surface, one would expect an efficient release of the loaded guest molecules into the cellular system.

6 Short summary/Kurzzusammenfassung

6.1 Short summary

Within this thesis different polyglycerol (PG) dendronized rylene dyes were synthesized and their photophysical properties determined as well as their possible application in two different fields tested. In the first part it was shown, that a high water-solubility could be introduced to the completely hydrophobic dye material by a substitution with PG-dendrons at the imide positions of perylene bisimide. Furthermore by just increasing the steric demand of the PG-dendrons by increasing the attached dendron generation (up to [G4]), the strong aggregation tendency was successfully suppressed thereby yielding highly fluorescent perylene bisimide dyes. Based on these findings, another set of bay functionalized perylene bisimides as well as the higher rylene homologs terrylene bisimide and quaterrylene bisimide bearing PG-dendrons were synthesized and their spectral characteristics determined. Due to their higher lying absorption and emission profiles these dye conjugates are of special interest for biological imaging as they are near or within the so-called optical window.

In the second part, the capability of PG dendronized rylene dyes to serve as a platform for the development of functional dyes was investigated. Therefore first an amphiphilic character was introduced to the PG dendronized perylene dye by attaching two hydrophobic alkyl chains instead of one PG-dendron yielding a classical amphiphile. This was successfully applied as solubilizing agent for single-walled carbon nanotubes (SWCNT) in an aqueous environment. It was shown, that this did not only solubilize and debundle SWCNTs very effectively into individual tubes but it also caused an efficient energy transfer from the perylene dye moiety to the SWCNTs. Although similar energy transfer processes are known from other fluorophores, e.g., porphyrines to SWCNTs, this was the first time that this phenomenon was observed for a water-soluble perylene based amphiphile. In the following, a closer inspection of the suspension revealed that besides this extraordinary property the surfactant is also able to enrich SWCNTs with specific chiralities. This is of great importance, because the optoelectronic properties of SWCNTs strongly depend on the chirality and there are only few post-growth sorting mechanisms available. To get more insight into the solubilization and the energy transfer processes, a whole library of perylene based surfactants was then synthesized and tested. As a result different parameters for the rational design of an ideal SWCNT-surfactant design could be obtained.

In the last part, one of the amphiphiles was used as a fluorescent membrane marker for bioimaging purposes. Therefore, the design was adapted to allow the best interaction with natural lipid bilayer

membranes. It was shown that this marker easily intercalates into artificial and natural membranes and due to its high photostability and water solubility outperforms many commercially available membrane labels.

6.2 Kurzzusammenfassung

In der vorliegenden Arbeit wurden verschiedene Polyglycerol (PG) dendronisierte Rylen Farbstoffe hergestellt, deren photophysikalischen Eigenschaften sowie Ihre mögliche Anwendung als funktioneller Farbstoff in zwei unterschiedlichen Themenfeldern untersucht. Im ersten Teil konnte gezeigt werden, dass durch eine einfache Substitution mit PG-Dendronen an den Imid Positionen von Perylenebisimid eine hohe Wasserlöslichkeit dieses komplett hydrophoben Farbstoffs erreicht werden kann. Zusätzlich dazu konnte durch eine sukzessive Erhöhung der Dendrimergeneration (bis [G4]) und damit des sterischen Anspruchs die extrem ausgeprägte Aggregationsneigung erfolgreich unterdrückt werden. Dies resultierte in hoch fluoreszenten, wasserlöslichen Perylenbisimiden. Basierend auf diesen Ergebnissen wurden in Folge sowohl bay funktionalisierte als auch höhere Rylen Homologe wie Terrylenbisimid oder Quaterrylenbismid mit PG-Dendronen modifiziert und ihre optischen Eigenschaften bestimmt. Durch ihre längerwelligen Absorptions- und Emissionseigenschaften sind diese Farbstoffkonjugate insbesondere für biologische Bildgebungsverfahren interessant, da sie sich nahe oder innerhalb des sogenannten optischen Fensters für biologisches Gewebe befinden.

Im zweiten Teil wurde untersucht inwiefern sich PG denronisierte Rylen Farbstoffe als Plattform für die Entwicklung von funktionellen Farbstoffen eigenen. Dafür wurde der PG-dendroniserte Perylen Farbstoff in eine klassische amphiphile Struktur umgewandelt indem ein PG-Dendron durch zwei Alkylketten ersetzt wurde. Dieser Farbstoff konnte erfolgreich als Tensid für die Solubilisierung von einwandigen Kohlenstoffnanoröhren (engl. SWCNT) in wässriger Umgebung eingesetzt werden. Desweiteren konnte gezeigt werden, dass neben der hoch effizienten Solubilisierung und Entbündelung der SWCNTs zu einzelnen Röhren ein effizienter Energietransfer vom Perylen Farbstoff in die SWCTNs stattfindet. Obwohl dieser Effekt von anderen Farbstoffen bekannt ist, insbesondere von Porphyrinen, ist dies das erste Mal, dass dieser Effekt bei wasserlöslichen Perylen basierten Amphiphilen auftritt. Darauf folgende Untersuchungen zeigten, dass der Farbstoff neben dieser außergewöhnlichen Eigenschaft auch zu einer Anreicherung von SWCNTs mit bestimmten Chiralitäten verwendet werden kann. Dies ist von besonderer Bedeutung, da die opto-elektronischen Eigenschaften von SWCNTs stark von der jeweiligen Chiralität abhängen und es bis dato nur sehr wenige Sortiermechanismen dafür gibt. Um ein tieferes Verständnis für den Solubiliserungs- und den Energietransferprozess zu erhalten wurde abschließend eine Bibliothek von Perylen basierten

Amphiphilen hergestellt und getestet. Daraus konnten verschiedene Parameter bezüglich des Designs eines idealen SCWNTs-Tensids abgeleitet werden.

Im letzten Teil der Arbeit wurde einer der amphiphilen Farbstoffe als fluoreszenter Membranmarker in der biologischen Bildgebung angewendet. Dafür wurde das Design so gewählt, das es eine bestmögliche Interaktion mit natürlichen Lipid-Doppelschichten gewährleistet. Es konnte gezeigt werden, dass dieser Marker sowohl in der Lage ist in künstliche Membranen als auch in natürliche Zellemembranen zu Interkalieren und dass seine hohe Photostabilität die von vielen kommerziell erhältlichen Membranmarkern übertrifft.

7 References

[1] H. Valladas, J. Clottes, J.-M. Geneste, M. A. Garcia, M. Arnold, H. Cachier, N. Tisnérat-Laborde, *Nature,* **2001**, *413*, 479.

[2] D. Jacoby, *Dumberton Oak Papers*, **200**4, *58*, 197-240.

[3] http://www.seilnacht.com/Lexikon/purp1.htm, **2006**.

[4] A. Kraft, *Bull. Hist. Chem*., **2008**, *33*, 61-67.

[5] K. Hubner, *Chem. Unserer Zeit*, **2006**, *40*, 274-275.

[6] A. Baeyer and A. Emmerling, *Ber. Dtsch. Chem. Ges*., **1870**, *3*, 514–517.

[7] R. M. Christie, *Colour Chemistry,* RSC Paperbacks Cambridge, **2001**, *6*.

[8] a.) H. Spanggaard and F. C. Krebs, *Sol. Energ. Mat. Sol. C.*, **2004**, *83*, 125-146. b.) G. S. Shankarling, K. J. Jarag, *Resonance*, **2010**, *15*, 804-818. c.) M. Clark, *Handbook of textile and industrial dyeing: Applications of dyes*, Woodhead publishing limited, Cambridge, **2011**.

[9] J. Griffiths, *Chem. Unserer Zeit*, **1993**, *27*, 21-31.

[10] K. Meyer, *Chem. Unserer Zeit*, **2002**, *36*, 178–192.

[11] J. Barber, *Chem. Soc. Rev*, **2009**, *38*, 185-196.

[12] E. Clar, *Chem. Ber.*, **1948**, *81*, 52.

[13] H. Langhals, *Heterocycles,* **1995**, *40*, 477-500.

[14] M. Zander, *Polycyclische Aromaten - Kohlenwasserstoffe und Fullerene*, Teubner Verlag, Stuttgart, **1995**.

[15] F. Würthner, *Chem. Commun*., **2004**, 1564-1579.

[16] C. Huang, S. Barlow and S. R. Marder, *J. Org. Chem.*, **2011**, *76*, 2386-2407.

[17] C. Li and H. Wonneberger, *Adv. Mater.*, **2012**, *24*, 613-636.

[18] M. Kardos, D.R.P. 276357, **1913**.

[19] a.) T. Maki and H. Hashimoto, *Kogyo Kagaku Zasshi*, **1951**, *54*, 544. b.) Y. Nagao, *Prog. Org. Coat.*, **1997**, *31*, 43-49.

[20] E. B. Faulkner, R. J. Schwartz, *High Performance Pigments*, Wiley-VCH, Weinheim, **2009**.

[21] a.) J. Perlstein, *Chem. Mater*., **1994**, *6*, 319-326. b.) K.-Y. Law, *Chem. Rev*., **1993**, *93*, 449-486. c.) P. M. Kazmaier and R. Hoffmann, *J. Am. Chem. Soc*., **1994**, *116*, 9684-9691.

[22] A. Rademacher, S. Märkle and H. Langhals, *Chem. Ber*., **1982**, *115*, 2927-2934

[23] S. Demming and H. Langhals, *Chem. Ber*., **1988**, *121*, 225-230.

[24] a.) H. Langhals, S. Demmig and T. Potrawa, *J. Prakt. Chem.*, **1991**, *333*, 733–748. b.) H. Langhals, J. Karolin and L. B.-Å. Johansson, *J. Chem. Soc., Faraday Trans.*, **1998**, *94*, 2919–2922.

[25] a.) M. Sadrai, L. Hadel, R. R. Sauers, S. Husain, K. Krogh-Jespersen, J. D. Westbrook and G. R. Bird, *J. Phys. Chem.*, **1992**, 7988-7966. b.) J. Vura-Weis, M. A. Ratner and M. R. Wasielewski, *J. Am. Chem. Soc.*, **2010**, *132*, 1738-1739.

[26] a.) H. Langhals, *Chimia*, **1994**, *48*, 503-505. (b) N. Pasaogullari, H. Icil and M. Demuth, *Dyes Pigments*, **2005**, *69*, 118-127.

[27] a.) F. Würthner, C. Thalacker, S. Diele and C. Tschierske, *Chem.–Eur. J.*, **2001**, *7*, 2245–2253. b.) E. H. A. Beckers, S. C. J. Meskers, A. P. H. J. Schenning, Z. Chen, F. Würthner and R. A. J. Janssen, *J. Phys. Chem. A*, **2004**, *108*, 6933–6937.

[28] a.) R. Reisfeld and G. Seybold, *Chimia,* **1990**,*44,* 295. b.) H. G. Löhmannsröben and H. Langhals, *Appl. Phys. B,* **1989**, *48,* 449-452.

[29] G. Seybold and G. Wagenblast, *Dyes Pigments*, **1989**, *11*, 303–317.

[30] J. C. Goldschmidt, M. Peters, A. Bösch, H. Helmers, F. Dimroth, S.W. Glunz and G. Willeke, *Sol. Energ. Mat. Sol. C.*, **2009**, *93*, 176-182.

[31] a.) I. Luka and H. Langhals, *Chem. Ber.*, **1983**, *116*, 3524-3528. b.) M. Adachi and Y. Nagao, *Chem. Mater*., **1999**, *11*, 2107-2114.

[32] P. J. Regensburger and J. J. Jakubowski, U. S. P. 3 904 407, **1975**.

[33] H. Quante, Y. Geerts and K. Müllen, *Chem. Mater*., **1997**, *9*, 495-500.

[34] H. O. Loufty, A. M. Hor, P. Kazmaler and M. Tarn, *J. Imag. Sci*., **1989**, *33*, 151-159.

[35] a.) H. Eilingsfeld and M. Patsch, (BASF AG) Ger. Pat. DE 2519790 A1, **1976**. b.) R. Ruediger and G. Seybold, (BASF AG) Ger. Pat. DE 3434059 A1, **1985**.

[36] W. Qiu, S. Chen, X. Sun, Y. Liu and D. Zhu, *Org. Lett.*, **2006**, *8*, 867–870.

[37] A. Böhm, H. Arms, G. Henning, P. Blaschka, (BASF AG) Ger. Pat. DE 19547209 A1, **1997**; *Chem. Abstr.* **1997**, *127*, 96569g.

[38] F. Würthner, V. Stepanenko, Z. Chen, C. R. Saha-Moeller, N. Kocher and D. Stalke, *J. Org. Chem.,* **2004**, *69*, 7933–7939.

[39] P. Rajasingh, R. Cohen, E. Shirman, L. J. W. Shimon and B. Rybtchinski, *J. Org. Chem.*, **2007**, *72*, 5973-5979.

[40] a.) Z. Chen, U. Baumeister, C. Tschierske and F. Würthner, *Chem. Eur. J*, **2007**, *13*, 450-465. b.) F. Würthner, *Pure Appl. Chem*., **2006**, *78*, 2341-2349.

[41] D. Dotcheva, M. Klapper and K. Müllen, *Macromol. Chem. Phys*., **1994**, *195*, 1905-1911.

[42] a.) L. Perrin and P. Hudhomme, *Eur. J. Org. Chem*, **2011**, 5427-5440. b.) M. Bagui, T. Dutta, S. Chakraborty, J. S. Melinger, H. Zhong, A. Keightey and Z. Peng, *J. Phys. Chem. A*, **2011**, *115*, 1579–1592.

[43] R. Gvishi, R. Reisfeld and Z. Buhrstein, *Chem. Phys. Lett.*, **1993**, *213*, 338-344.

[44] P. Pösch, M. Thelakkat and H. W. Schmidt, *Synth. Met.*, **1999**, *102*, 1110–1112.

[45] a.) P. Osswald and F. Würthner, *Chem. Eur. J.*, **2007**, *13*, 7395-7409. b.) P. Osswald, D. Leusser, D. Stalke and F. Würthner, *Angew. Chem*., **2005**, *117*, 254–257; *Angew. Chem. Int. Ed.,* **2005**, *44*, 250–253.

[46] E. Fron, G. Schweitzer, P. Osswald, F. Würthner, P. Marsal, D. Beljonne, K. Müllen, F. C. De Schryver and M. Van der Auweraer, *Photochem. Photobiol. Sci*., **2008**, *7*, 1509-2521.

[47] Y. Zhao and M. R. Wasielewski, *Tetrahedron Lett.,* **1999**, *40*, 7047-7050.

[48] a.) A. S. Lukas, Y. Zhao, S. E. Miller and M. R. Wasielewski, *J. Phys. Chem. B*, **2002**, *106*, 1299. b.) R. K. Dubey, A. Efimov and H. Lemmetyinen, *Chem. Mater.,* **2011**, *23*, 778–788.

[49] a.) F. Würthner, P. Osswald, R. Schmidt, T. E. Kaiser, H. Mansikkämaki and M. Könemann, *Org. Lett.* **2006**, *8*, 3765–3768. b.) R. Schmidt, M. M. Ling, J. H. Oh, M. Winkler, M. Könemann, Z. Bao and F. Würthner, *Adv. Mater.*, **2007**, *19*, 3692–3695.

[50] M. J. Ahrens, M. J. Fuller and M. R. Wasielewski, *Chem. Mater.*, **2003**, *15*, 2684–2686.

[51] a.) N. V. Handa, K. D. Mendoza and L. D. Shirtcliff, *Org. Lett*., **2011**, *13*, 4724-4727. b.) M. Bagui, T. Dutta, H. Zhong, S. Li, S. Chakraborty, A. Keightley and Z. Peng, *Tetrahedron*, **2012**, *68*, 13, 2806–2818.

[52] C. C. Chao, M. K. Leung, Y. O. Su, K. Y. Chiu, T. H. Lin, S. J. Shieh and S. C. Lin, *J. Org. Chem*. , **2005**, *70*, 4323−4331.

[53] a.) C. L. Eversloh, C. Li and K. Müllen, *Org. Lett*., **2011**, *13*, 4148-4150. b.) U. Rohr, P. Schlichting, A. Böhm, M. Gross, K. Meerholz, C. Bräuchle and K. Müllen, *Angew. Chem*., **1998**, *110*, 1463-1467; *Angew. Chem., Int. Ed*., **1998**, *37*, 1434–1437. c.) S. Müller and K. Müllen, *Chem. Commun.*, **2005**, 4045–4046.

[54] H. Langhals and S. Kirner, *Eur. J. Org. Chem.*, **2000**, 365–380.

[55] H. Qian, C. Liu, Z. Wang and D. Zhu, *Chem. Commun.*, **2006**, 4587-4589.

[56] H. Langhals and P. Blanke, *Dyes Pigments,* **2003**, *59*, 109–116.

[57] a.)L. Feiler, H. Langhals and K. Polborn, *Liebigs Ann.* **1995**, 1229–1244. b.) W. Helfer and A. Böhm, (BASF AG), DE 19501737 A1, **1996**.

[58] a.) Y. Nagao, Y. Abe and T. Misono, *Dyes Pigments*, **1991**, *16*, 19–25. b.) H. Quante and K. Müllen, *Angew. Chem.*, **1995**, *107*, 1487-1489; *Angew. Chem. Int. Ed.*, **1995**, *34*, 1323-1325.

[59] J. Hofkens, L. Latterini, G. De Belder, T. Gensch, M. Maus, T. Vosch, Y. Karni, G. Schweitzer, F.C. De Schryver, A. Hermann and K. Müllen, *Chem. Phys. Lett*., **1999**, 1-9.

[60] K.-y. Tomizaki, P. Thamyongkit, R. S. Loewe, J. S. Lindsey, *Tetrahedron*, **2003**, *59*, 1191–1207.

[61] a.) P. D. Zoon, and A. Brouwer, *ChemPhysChem*, **2005**, *6*, 1574–1580. b.) M. J. Fuller and M. R. Wasielewski, *J. Phys. Chem. B,* **2001**, *105*, 7216–7219.

[62] a.) M. A. Miller, R. K. Lammi, S. Prathapan, D. Holten and J. S. Lindsey, *J. Org. Chem*., **2000**, *65*, 6634-6649. b.) D. Veldman, S. M. A. Chopin, S. C. J. Meskers and R. A. J. Janssen, *J. Phys. Chem. C.*, **2008**, *112*, 8617-8632.

[63] C. Li, J. Schöneboom, Z. Liu, N. G. Pschirer, P. Erk, A. Herrmann and K. Müllen, *Chem. Eur. J*, **2009**, *15*, 878-884.

[64] H. Langhals, G. Schönmann and L. Feiler, *Tetrahedron Lett.*, **1995**, 6423-6424.

[65] H. Langhals, J. Büttner and P. Blanke, *Synthesis*, **2005**, 364-366.

[66] H. Quante and K. Müllen, *Angew. Chem.*, **1995**, 34, 1323-1325; *Angew. Chem. Int. Ed.*, **1995**, *34*, 1323-1325.

[67] T. Yamamoto, A. Morita, Y. Miyazaki, Y. Maruyama, H. Wakayama, Z. Zhou, Y. Nakamura and T. Kanbara, *Macromolecules*, **1992**, *25*, 1214-1223.

[68] Y. Geerts, H. Quante, H. Platz, R. Mahrt, M. Hopmeier, A. Böhm and K. Müllen, *J. Mater. Chem.*, **1998**, *8*, 2357-2369.

[69] F. Nolde, W. Pisula, S. Müller, C. Kohl and K. Müllen, *Chem. Mater*, **2006**, *18*, 3715-3725.

[70] F. O. Holtrup, G. R. J. Müller, H. Quante, S. De Feyter, F. C. De Schryver and K. Müllen, *Chem. Eur. J.*, **1997**, *3*, 219-225.

[71] F. Nolde, J. Qu, C. Kohl, N. G. Pschirer, E. Reuther and K. Müllen, *Chem. Eur. J.*, **2005**, *11*, 3959-3967.

[72] N. G. Pschirer, C. Kohl, F. Nolde, J. Qu and K. Müllen, *Angew. Chem*., **2006**, *118*, 1429-1432; *Angew. Chem. Int. Ed*., **2006**, *45*, 1401-1404.

[73] T. Weil, E. Reuther,C. Beer and K. Müllen, *Chem. Eur. J.*, **2004**, *10*, 1398-1414.

[74] Y. Avlasevich, S. Müller, P. Erk and K. Müllen, *Chem. Eur. J.*, **2007**, *13*, 6555-6561.

[75] J. E. Bullock, M. T. Vagnini, C. Ramanan, D. T. Co, T. M. Wilson, J. W. Dicke, T. J. Marks and M. R. Wasielewski, *J. Phys. Chem. B*, **2010**, *114*, 1794-1802.

[76] a) S. Murai, F. Kakiuchi, S. Sekine, Y. Tanaka, A. Kamatani, M. Sonoda and N. Chatani, *Nature*, **1993**, *366*, 529-531. b) F. Kakiuchi and S. Murai, *Acc. Chem. Res*., **2002**, *35*, 826-834.

[77] S. Nakazono, Y. Imazaki, H. Yoo, J. Yang, T. Sasamori, N. Tokitoh, T. Cédric, H. Kageyama, D. Kim, H. Shinokubo and A. Osuka, *Chem. Eur. J.*, **2009**, *15*, 7530-7533.

[78] S. Nakazono, S. Easwaramoorthi, D. Kim, H. Shinokubo and A. Osuka, *Org. Lett*., **2009**, *11*, 5426-5429.

[79] a.) W. E. Ford and P. V. Kamat, *J. Phys. Chem*., **1987**, *91*, 6373-6380. b.) E. M. Ebeid, S. A. El-Daly and H. Langhals, *J. Phys. Chem*., **1988**, *92*, 4565-4568.

[80] T. Teraoka, S. Hiroto, and H. Shinokubo, *Org. Lett*., **2011**, *13*, 2532-2535.

[81] a.) G. Battagliarin, C. Li, V. Enkelmann and K. Müllen, *Org. Lett.*, **2011**, *13*, 3012-3015. b.) G. Battagliarin, Y. Zhao, C. Li and K. Müllen, *Org. Lett*., **2011**, *13*, 3399-3401.

[82] H. Eilingsfeld and M. Patsch, (BASF AG), Ger. Pat. DE 2456738 A1, **1976**,

[83] R. Stolarksi and K. J. Fiksinski, *Dyes Pigments*, **1994**, *24*, 295-303.

[84] X. Mo, H.-Z. Chen, M.-M. Shi and M. Wang, *Chem. Phys. Lett*., **2006**, *417*, 457-460.

[85] C. Xue, R. Sun, R. Annab, D. Abadi and S. Jin, *Tetrahedron Lett*., **2009**, *50*, 853-856.

[86] X. Mo, M.-M. Shi, J.-C. Huang, M. Wang and H.-Z. Chen, *Dyes Pigments*, **2008**, *76*, 236-242.

[87] L. Yang, M. M. Shi, M. Wang and H. Chen, *Tetrahedron*, **2008**, *64*, 5404-5409.

[88] S. A. El-Daly, M. K. Awad, S. T. Abdel-Halim and D. A. Dowidar, *Spectrochim Acta A*, **2008**, *71*, 1063-1069.

[89] J. Kelber, H. Bock, O. Thiebaut, E. Grelet and H. Langhals, *Eur. J. Org. Chem*., **2011**, 707-712.

[90] I. Seguy, P. Jolinat, P. Destruel, R. Mamy, H. Allouchi, C. Courseille, M. Cotrait and H. Bock, *ChemPhysChem*, **2001**, *7*, 448-452.

[91] M. Hof, R. Hutterer and V. Fidler, *Fluorescence Spectroscopy in Biology: Advanced Methods and their Applications to Membranes, Proteins, DNA, and Cells*, Springer-Verlag, Heidelberg, **2005**.

[92] M. S. T. Goncalves, *Chem. Rev*., **2009**, *109*, 190-212.

[93] W. E Mörner, *Nat. Methods*, **2006**, *3*, 781-782.

[94] a.) S. W. Hell and J. Wichmann, *Opt. Lett*., **1994**, *19*, 780-782. b.) T. A. Klar and S. W. Hell, *Opt. Lett*., **1999**, *24*, 954-956.

[95] M. J. Rust, M. Bates and X. Zhuang, *Nat. Methods*, **2000**, *3*, 793-796.

[96] E. Betzig, G. H. Patterson, R. Sougrat, O. W. Lindwasser, S. Olenych, J. S. Bonifacino, M. W. Davidson, J. Lippincott-Schwartz and H. F. Hess, *Sciene*, **2006**, *313*, 1642-1645.

[97] M. Fernández-Suárez and A. Y. Ting, *Nat. Rev. Mol. Cell. Bio*., **2008**, *9*, 929-943.

[98] A. Margineanu, J. Hofkens, M. Cotlet, S. Habuchi, A. Stefan, J. Qu, C. Kohl, K. Müllen, J. J. Vercammen, Y. Engelborghs, T. Gensch and F. C. De Schryver, *J. Phys. Chem. B*, **2004**, *108*, 12242-12251.

[99] M. Kasha, H. R. Rawls and M. Ashraf El-Bayoumi, *Pure Appl. Chem*., **1965**, *11*, 371-392.

[100] E. E. Jelley, *Nature*, **1936**, *138*, 1009-1010.

[101] G. Scheibe, *Angew. Chem*. , **1937**, *50*, 212-219.

[102] T. E. Kaiser, H. Wang, V. Stepanenko and F. Würthner, *Angew. Chem.* , **2007**, *119*, 5637-5640; *Angew. Chem. Int. Ed.*, **2007**, *46*, 5541-5544.

[103] R. F. Fink, J. Seibt, V. Engel, M. Renz, M. Kaupp, S. Lochbrunner, H. Zhao, J. Pfister, F. Würthner and B. Engels, *J. Am. Chem. Soc*, **2008**, *130*, 12858-12859.

[104] a.) A. S. Davydov, *Zh. Eksp. Teor. Fiz*. **1948,** *18*, 210-218. b.) A. S. Davydov, Theory of Molecular Excitons. Translated from the Russian by Michael Kasha and Max Oppenheimer, **1962**, 174.

[105] F. Würthner, T. E. Kaiser and C. R. Saha-Möller, *Angew. Chem*., **2011**, *123*, 3436-3473; *Angew. Chem. Int. Ed.*, **2011**, *50*, 3376-3410.

[106] E.-Z. M. Ebeid and S. A. El-Daly*, J. Phys. Chem*., **1988**, *92*, 4565-4568.

[107] D. Görl, X. Zhang and F. Würthner, *Angew. Chem*., **2012**, *124*, 6434-6455; *Angew. Chem. Int. Ed.*, **2012**, *51*, 6328-6348.

[108] W. E. Ford, *J. Photochem*., **1987**, *37*, 189-204.

[109] G. Schnurpfeil, J. Stark and D. Wöhrle, *Dyes Pigments*, **1994**, *27*, 339-350.

[110] H. Langhals, Ger. Pat. DE 3703513, **1987**.

[111] H. Langhals, W. Jona, F. Einsiedl and S. Wohnlich, *Adv. Mater*, **1998**, *10*, 1022-1024.

[112] J. H. Ryu, C. J. Yang, Y. S. Yoo, S. G. Lim and M. Lee, *J. Org. Chem*., **2005**, *70*, 8956-8962.

[113] R. Samudrala, X. Zhang, R. M. Wadkins and D. L. Mattern, *Bioorg. Med. Chem*. , **2007**, *15*, 186-193.

[114] H.-A. Klok, J. R. Hernandéz, S. Becker and K. Müllen, *J. Polym. Sci. A: Polym. Chem*., **2001**, *39*, 1572-1583.

[115] J. Hernandéz Rodriguez, Dissertation, Johannes Gutenberg Universität (Mainz), **2003**.

[116] M. Yin, C. R. W. Kuhlmann, K. Sorokina, C. Li, G. Mihov, E. Pietrowski, K. Koynov, M. Klapper, H. J. Luhmann, K. Müllen and T. Weil, *Biomacromolecules*, **2008**, *9*, 1381-1389.

[117] D. Liu, S. De Feyter, M. Cotlet, A. Stefan, U.-M. Wiesler, A. Herrmann, D. Grebler-Köhler, J. Qu, K. Müllen and F. C. De Schryver, *Macromolecules*, **2003**, *36*, 5918-5925.

[118] U. Resch-Genger, M. Grabolle, S. Cavaliere-Jaricot, R. Nitschke and T. Nann, *Nat. Methods*, **2008**, *5*, 763-775.

[119] C. Kohl, T. Weil, J. Qu and K. Müllen, *Chem. Eur. J*., **2004**, *10*, 5297-5310.

[120] T. Tang, K. Peneva, K. Müllen and S. E. Webber, *J. Phys. Chem. A*, **2007**, *111*, 10609-10614.

[121] K. Penava, G. Mihov, F. Nolde, S. Rocha, J.-I. Hotta, K. Braeckmans, J. Hofkens, H. Uji-I, A. Herrmann and K. Müllen, *Angew. Chem*., **2008**, *120*, 3420-3423; *Angew. Chem. Int. Ed*., **2008**, *47*, 3372-3375.

[122] K. Penava, G. Mihov, A. Herrmann, N. Zarrabi, M. Börsch, T. M. Duncan and K. Müllen, *J. Am. Chem. Soc.*, **2008**, *130*, 5398-5399.

[123] K. Peneva, K. Gundlach, A. Herrmann, H. Paulsen and K. Müllen, *Org. Biomol. Chem*., **2010**, *8*, 4823-4826.

[124] F. J. Céspades-Guiaro, A. B. Ropero, E. Font-Sanchis, Á. Nadal, F. Fernández-Lazaro and Á. Sastre-Santos, *Chem. Commun*., **2011**, *47*, 8307-8309.

[125] C. D. Schmidt, C. Böttcher and A. Hirsch, *Eur. J. Org. Chem*., **2007**, 5497-5505.

[126] B. Gao, H. Li, H. Liu, L. Zhang, Q. Bai and X. Ba, *Chem. Commun*., **2011**, *47*, 3894-3896.

[127] V. J. Pansare, S. Hejazi, W. J. Faenza and R. K. Prud´homme, *Chem. Mater*., **2012**, *24*, 812-827.

[128] J. Rodríguez-Hernández, J. Qu, E. Reuther, H.-A. Klok and K- Müllen, *Polym. Bull*., **2004**, *52*, 57-64.

[129] C. Jung, B. K. Müller, D. C. Lamb, F. Nolde, K. Müllen and C. Bräuchle, *J. Am. Chem. Soc*., **2006**, *128*, 5283-5291.

[130] C. Jung, N. Ruthardt, R. Lewis, J. Michaelis, B. Sodeik, F. Nolde, K. Penava, K. Müllen and C. Bräuchle, *ChemPhysChem*, **2009**, *10*, 180-190.

[131] a.) D. Rehm, A. Weller, *Ber. Bunsenges. Phys. Chem.* **1969**, *73*, 834-845 b.) M. W. Holman, R. Liu, L. Zang, P. Yan, S. A. DiBenedetto, R. D. Bowers and D. A. Adams, *J. Am. Chem. Soc.,* **2004**, *126*, 16126-16133.

[132] M. Davies, C. Jung, P. Wallis, T. Schnitzler, C. Li, K. Müllen and C. Bräuchle, *ChemPhysChem*, **2011**, *12*, 1588-1595.

[133] R. Marquis, C. Greco, I. Sadokierska, S. Lebedkin, M. M. Kappes, T. Michel, L. Alvarez, J.-L. Sauvajol, S. Meunier and C. Mioskowski, *Nano Lett*., **2008**, *8*, 1830-1835.

[134] E. Buhleier, W. Wehner and F. Vögtle, *Synthesis*, **1978**, *78*, 155-158.

[135] F. Vögtle, G. Richardt and N. Werner, *Dendritische Moleküle*, Teubner Verlag, Wiesbaden, **2007**.

[136] M. J. Maciejewski, *J. Macromol. Sci. A,* **1982**, *17*, 689-703.

[137] P. G. De Gennes and H. Hervet, *J. Physique Lett*., **1983**, *44*, 351-360.

[138] R. G. Denkewalter , J. Kolc and W. J. Lukasavage, US Pat. 4289872, **1981**, A 19810915.

[139] D.A. Tomalia, H. Baker, J. Dewald, M. Hall, G. Kallos, S. Martin, J. Roeck, J. Ryder, P. Smith, *Polymer J.,* **1985**, *17*, 117-132.

[140] M. V. Walter and M. Malkoch, *Chem. Soc. Rev.*, **2012**, *41*, 4593-4609.

[141] A. W. Bosman, H. M. Janssen and E. W. Meijer, *Chem. Rev*., **1999**, *99*, 1665-1688.

[142] C. J. Hawker and J. M. J. Fréchet, *J. Am. Chem. Soc*., **1990**, *112*, 7638-7647.

[143] a.) E. M. M. De Brabander van den Berg and E. W. Meijer, *Angew. Chem*, **1993**, *105*, 1370-1372; *Angew. Chem. Int. Ed*., **1993**, *32*, 1308-1311. b.) C. Wörner and R. Mühlhaupt, *Angew. Chem.*, **1993**, *105*, 1367-1370; *Angew. Chem. Int. Ed*., **1993**, *32,* 1306-1308.

[144] G. R. Newkome, Z. Yao, G. R. Baker and V. K. Gupta, *J. Org. Chem.*, **1985**, *50*, 2003-2004. b.) A. B. Padias, H. K. Hall, D. A. Tomalia and J. R. Mcconnell, *J. Org. Chem*., **1987**, *52*, 5305-5312.

[145] H. Ihre , A. Hult , and E. Soderlind, *J. Am. Chem. Soc.,***1996**, *118*, 6388–6395 .

[146] J.-P. Majoral and A.-M. Caminade, *Chem. Rev.,* **1999**, *99*, 845-880.

[147] A.-M. Camiade, C. –O. Turrin, R. Laurent, A. Ouali, B. Delavaux-Nicot, *Dendrimers: Towards Catalytical, Material and Biomedical Uses*, Wiley-VCH, Weinheim, **2011**.

[148] S. Hecht and J. M. J. Fréchet, *Angew. Chem*., **2001**, *113*, 76-94; *Angew. Chem. Int. Ed*., **2001**, *40*, 74-91.

[149] P. J, Dandliker, F. Diederich, A. Zingg, J. P. Gisselbrecht, M. Gross, A. Louati and E. Sanford, *Helv. Chim. Acta*, **1997**, *80*, 1773–1801.

[150] P. J. Dandliker, F. Diederich, M. Gross, C. B. Knobler, A. Louati and E. M. Sanford, *Angew. Chem.*, **1994**, *106*, 1821-1824; *Angew. Chem. Int. Ed*., **1994**, *33*, 1739-1742.

[151] P. Wu, X. Chen, N. Hu, U. Tam, O. Blixt, A. Zettl and C. R. Bertozzi, *Angew. Chem*., **2008**, *120*, 5100-5103; *Angew. Chem. Int. Ed*., **2008**, *47*, 5022–5025.

[152] M. W. P. L. Baars, R. Kleppinger, M. H. J. Koch, S.-L. Yeu and E. W. Meijer, *Angew. Chem.*, **2000**, *112*, 1341-1342; *Angew. Chem. Int. Ed*., **2000**, *39*, 1285–1288.

[153] S. M. Ryan, G. Mantovani, X. X. Wang, D. M. Haddleton and D. J. Brayden, *Expert Opin. Drug Del.*, **2008**, *5*, 371-383.

[154] A. E. Beezer, A. S. H. King, I. K. Martin, J. C. Mitchel, L. J. Twyman and C. F. Wain, *Tetrahedron*, **2003**, *59*, 3873-3380.

[155] A. M. Caminade and J. P. Majoral, *Prog. Polym. Sci*., **2005**, *30*, 491-505.

[156] T. R. Krishna, M. Parent, M. H. V. Werts, L. Moreaux, S. Gmouh, S. Charpak, A.-M. Caminade, J.-P. Majoral and M. Blanchard-Desce, *Angew. Chem*., **2006**, *118*, 4761-4764; *Angew. Chem. Int. Ed.*, **2006**, *45*, 4645–4648.

[157] B. Zhu, Y. Han, M. H. Sun and Z. S. Bo., *Macromolecules*, **2007**, *40*, 4494−4500.

[158] C. Ornelas, R. Lodescar, A. Durandin, J. W. Canary, R. Pennell, L. F. Liebes and M. Weck, *Chem. Eur. J*., **2011**, *17*, 3619–3629.

[159] I. B. Rietveld, E. Kim and S. A. Vinogradov, *Tetrahedron*, **2003**, *59*, 3821–3831.

[160] S. Xiao, N. Fu, K. Peckham and B. D. Smith, *Org. Lett*., **2010**, *12*, 140–143.

[161] S. M. Grayson and J. M. J. Fréchet, *Chem. Rev*., **2001**, *101*, 3819-3867.

[162] M. Wyszogrodzka, K. Möws, S. Kamlage, J. Wodzińska, B. Plietker and R. Haag, *Eur. J. Org. Chem.*, **2008**, 53–63.

[163] B. Trappmann, K. Ludwig, M. R. Radowski, A. Shukla, A. Mohr, H. Rehage, C. Böttcher and R. Haag, *J. Am. Chem. Soc*., **132**, 11119-11124.

[164] M. Wyszogrodzka and R. Haag, *Langmuir*, **2009**, *25*, 5703-5712.

[165] H. Nemoto, J. G. Wilson, H. Nakamura and Y. Yamamoto, *J. Org. Chem*., **1992**, *57*, 435.

[166] M. Jayaraman and J. M. J. Fréchet, *J. Am. Chem. Soc.*, **1998**, *120*, 12996-12997.

[167] M. Wyszogrodzka and R. Haag, *Chem. Eur. J.,* **2008**, *14*, 9202–9214.

[168] R. Haag, A. Sunder and J.-F. Stumbé, *J. Am Chem. Soc*., **2000**, *122*, 2954-2955.

[169] T. Ooya, J. Lee and K. Park, *Bioconjugate Chem*., **2004**, 1221-1229.

[170] S. L. Elmer, S. Man and S. C. Zimmerman, *Eur. J. Org. Chem*., **2008**, 3845-3851.

[171] R. K. Kainthan, J. Janzen, E. Levin, D. V. Devine and D. E. Brooks, *Biomacromolecules*, **2006**, *7*, 703-709.

8 Curriculum Vitae (Lebenslauf)

Der Lebenslauf ist in der Online-Version aus Gründen des Datenschutzes nicht enthalten.